Propositions

added to the thesis

Towards a High Brightness, Monochromatic Electron Impact Gas Ion Source

by Vipin Tondare

[1] The performance of a well-designed charged particle optical system ultimately depends on the quality of its charged particle source, and therefore research on charged particle sources is more interesting than other research topics in charged particle optics.

[2] Cold field electron emission sources are not unsuitable for focused beam applications provided that one maintains a gas pressure around the source of well below 10^{-12} Torr (ultra high vacuum).

F. Charbonnier, Appl. Surf. Science, **94/95**, 26 (1996)

[3] One of the best approaches to obtain a stable field electron emission current at almost stable voltage in poor vacuum conditions could be to (a) operate the tip below the sputtering threshold of the tip material (b) use a proper feedback system on the tip voltage and (c) collect the reference current or the information for the feedback not only from the extractor but also from the target.

[4] Carbon nanotube is found to be the 'best' candidate among all the known materials that have been studied as cold field electron emitters for industrial applications. However, the 'best' is not good enough!

[5] Recent proposals on ultra-cold plasma gas ion source and laser cooled gas ion source for focused ion beam (FIB) applications look promising. However, it is not clear yet as to what extent these sources will be sufficiently easy to operate and maintain for day-to-day industrial applications of FIB machines.

B. J. Claessens et.al. Phy. Rev. Lett. **95**, 164801, (2005)
and B.G. Freinkman et.al. Microelectron. Eng. **73-74**, 139 (2004)

[6] Only one conclusion can be drawn from the experiments with supertip liquid metal ion sources and that is that they cannot replace an ordinary liquid metal ion source.

S.T.Purcell et. al. Nanotechnology **12**, 168 (2001)
and S.T.Purcell and V.T. Binh, J.Vac.Sci.Technol.**B 19**, 79 (2001)

[7] Gas field ionization is an intrinsically wonderful way to produce high brightness, monochromatic ion beam. However, plasma gas ion sources are presently accepted because of their robustness and reliability. This means that one must not keep talking about high brightness and low energy spread of an ion source while ignoring the ion source reliability.

[8] Thermal field electron impact gas ion source is the only gas ion source that has been proposed by considering all of the main requirements simultaneously, that is (a) high brightness (b) low energy spread (c) ion emission stability (d) ion source life-time (e) minimum ion current from the source and (f) room temperature operation.

[9] First publishing research in a scientific journal and only then thinking about applying for a patent is the logical way and is beneficial for progress in scientific research. The European Patent Office should allow such a thing, just like the patent offices in the United States of America and a few other countries do!

[10] The Ga-liquid metal ion source used for digging the holes in the Si_3N_4 membranes of the gas target did not realize that it was digging its own grave.

Stellingen

behorende bij het proefschrift:

Naar een Monochromatische Elektronimpact Gas-Ionenbron met Hoge Helderheid

door Vipin Tondare

[1] De prestaties van een goed ontworpen deeltjesoptisch systeem zijn uiteindelijk afhankelijk van de kwaliteit van de gebruikte elektronen- of ionenbron en daarom is onderzoek naar zulke bronnen interessanter dan andere onderzoeksonderwerpen in de deeltjesoptica.

[2] Koude veldemissie elektronenbronnen zijn niet ongeschikt voor toepassingen van gefocusseerde bundels onder de voorwaarde dat de gasdruk rond de bron ruim onder de 10^{-12} torr (ultra-hoog vacuüm) blijft.

F. Charbonnier, Appl. Surf. Sci. **94/95**, 26 (1996)

[3] Voor het verkrijgen van een stabiele veldemissiestroom bij nagenoeg stabiele spanning in slechte vacuüm condities zou één van de beste benaderingen kunnen zijn om (a) de tip beneden de sputter-drempel van het tipmateriaal te laten werken, (b) een geschikt terugkoppelingssysteem op de tipspanning toe te passen en (c) de referentiestroom of -informatie voor de terugkoppeling niet alleen van de extractor maar ook van het target te verzamelen.

[4] Koolstofnanobuisjes blijken van alle bekende materialen die zijn bestudeerd als koude veldemitters de 'beste' kandidaten voor industriële toepassingen. Echter, het 'beste' is niet goed genoeg!

[5] Recente voorstellen met betrekking tot ultra-koude plasma-ionenbronnen en lasergekoelde gas-ionenbronnen voor toepassingen van gefocusseerde ionenbundels (FIB) lijken veelbelovend. Echter, het is nog niet duidelijk in hoeverre deze bronnen voldoende eenvoudig te opereren en onderhouden zullen zijn voor industriële toepassingen van FIB machines.

B. J. Claessens *et al.*, Phys. Rev. Lett. **95**, 164801 (2005)
en B.G. Freinkman *et al.*, Microelectron. Eng. **73-74**, 139 (2004)

[6] Slechts één conclusie kan worden getrokken uit de experimenten met supertip vloeibaar-metaal-ionenbronnen en die is dat deze gewone vloeibaar-metaal-ionenbronnen niet kunnen vervangen.

S.T.Purcell *et al.*, Nanotechnology **12**, 168 (2001)
en S.T.Purcell en V.T. Binh, J. Vac. Sci. Technol. B **19**, 79 (2001)

[7] Veldionisatie van gassen is een intrinsiek geweldige manier om monochromatische ionenbundels met hoge helderheid te produceren. Echter, plasma-ionenbronnen zijn op dit moment geaccepteerd vanwege hun robuustheid en betrouwbaarheid. Dit betekent dat men niet over de hoge helderheid en lage energiespreiding van een ionenbron moet blijven praten, daarbij de betrouwbaarheid van de ionenbron negerend.

[8] Thermische veld elektronimpact gas-ionenbronnen zijn de enige gas-ionenbronnen die zijn voorgesteld door het gelijktijdig beschouwen van alle belangrijke vereisten, te weten (a) hoge helderheid, (b) lage energiespreiding, (c) hoge ionenemissiestabiliteit, (d) lange levensduur van de ionenbron (e), minimum ionenstroom van de bron en (f) mogelijkheid tot werken bij kamertemperatuur.

[9] Het eerst publiceren van onderzoek in een wetenschappelijk tijdschrift en pas dan overwegen een patent aan te vragen is de logische gang van zaken en is gunstig voor de voortgang in wetenschappelijk onderzoek. Het Europees Octrooibureau zou dit moeten toestaan, net als de octrooibureaus in de Verenigde Staten van Amerika en een aantal andere landen!

[10] De Ga vloeibaar-metaal-ionenbron die gebruikt werd om de gaten te graven in de Si_3N_4 membranen van het gas target realiseerde zich niet dat hij zijn eigen graf aan het graven was.

Towards a High Brightness, Monochromatic Electron Impact Gas Ion Source

Vipin Nagnath TONDARE

Towards a High Brightness, Monochromatic Electron Impact Gas Ion Source

P r o e f s c h r i f t

ter verkrijging van de graad van doctor
aan de Technische Universiteit Delft,
op gezag van de Rector Magnificus prof. dr. ir. J. T. Fokkema,
voorzitter van het College voor Promoties,
in het openbaar te verdedigen op dinsdag 20 juni 2006 om 17:30 uur

door

Vipin Nagnath TONDARE

Master of Philosophy (physics), University of Pune, Pune City, Maharashtra, India
geboren te Aurangabad City, Maharashtra, India.

Dit proefschrift is goedgekeurd door de promotor:

Prof. dr. ir. P. Kruit

Samenstelling Promotiecommissie:

Rector Magnificus	voorzitter
Prof. dr. ir. P. Kruit	Technische Universiteit Delft, promotor
Prof. dr. A. Schmidt-Ott	Technische Universiteit Delft
Prof. dr. H.W.M. Salemink	Technische Universiteit Delft
Prof. dr. ir. J.J.M. Braat	Technische Universiteit Delft
Prof. dr. I.M.de Schepper	Technische Universiteit Delft
Dr. G.N.A. van Veen	FEI Company, Eindhoven

Het onderzoek beschreven in dit proefschrift is financieel ondersteund door
de Stichting voor Fundamenteel Onderzoek der Materie (FOM) -
Philips Laboratorium zonder Muren

Preface

The work described in this thesis was done under a research project (FOM-Project 00PF84-FOM-Philips Laboratorium zonder Muren) in the period from August 2001 to January 2006 at Delft University of Technology in the Charged Particle Optics Group of prof. dr. ir. P. Kruit. The aim of this project was to investigate new approaches to obtain high-brightness, monochromatic and operationally reliable noble gas ion sources and if possible, to develop such a noble gas ion source for focused ion beam (FIB) machines.

A FIB machine is a particle optical instrument designed with the aim to focus a large amount of current in the smallest possible spot onto a specimen. However, for the successful operation of such a FIB machine, one needs a high brightness, monochromatic and operationally reliable ion source. FIB machines have tremendous applications in materials science, the semiconductor industry or nanotechnology in general. At present, gallium-liquid-metal ion sources (Ga-LMIS) are widely used in FIB machines, which is mainly because these sources meet some important requirements such as ion-source brightness and reliability. The problem of using a metal ion source is that the metal ions change the electric or magnetic properties of the specimen under fabrication or under inspection. It is expected that there will be a great demand for high brightness, monochromatic and operationally reliable noble gas ion sources in the near future.

The concept of electron impact gas ion sources for focused beam applications exists in our research group since more than twenty years. In 1985, Barth and co-workers [Microelectron. Eng. **3**, (1985) 147] from our group suggested that if an electron impact gas ion source (ions formed due to bombardment of electrons with atoms or molecules) is operated in non-plasma mode (that is, at room temperature) and if the ionization region is at micron scale, then the ion source brightness can be much higher. They used a conventional thermionic electron emitter to deliver the electrons into the gas ionization region. They concluded that to achieve an ion source reduced brightness $\geq 10^4 A/m^2SrV$ more electron current was needed. The concept of electron impact ion sources looked promising but, that in order to focus a large amount of electron current in a small ionization region a high-brightness, monochromatic electron source (better than a thermionic electron source) was required.

The obvious choice was a cold field electron emitter, the electron emitter known as a high-reduced brightness and monochromatic electron source. The concept of cold field electron impact gas ion sources (described in Chapter 3, Fig. 1) without a current regulator system did exist in our research group in the late 1990s, which is before the beginning of this PhD project.

In the first project meeting at the beginning of this PhD project in the month August 2001, we reached the conclusion that the concept of a cold field electron impact gas ion source is certainly a powerful concept; such an ion source can have a reduced brightness comparable to a Ga-LMIS and an energy spread much smaller than a Ga-LMIS. Other attractive features of this concept are its compact design and its simplicity compared to the ion source reported by Barth and co-workers (mentioned above). We then also expressed our doubts about the performance of a cold field electron source in poor vacuum conditions (that is very close to the ionization region). This is because it is well known that the successful operation of a field electron source, that is long-term, stable electron emission at an applied voltage, requires ultra-high vacuum conditions (pressure $< 10^{-12}$ Torr) around the electron

source. It was clear that the performance of the ion source would become seriously affected if the electron source could not deliver electrons into the ionization region at a constant rate and at constant electron energy or if the lifetime of the electron source would be too short. This led to thinking about a completely different research problem, namely "can we really have successful operation of cold field electron sources in poor vacuum conditions?"

It was also realized that various types of ion sources and cold field electron sources have been studied for several decades by other researchers. At times we thought that we had a novel idea of making gas ion sources for FIB applications, but eventually, we only discovered problems and understood why other researchers might not have tried those paths. It was absolutely necessary to take a critical look at the history and the status of the research on high brightness noble gas ion sources and cold field electron sources. It was also a must to answer the question of how our ion source concept is novel and better than other existing ion sources.

From the beginning of the project we started working on field emission experiments to check whether the cold field electron impact gas ion source concept is feasible. This work can be found in Chapter 3. As far as an electron impact ion source is concerned it was clear to us that to achieve a large ion current density we needed more electron current delivery into the gas ionization chamber. We also knew that this could only be achieved if we placed a point electron source very close to the gas target because the use of lenses to form an electron probe introduces aberrations, which would make it impossible to achieve maximum electron current density at the ionization region. It seemed that there was no alternative for the design of a cold field electron impact gas ion source. This design was much simpler and much more effective than the one reported by Barth and co-workers (mentioned above). We spent almost 80% of the total project time on cold field emission experiments (Chapter 3) and we believe that this time was well spent.

Finally, this thesis is about two types of gas ion sources (a) the thermal field electron impact gas ion source (Chapter 2) and (b) the cold field electron impact gas ion source (Chapter 3), the ones we have considered as potential candidates for FIB applications.

It was challenging as well as a bit risky to work as a PhD student on this project because the research topics of gas ion sources and cold field electron sources are several decades old and well studied. A considerable amount of time had to be spent on a literature survey, which was absolutely essential.

This PhD thesis has mainly evolved due to several useful discussions with prof. dr. ir. P. Kruit (the project leader). The original aim of the PhD project has been more or less achieved in that we have investigated new approaches for making gas ion sources for FIB applications and we have tried to build a prototype.

Two new PhD students will start working on 'thermal field electron impact gas ion sources' some time in 2006.

Outline of the thesis

Chapter 1:

Chapter 1 is a critical review on gas ion sources for focused beam applications. First of all, in Section 1.1, a FIB machine is described briefly. In Section 1.1, several useful up-to-date references can be found about FIB machines and their wide range of applications. After stating the problem of the use of a Ga-LMIS in FIB machines, a Ga-LMIS is described in terms of its design, working principal and

properties, including several useful references for the benefit of the reader. This also makes clear that when discussing a noble gas ion source for FIB applications, we should compare its properties with the successful Ga-LMIS. Section 1.2 is devoted to clarify the meaning of 'the quality of a charged particle beam'. While reading Section 1.2, it will become clear to anyone why one should have charged particle sources with high brightness and low energy spread for the successful performance of an optical column. More detailed information on the subject can be found in the references for Section 1.2. After understanding the meaning of the quality of a charged particle beam and considering the properties of a Ga-LMIS, one can understand the strengths and weaknesses of a Ga-LMIS. For instance, the strength of a Ga-LMIS is its operational reliability where as the high-energy spread is its weakness.

In Section 1.3, several noble gas ion sources are described with the aim of understanding why those gas ion sources were so far unsuccessful for FIB applications. As one can understand from Section 1.3, gas field ionization is the best way to produce high-brightness and monochromatic beams but these sources lack reliability. The supertip-gas field ion source (Sub-section 1.3.1.1c) is an example of the futile efforts by several researchers to develop a gas ion source for FIB applications. The needle-in-capillary type gas field ion source (Sub-Section 1.3.1.3) brings some hope but is still unproven and has not been widely tested. High-temperature plasma gas ion sources (described in Sub-Section 1.3.2) are robust and reliable but are still struggling to achieve a high brightness beam required for FIB applications. In Sub-Section 1.3.3., a number of different ways to develop gas ion sources are described. Proposals such as a novel laser ion source (described in Sub-Section 1.3.3.1) looks promising and worth investigating but it is not clear yet how easy it would be to operate and maintain such a gas ion source in day-to-day applications of FIB machines.

Section 1.4 gives the present status of noble gas ion source research for FIB applications.

In summary, Chapter 1 gives clear understanding that there is a need and some room left for research on gas ion sources for FIB applications.

Chapter 2:

In Chapter 2, we propose the concept of the 'thermal field electron impact gas ion source'. The basic concept of electron impact ion sources for FIB application is the same as that reported by Barth and co-workers (mentioned above) where one operates an electron impact ion source in non-plasma mode by keeping the ionization region as small as possible. The difference is the ultra small gas ionization chamber where one can maintain a maximum gas pressure and operate the ion source without forming plasma inside or outside the gas ion chamber. Of course, the thermal field electron source (also known as Schottky electron gun), which is a high brightness, monochromatic and reliable electron source, can deliver more current in a small ionization region than conventional thermionic electron sources. Actually, the main differences between the concepts of the cold field electron impact gas ion source (the concept that existed before this PhD project) and the concept of the thermal field electron impact gas ion source are the electron source used for creating the gas ions and the use of lenses.

From Chapter 1, it has become clear that until now gas ion sources have been unsuccessful because while designing those sources researchers did not consider all of the desired properties of an ion source for FIB applications simultaneously.

As one can understand after reading Chapter 2, the thermal field electron impact gas ion source is the only gas ion source that has been proposed by considering (i) high brightness (ii) low energy spread (iii) ion emission stability (iv) ion source lifetime (v) minimum ion current from the source and (vi) room temperature operation etc. simultaneously.

In chapter 2, before explaining the concept of the ion source, the electron impact ionization process is explained in Section 2.2. This gives an idea of a number of parameters such as the electron current, the gas particle density, the length of the gas ionization chamber, the ion current and the partial ionization cross-section with respect to the electron energy.

After giving earlier experimental results and experimental conditions of measuring the partial electron impact ionization cross-section for argon gas [Rejoub et.al. Phys. Rev. A, **65**, (2002) 042713] in Section 2.2, the concept of the 'thermal field electron impact gas ion source' is described in Section 2.3. A relatively high pressure can be maintained (in the molecular flow regime) in between two closely spaced (submicron distance) parallel plates, each with holes on the axis. Outside the chamber, on the axis, the gas particle density can be extremely small. Such a design of a gas chamber at millimeter scale and made for different reason existed in the literature [J. Peatross and D.D. Meyerhofer, Rev. Sci. Instrum, **64(11)**, (1993) 3066]. The thermal field electron gun is used to deliver electrons into the ultra-small gas ionization chamber with a length approximately equal to the diameter of a hole on the axis. In Section 2.3, equation 3 gives the relation between the reduced brightness and the ion current density.

In the Section 2.4, first of all two different pressures are assumed in such a way that one can use the experimentally measured data of the partial ionization cross-section of argon gas (Rejoub et.al., 2002) to estimate the possible ion current density. Equations 4 and 5 give the relation between the electron current density, the ion current density, the partial ionization cross-section and the gas particle density. After estimating the maximum electron current density that can be achieved from a thermal field electron gun at different electron energies (< 1000 V) using a computational recipe from a recent paper [Kruit et.al., J. Appl. Phys. **99**, (2006) 024315], with the help of Equations 3, 4 and 5, the reduced brightness at two different pressures and a few different electron energies has been estimated. The dimension of the gas target can be ~100nm (the spacing between the two plates ~100nm and the diameter of each hole ~100nm). The ion energy spread is mostly dependent on the applied voltage difference. The maximum voltage difference is assumed in such a way that the electric field should not be so high as to cause field induced gas discharges. The ion beam emission is considered to be in the pencil beam regime, which means that interactions between the charged particles are negligible.

The reliability of this ion source (operated at room temperature) can be better than gas field ion sources because it does not depends on the surface properties of the material, which are difficult to control. The operation of a thermal field electron gun can be sufficiently smooth as it can be kept in ultra-high vacuum. Section 2.5 gives the conclusion of the predicted performance of the ion source, which is comparable to or even better (i.e. low energy spread) than that of Ga-LMIS.

Although the construction of an ion source looks almost equal to an optical column, we believe that it would also be possible to fabricate a dual-beam system (electron and ion beam) in such a way that the electron source used here can be used not only for creating the ions but also as a separate low-energy electron probe.

Chapter 3:

Chapter 3, mainly describes the field emission experiments done to check whether the cold field electron impact gas ion source concept is feasible. The field emission study reported in this chapter can also be of interest to a wider field emission or vacuum microelectronics community. Section 3.1 explains the concept of the ion source (already existing prior to this PhD project).

Section 3.2 is a brief literature survey that gives the impression that cold field emitters have already been studied extensively, as this research topic is several decades old. It also shows the results from the literature and concludes that novel materials such as chemical-vapor-deposited diamond films or carbon nanotubes may not be enough to develop field emission devices that can be operated in industrial vacuum ($> 10^{-7}$mbar) conditions. The conditions for stable electron emission at stable voltage are given and it is concluded that there has to be some active mechanism that will stabilize the electron current at stable tip voltage. Section 3.2 also assesses the success and limitations of some of the excellent ways reported in the literature (for instance, MOSFET-structured silicon field emitters, the use of a resistive sheet and the use of feedback on the tip- to-anode distance) to stabilize the field emission current in industrial vacuum conditions.

In Section 3.3, first of all the aim of our field emission experiments is given, namely to experimentally simulate the field emission tip behavior when placed in front of the gas target. Several things were taken into account while designing the experiments. It was decided to use feedback on the tip voltage to stabilize the field emission current as it has a number of advantages over the approach of using feedback on the tip-to anode distance.

Subsections 3.3.1 and 3.3.2 describes the experiments of making sharp tungsten tips and the study of the field emission image of an unclean field emission tip, respectively.

Subsections 3.3.3 describes our attempt to stabilize the field emission current using a current regulator system (feedback on the tip voltage). A feedback circuit was built. The experimental set up was designed in such way that it was possible to perform field emission experiment at ~ 90 V and vary the gas pressure. The separation distance of the tip and the anode could be watched through an optical microscope. The short-term as well as long-term fluctuations and lifetime of the tip were studied in poor vacuum conditions.

Subsections 3.3.4 describes our attempt to achieve a stable electron beam current through an aperture. A field emission shadow microscope was built. It was possible to bring the field emission tip close to the aperture (micron scale) of a grid using a scanning tunneling microscope. We also used an improved feedback circuit. The stability of the electron beam through the aperture was measured. A post-inspection of the grid for possible damage was also performed.

It is clear that the results are quite encouraging but that further work is needed. For instance, as described in Section 3.4, if one makes a rigid assembly similar to a double-gated field emitter with feedback on the tip voltage, operates a carbon based tip below the sputtering threshold and collects the reference current (or information) not only from the gates but also from the target then, it could be possible to make a ‘cold field electron impact gas ion source’. In this way, one can expect a stable current at relatively stable voltage and long life for the field emission tip.

Interestingly, this could also be a way to fabricate a cold field emission gun for an electron microscope that does not require an sputter ion pump to maintain ultra high vacuum.

Chapter 4:

Chapter 4 is all about fabricating a sub-micron scale gas target for the 'thermal field electron impact gas ion source'. To the best of our knowledge there is no published report of fabricating such a submicron scale (~100 nm) gas target.

Section 4.2 describes the fabrication process (lithographic steps). Basically, two 100nm thick Si_3Ni_4 membranes, covered with a 10-nm thick molybedenum layer, are fabricated as two parallel plates. The membranes are electrically isolated by electron beam resist (PMMA 950K). A focused ion beam is used to drill holes (diameter ~100 nm) through both the membranes.

As one can see in Section 4.2, it is really possible to maintain two separate membranes that are electrically isolated with the help of electron beam resist (PMMA 950K).

Section 4.3 shows the scanning electron micrographs of the gas target with different hole sizes.

Several things will be clear only after use of the gas target for creating the gas ions. The gas target may become damaged even in the concept of a 'thermal field electron impact gas ion source'. Therefore, the fabrication process of the gas target is designed in such a way that several gas targets can be fabricated in one batch. The gas target should be cost-effective and replacing it should be as easy as replacing a specimen in FIB machines.

Although several new ideas can be thought of for making the gas target, we believe that these fabricated gas targets can be sufficient for a pilot experiment.

Chapter 5:

Chapter 5 describes an experimental setup to conduct the 'thermal field electron impact gas ion source' experiments.

Section 5.2 is all about the design of a thermal field electron gun that can deliver a maximum electron current into the 100nm size gas target.

Section 5.4 shows that the gas target that we are using is not an ideal one as due to the thickness of the silicon wafer used to support the Si_3Ni_4 membranes a lens effect may occur, which may spoil the quality of the ion beam. However, these gas targets can be used for the first experiments but eventually, the gas target will have to be modified.

Section 5.5 shows the built experimental setup of the thermal field electron gun as well as the ion optical column. The first experiments can be performed using this experimental set up.

V.N. Tondare
Delft, June 2006

Acknowledgements

First of all, I gratefully acknowledge my thesis supervisor, prof. dr. ir. P. Kruit for giving me an opportunity to work on this project and for his several useful suggestions throughout the duration of this PhD project that made this thesis possible. I also gratefully acknowledge my official employer 'de Stichting voor Fundamenteel Onderzoek der Materie' (FOM), The Netherlands and Philips Company, The Netherlands for the financial support.

I sincerely acknowledge the members of scientific staff of our research group Dr. N.J. van Druten (Ex-member), Dr. C.W. Hagen and Dr. J.E. Barth. The discussions with these people have benefited me.

I would like to thank A.H.M. Coppens, a member of our technical staff, for his leading role in fabricating (in DIMES, Delft) the gas target that was required for the thermal field electron impact gas ion source. I also would like to thank a present PhD student and a former MSc student, Ir. M.S. Bronsgeest and Ir. M. Bezuijen from our research group, who were already working on thermal field electron sources for their work and they helped me very much in designing the low energy electron probe that was required for the thermal field electron impact gas ion source.

I specially thank J. Nonhebel and J. de Looff, members of our technical staff. Their technical assistance throughout the duration of this PhD project is invaluable. I also thank R. Radhoe and S. van Berloo for their technical assistance under the supervision of J. Nonhebel.

I thank P.W. van Harrewijn, M. Pelle and F. Berwald, members of our technical staff for their technical assistance along with J. Nonhebel and J. de Looff, while building the experimental setup of the thermal field electron impact gas ion source.

I am thankful to Drs. A.E. van Diepen, a member of our scientific staff, for reading the manuscripts of this thesis and providing the dutch translations of the propositions attached to this thesis and of the summary and conclusions of this thesis.

I am also thankful to our group secretaries E.P. van der Most and M.A.H. Moor for their always-prompt help in dealing with office paper work.

I take this opportunity to thank FEM/FIM Laboratory, Department of Physics, University of Pune, Pune City, Maharashtra, India and in particular, Dr. N. Pradeep (Ex-member of the laboratory). The research training that I received there was very useful while working on 'cold field electron impact noble gas ion source' concept here, in Delft.

Finally, I want to thank my family and friends for their encouragement and moral support during this PhD work.

V.N. Tondare
Delft, June 2006

Contents

Chapter 1

*Quest for high brightness, monochromatic noble gas ion sources**

V. N. Tondare

Abstract

Focused ion beam (FIB) machines are key tools for state-of-the art sample preparation in electron microscopy, for characterization and repair in material sciences, for the semiconductor industry and for nanotechnology in general. Liquid-metal ion sources (LMIS) are widely used in FIB machines because they meet the minimum ion source requirements such as source brightness and reliability. However, in FIB machines, noble-gas ion sources are favorable for sputtering, beam-induced etching and deposition, because the implanted ions do not change the electrical behavior of the substrate significantly. There are several efforts by various researchers to develop noble-gas ion sources that can be used in FIB machines instead of LMIS. The gas ion sources could not meet the minimum ion source requirements. Therefore, LMIS are still a popular choice among FIB machine users. This review article takes a critical look at the reported efforts in the literature to develop noble gas ion sources for FIB machines.

***** Critical review, V. N. Tondare, J. Vac. Sci. Technol. A., **23(6)**, (2005) 1498.

1.1 Focused Ion Beam Machine

Focused ion beam (FIB) machines [1] look very similar to the more familiar scanning electron microscopes (SEM). FIB machines consist of three major parts, namely the ion source, the ion column and the sample stage. The main difference between the two machines is that in a SEM an electron beam is used, whereas in an FIB machine, an ion beam (mostly Ga^+) is used. Figure 1 shows the working principle of an FIB machine. As shown in Fig. 1, an FIB machine involves the transmission of a parallel ion beam between two lenses. A number of apertures are used to select the beam current. The beam energy typically is 30 or 50 keV. The beam is raster-scanned over the sample, which is mounted in a vacuum chamber. Ions can be focused into diameters smaller than 0.1μm with current densities of several A/cm^2.

FIB machines are an integral part of material science and the semiconductor industry due to their day-to-day tremendous applications [1]. For example, FIB machines can be used for 1) specimen preparation for transmission electron microscopy, 2) in-situ cross-sectioning and analysis of a fabricated device, 3) gas-assisted milling and deposition, 4) mask repair and micro-machining 5) scanning ion microscopy, 6) lithography, etc. More details about FIB machines and their applications can be found elsewhere [1].

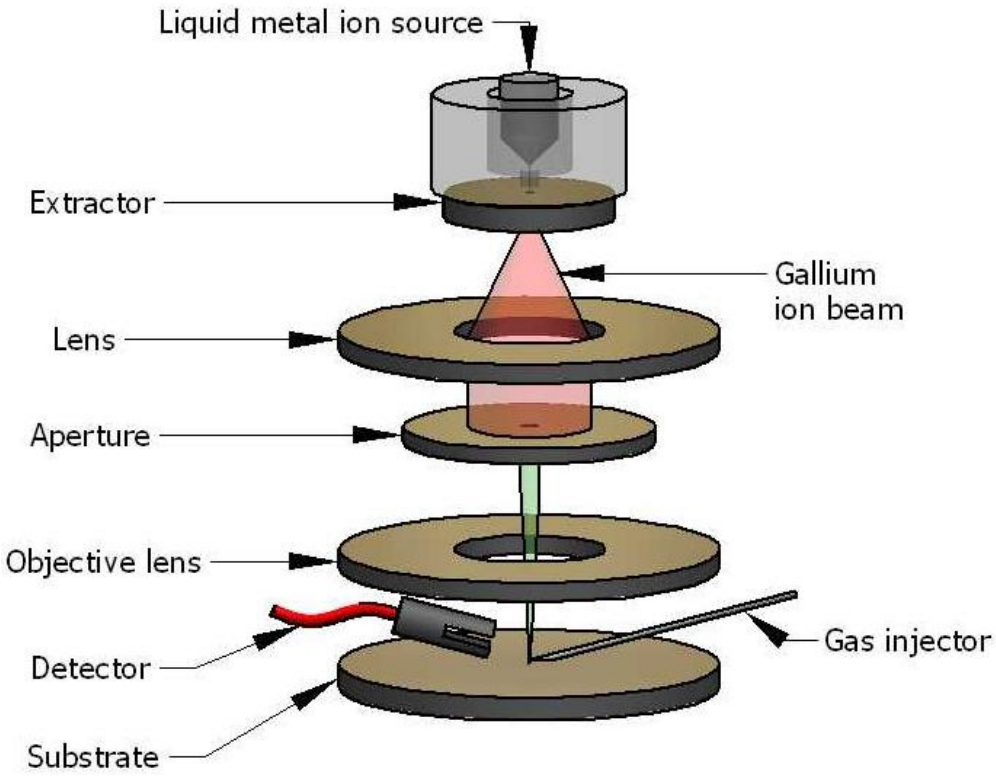

FIG. 1. Schematic of a typical Focused Ion Beam Machine. Adapted from Ref. [1].

One of the main drawbacks of FIB machines is that contamination is inevitable due to the use of liquid-metal ions, so a noble-gas ion source is very much desired. Ga ions not only change the electrical properties but can also affect the magnetic properties of the devices [2]. Gallium staining [3,4] due to deposition of gallium ions in the quartz substrate during FIB repair of a photo-mask is another important issue that limits the use of FIB machines. If a suitable noble-gas ion source can be developed, the usefulness of FIB machines will also increase. Before we discuss the efforts by other researchers to develop noble-gas ion sources for FIB machine, it is useful to present some information about liquid metal ion sources (LMIS).

1.1.1 Liquid-metal ion source

There are several types of LMIS available such as needle-type LMIS, capillary-type LMIS and impregnated-type LMIS [5,6]. The needle ionizer [7-9] is most commonly used. As shown in Fig. 2(a), needle-type liquid-metal ion sources usually consist of a blunt tip (usually tungsten with a radius of a few microns). The reservoir of liquid metal is maintained at the other end of the tip. The tip faces an extraction aperture. An electric field can be applied across the tip and the aperture. After heating the reservoir to a suitable temperature, the metal flows down and wets the tip. The metal used in LMIS can essentially be any composition having high surface tension, low vapor pressure in its molten state and not corroding the tip itself [1]. Gallium (melting point ~300K) is considered the most suitable and is most widely used but several metals and alloys can be used for different applications [1,7,10 and 11].

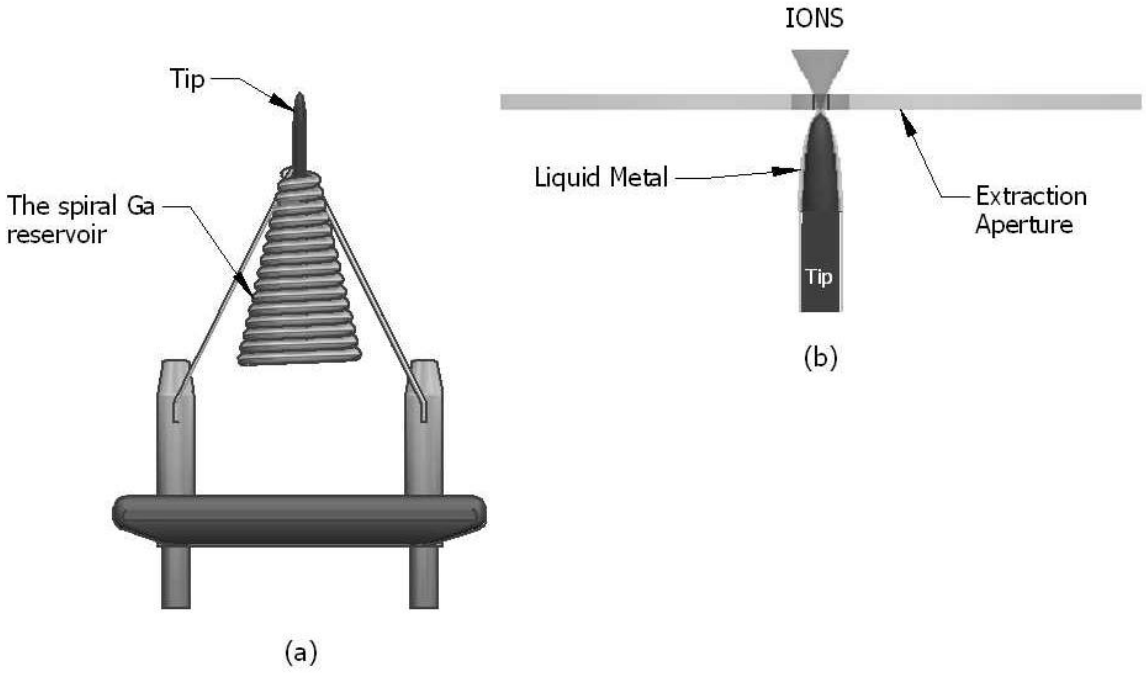

FIG. 2. Needle type liquid metal ion source used in FIB machine. Adapted from Ref. [7]. (a) Liquid metal ion source. (b) Ion emission process.

The strong electric field applied displaces the metal that is in a molten state. The liquid metal gets pulled into a cone, which is known as the Taylor-Gilbert cone [12]. The strong electric field causes field evaporation of the liquid metal at the apex of the Taylor-Gilbert cone. The positive ions (see Fig. 2(b)) from the apex of the Taylor-Gilbert cone start flying out towards the extraction aperture forming a positive-ion beam. The radius of this emitting apex may be 1.5-3 nm [12]. Forbes [12] has explained the basic working principle of LMIS. LMIS (at low current levels) are also known as liquid-metal field ionization sources or field emission ion sources. The field ionization [13] process is a quantum mechanical tunneling process that starts taking place at a high electric field (10^{10}V/m). Electrons tunnel from trapped atoms or molecules (trapping in the vicinity of the tip due to the high electric field) into the tip, resulting in ionization of atoms or molecules in the vicinity of the tip. Field evaporation [13] is a similar process as field ionization. More details about field-ionization and field-evaporation mechanism can be found elsewhere [13].

1.1.2 Properties of liquid-metal ion sources

Several properties of LMIS can be found elsewhere [1, 5-7,10 and 11]. Actually, from an electron optical perspective only two properties are really important, and those are the reduced brightness and the ion energy spread. Ion-source properties with respect to reliability, such as current stability and lifetime, are also important. The typical values are given in the table 1. The lifetime of LMIS depends upon the ion current level. A typical LMIS (Ga) can have a useful lifetime >2000 hours for a 2-μA current level. For FIB applications, the ion-current stability is an important requirement as well as the requirement that the ion source should have at least 1-nA current at the source. LMIS can have a much larger current.

Table 1. The typical properties of Ga-LMIS [1]

Reduced brightness	~ $1 \cdot 10^6$A/m^{2}SrV
Ion energy spread	~ 5-10 eV
Ion current stability	~ (±2%) on a minute scale
Ion source lifetime	~ (>2000-hours with ion current ~2 μA)

1.2 The Quality of a Charged Particle Beam

The quality of a charged particle beam is determined by the final spot size and also the current density at the specimen [14]. The smaller spot size and high current density is always desirable. The obtainable high quality of a charged particle beam mainly depends on the properties of the charged particle source, the properties of the optical system and the coulomb interactions in the beam [14].

As stated earlier, from an optical perspective, one wants to know primarily the two properties of a charged particle source and those are the reduced brightness and the initial (intrinsic) energy spread. The initial (intrinsic) energy spread is an inherent beam energy spread related to the temperature of the charged particle emitting surface [15]. By

the end of this section 1.2, one will understand: Do the values of these two quantities (reduced brightness and initial energy spread of a charged particle source) remain the same in an entire optical column? And, what is the role of these two quantities in the performance of an optical system?

The reduced brightness [16, 17] of point sources (see, Fig. 3) is defined as:

$$B_r = \frac{I}{A\Omega V} \tag{1}$$

Where B_r is the reduced brightness (Unit: A/m^{2}SrV), I is the current, A is the virtual source size, Ω is the solid angle, and V is the acceleration voltage

The reduced brightness of thermionic electron emitters or plasma ion sources is usually estimated by the following equation:

$$B_r = \frac{eI}{\pi^2 r^2 kT} \tag{2}$$

Where B_r is the reduced brightness (Unit: A/m^{2}SrV), I is the current, e is the electron charge, r is the radius of the charged particle emitting area, k is the Boltzmann constant, and T is the temperature of the emitting surface.

This definition of the reduced brightness has real physical meaning where every term of the equation and the unit is clearly given [16]. Reduced brightness is conserved throughout the optical system, that means at any focus of the charged particle beam one can expect the same value of the reduced brightness and this can be always irrespective of the imaging conditions or the value of the charged particle energy. However, one should use the size of the first-order image and not any observed probe size [16].

The properties of an electron optical system are determined by the aberrations of the optical elements [14]. The effect of chromatic aberration in optical systems is that lenses bring charged particles of different wavelength (energy) to focus at different points along the optical axis. The higher energy (shorter-wavelength) charged particles are brought to focus further from the lens than those of lower energy. If energy spread is large, a lens has no unique focal length which will give rise to a disc of confusion rather than a point focus. This adversely affects the resolution attainable with the optical system. Even with perfectly 'monochromatic' charged particles a lens can suffer from spherical aberration. Charged particles travelling far from the optical axis are brought to focus closer to the lens than those near the axis. To minimize the effect of spherical aberration in an optical system the rays which are near the optical axis are only used. In FIB system, mainly, the aberrations of the sources extraction lens and the final projector lens are dominant [18]. There are well known design principles to reduce lens aberrations. However, the problem of determining the effects of coulomb interactions (interactions between charged particles in the beam) is very complicated [19]. These coulomb interactions depend on several system parameters including particle mass, beam energy, beam current, beam convergence angle, source properties, length of optical column, cross over size and position [19]. The effects caused by coulomb interactions are of three types: the space charge effect, the Boersch effect and the trajectory displacement effect [14].

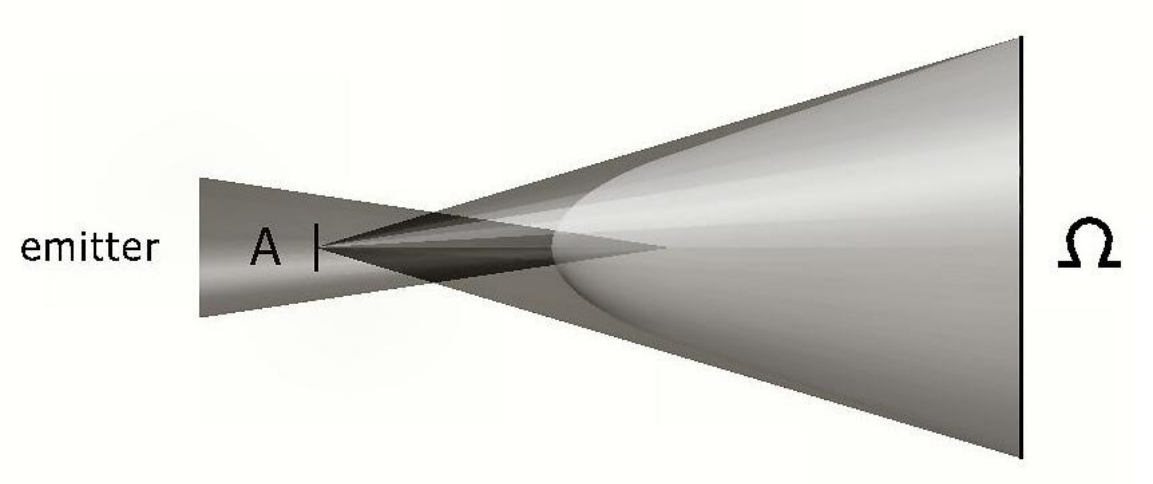

FIG. 3. Definition of reduced brightness.
(The figure shows an emitter emitting charged particles into solid angle Ω (Sr), A (m^2) is the virtual source size of the emitter).

In a first order approximation the space charge effect that is a broadening of the beam caused by average charge density, can only cause a defocusing (negative lens). This defocusing can be corrected in the optical system [14]. The Boersch effect and the trajectory displacement effect lead to axial and lateral displacements of the charged particles respectively. Boersch effect results in an energy broadening and the trajectory displacement effect results in a broadening of the spatial particle distribution. These last two effects (Boersch and the trajectory displacement) are of statistical nature, due to the coulomb repulsion of individual pairs of the charged particles. The unwanted results of those two effects can not be corrected in the optical system [14]. One has to try to maintain these coulomb interactions effects as minimum as possible in an optical system. Low energy focused ion beams with a high current density are desirable for low damage maskless processing [20]. However, the effect of coulomb interactions can be dominant in the systems operating at high beam current or low beam voltage [21].

Energy broadening due to coulomb interactions is the biggest concern for obtaining the quality charged particle beams [22, 23]. Energy spread in charged particle beams often reach widths of several electron volts, even if initial energy spread at the source amounts to only a fraction of an electron volt [24]. It is clear that such broadened energy spread result from the processes that act along the beam [24]. The two types of energy spreading mechanisms have been briefly reviewed by Mair [23]. The first one is non-laminar (collision-dominated) and the second one is laminar (collisionless).

In the collision-dominated mechanisms, momentum is transferred from the transverse motion components to the axial component via collisions. This leads to large energy spread. This was first studied for high-density electron beams. Zimmermann [25] showed a relationship between energy spread and current density j as follow.

$$\Delta E^2 = \Delta E_0{}^2 + Cj^{1/2} \tag{3}$$

Where, ΔE_0 is an initial or intrinsic energy spread. The constant C strongly depends on the mean free path between collisions in the beam and weakly on the current density j.

The model for the laminar (collisionless) energy broadening mechanism was developed by Knauer [24] for the case of field emitted electron and ions. He understood that the beams that originate at point sources are mostly collision-free since they diverge so rapidly that even particles with large transverse motions can not cross paths. He assumed that the energy broadening comes in collisionless beam by a process where steady coulomb repulsion between neighbouring particles converts potential energy into kinetic energy. Since beam particles are distributed randomly, this mechanism can also lead to energy broadening. He came with the following equation that gives relationship between energy spread (ΔE) and angular beam intensity (I_Ω).

$$\Delta E = 5.8\pi \frac{e}{4\pi\varepsilon_0}\left(\frac{m}{Vo}\right)^{1/3} r_o{}^{-1/3} I_\Omega{}^{2/3} \tag{4}$$

Where, e = the electron charge, ε_0= electric constant, m = mass of the particle, V_0= the beam extraction voltage and r_0=radius of the source.

Knauer had developed his model on the basis of many simple assumptions. However it has been proved that Knauer's model reasonably works for small diverging beams (collisionless) of high brightness that is the field emitted electron and ion beams [23,26].

It is clear that the initial energy spread does not remain the same but it evolves due to coulomb interactions [22]. When one uses a very fine particle probe containing high current, inevitably the particles will start to interact through their coulomb repulsive forces [27]. To have minimum broadening of energy spread the beam crossovers in the optical system should be kept minimum [28].

The most complete theoretical analysis of coulomb interactions has been so far given by Jansen [29]. The previous attempts and several useful references on the study of coulomb interactions in charged particle beams can be found in his work. According to Kruit et al [27,30], they have used Jansen' theory and tried to represent the effect of coulomb interactions in a comprehensive way [27]. They have derived user friendly equations [27,30]. According to them [27], the absolute maximum current ever obtainable in a given probe size in chromatic aberration limited or spherical aberration limited optical system is as follow.

The chromatic-aberration-limited current I_c in a total probe of $FW_{50} = d_t$ is:

$$I_c = 5.4 \frac{d_t^4 B_r E^3}{C_c^2 \Delta E^2} \tag{5}$$

where FW50 is the beam size of diameter containing 50% of the beam current, d_t is the spot size, E is the particle energy, C_c is the total chromatic aberration coefficient of the system and ΔE is the FWHM of a Gaussian energy distribution.

The spherical-aberration-limited current I_s in a total probe of $FW_{50} = d_t$ is:

$$I_s = 2.44 \frac{d_t^{8/3} B_r E}{C_s^{2/3}} \tag{6}$$

Where C_s is the total spherical aberration coefficient of the system.

These equations (5 and 6) are valid for FIB machines as well as electron microscopes in general, if one deals with small amounts of current on the specimen. The minimum and best information from these equations (5 and 6) can be extracted is very simple and that is that we should have high reduced brightness and minimum possible energy spread to obtain a high quality charged particle beam.

If one optimizes an optical system by considering lens aberrations and coulomb interactions simultaneously [31], finally, it all comes to the reduced brightness of the source and initial energy spread of the source. For instance, in an optimized electron optical instrument (say electron microscope) the Lanthanum hexaboride (LaB_6) thermionic emitters can give high quality beam than the tungsten (W) thermionic emitters. A LaB_6 thermionic emitter has better reduced brightness than W thermionic emitter [32].

The purpose of this chapter is not to give a review or address issues of the optimization of optical columns by considering coulomb interactions in the system. Nevertheless, we tried to explain the meaning of high quality charged particle beam and importance of high reduced brightness as well as smallest intrinsic energy spread of the source. The expectations of FIB machine users or electron microscope users are always high. They always want to have a charged particle source of highest reduced brightness and smallest intrinsic energy spread to obtain high quality beam. By these expectations,

the LMIS are neither very bright (only ~ $1 \cdot 10^6$ A/m^{2}SrV) nor monochromatic (energy spread > 5eV).

1.3 Noble Gas Ion Sources for FIB Machines

Noble gas ions can be produced by bombardment of electrons, atoms or ions with noble gas atoms or molecules, or by exposing gas atoms or molecules to high electric fields or irradiation [33, 34]. Several noble gas ion sources exist [34], which can be classified according to their working principles or their designs. However, in this review article we will discuss only those noble gas ion source designs and their technical aspects that were claimed to be potential candidates for FIB applications.

1.3.1 Gas field ion sources

Sources based on the field ionization process are known as gas field ion sources (GFIS). This ionization process [13], which takes place at a high electric field ($\geq 10^{10}$ V/m), has been applied in field ion microscopy as well as in GFIS [13]. Several researchers have studied different types (geometries) of GFIS, such as needle type GFIS, capillary type GFIS, impregnated type GFIS, and needle-in-capillary type GFIS. The history of GFIS starts earlier than that of LMIS [13]. Needle type GFIS have been widely studied for focused beam applications. One of the main drawbacks in gas field ionization concerning industrial applications is that the tip surface needs to be cooled to < 77 K for effective ionization. Recently, needle-in-capillary type GFIS have been proposed by a few researchers claiming room temperature operation. We will try to evaluate each of these concepts separately to understand the overall status of GFIS for FIB applications.

1.3.1.1 Needle type GFIS

Needle type GFIS can be divided into three different categories, *viz.*. needle type GFIS with cold finger, without cold finger, and super-tip.

1.3.1.1. a *Needle type GFIS with cold finger*

After the success of field-ion microscopy [Muller in ref 13], it was realized that it is perhaps possible to develop a high-brightness noble gas ion source with smaller energy spread. In fact, such an ion source essentially requires exactly the same things as a field-ion microscopy experiment. A needle type field-ion emitter [35-42] uses a sharp (see Fig. 4) metal tip (typically, tungsten or iridium). The cold finger (temperature < 77K) is attached to the tip to lower its temperature. The noble gas is inserted into an UHV system (minimum possible background pressure < 10^{-10} mbar) with a typical pressure of 10^{-3} to 10^{-2} mbar. The noble gas, which is at room temperature, tries to accommodate at the surface of the tip. A positive voltage is applied to the ion emitter.

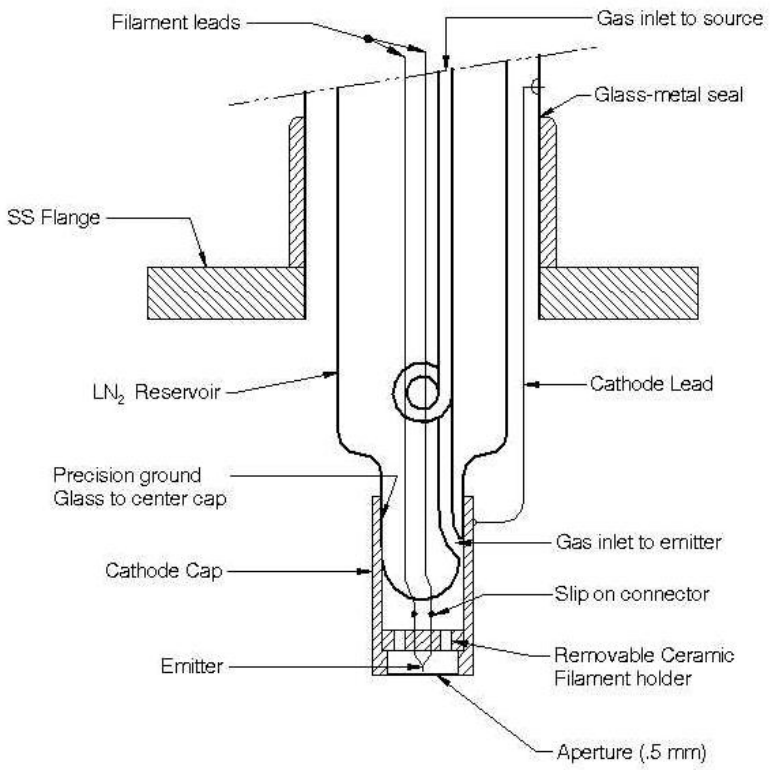

FIG. 4. Schematic of Gas Field Ion Source (conventional type with cold finger). Adapted from Ref. [37].

At high electric fields ($\geq 10^{10}$ V/m), near the vicinity of the tip, appreciable field ionization takes place. Ionization takes place due to the tunneling of electrons from the gas particles into the tip (needle). In the 1970s, Levi-Setti, Orloff and Swanson did excellent work on GFIS [35-37]. Unfortunately, GFIS are not only difficult to maintain but are also not very reliable; for example, a change in temperature or residual gas atoms (extremely small impurities in the noble gas) can cause fluctuations in the ion current. The emission characteristics and the stability of helium field-ion source at different temperatures and gas pressures have been well studied by Horiuchi et al. [40]. A study on the field-ion current variation with respect to the noble gas pressure was also reported by Sato [41]. The authors found that the ion current does not increase with an increase in pressure beyond ~10^{-2} mbar [40, 41].

1.3.1.1. b *Needle type GFIS without cold finger*

Though GFIS have their origin in classical field-ion microscopy experiments, for industrial applications it is advantageous to have an ion source that does not require a cold finger. A few attempts of developing field-ion gun at room temperature have been reported in the literature [43]. Not many researchers have tried to develop high brightness GFIS without cold finger. The main reason of that is the common knowledge from field ion microscopy experiments and that is that the cold finger improves ionization

probability or ion current and hence, the reduced brightness [43]. Nevertheless, Allan et al [43] found that iridium (Ir) field ion emitter can give better results than tungsten (W) field ion emitter.

1.3.1.1. c Needle type GFIS with supertip

For quite a few years, several researchers have tried to create ultimate high-brightness noble gas field-ion sources [44-59]. A supertip is a nanometric protrusion that can be formed on a regular tip.

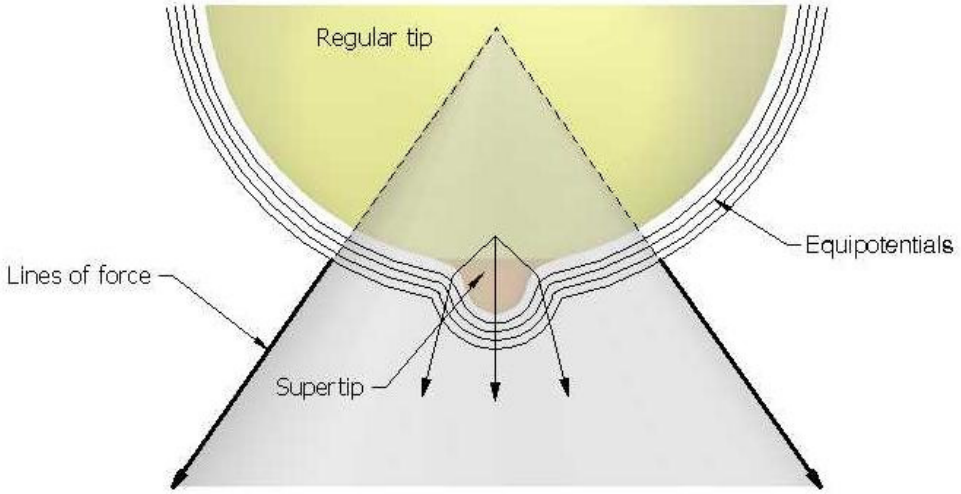

FIG. 5. Super tip and the lens effect. Adapted from Ref. [Gomer in 13].

In the 1980s, Hanson, Siegel and Schwoebel [44-47] carried out gas-field-ion experiments with supertip emitters. Obviously, the aim was to achieve more angular current density and brightness with such an emitter. A supertip-GFIS also uses a cold finger. Kalbitzer and co-workers [48-56] and other researchers [57-59] have extensively studied supertip-GFIS. According to Kalbitzer, supertip-GFIS can have a reduced brightness as high as $3 \cdot 10^{11} A/m^2 SrV$ [50]. This claim of super high reduced brightness is based upon an estimation of the virtual source size of the supertip by Kalbitzer and co-workers [52]. According to Kalbitzer, a supertip of radius ~ 1 nm formed on a regular tip can have a virtual source size of ~ 0.1 nm [50]. I believe that the procedure [52] used for the estimation of the virtual source size of the supertip should be verified again. For example, it can be checked, how different the virtual source size of a supertip (radius ~ 1 nm) formed on a regular tip (radius of a few 100 nm) can be from that of the virtual source size of a regular tip (radius ~1 nm). Already in 1961, R. Gomer [in ref 13] has discussed that a small bump (supertip) on a regular tip can give a lens effect. As shown in Fig. 5, the lines of force from such a small bump become more parallel compared to that of a regular tip. Therefore, the estimated value of the virtual source size of ~ 0.1 nm for a supertip of ~ 1-nm radius seems too optimistic.

Anyway, it should be noted that irrespective of their claim about its virtual source size estimation and reduced brightness, it is a fact that supertip-GFIS have not been employed in FIB machines because of their unreliability. The lifetime of these ion sources cannot compete with that of LMIS.

Interestingly, the supertip concept does not exist only in GFIS but also in LMIS. Purcell et al. [60,61] have worked on supertip-LMIS. It appears from their experimental results that the supertip-LMIS are not reliable (maintenance, ion-current stability, lifetime of supertip, etc.), and, therefore, conventional needle type LMIS are still widely used for FIB machines.

1.3.1.2 Capillary type and impregnated type GFIS

The capillary type GFIS has a long history [6]. In this type of GFIS, the gas is fed through a small capillary. The field ionization occurs at the gas exit (at the peripheral edge of the capillary) of the capillary itself. The Spindt field ionizer [62] can be considered in this category (see Fig. 6(a)). FIBs were proposed as one of the several applications [62]. Spindt type field-ion sources have not been studied widely for FIB applications. I believe that the next step could be, to scale down the device (say, sub-100nm) in order to reduce the virtual source size and probably, increase the field ionization current with more gas pressure in.

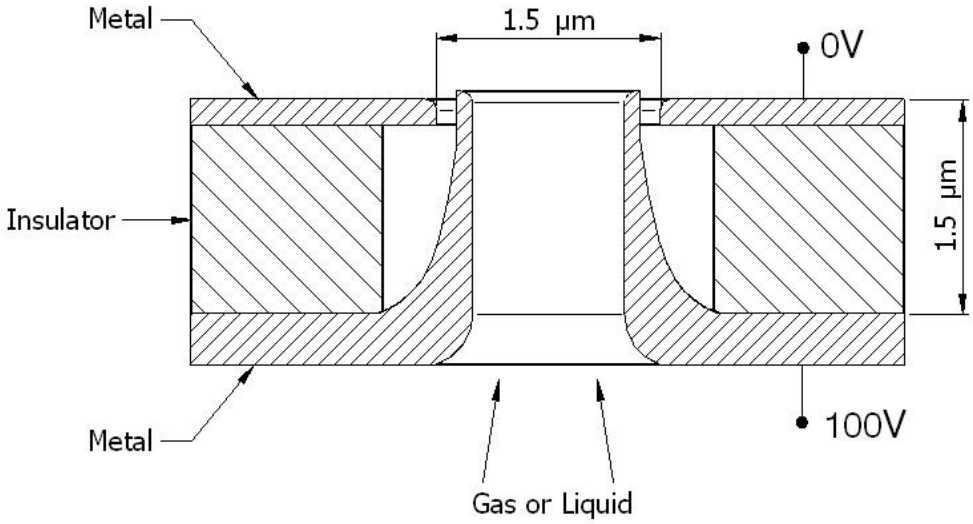

FIG. 6. (a) Spindt field ionizer. Adapted from Ref. [62]

An impregnated type GFIS (see Fig. 6(b)) was studied by Teraoka *et al.* [63] as a high-brightness GFIS. As shown in Fig. 6(b), the proposed ion source consists of a stainless steel tube with a palladium needle. Hydrogen permeates through the needle, which is maintained at a high temperature, and is released into the vacuum chamber. Although, it was an innovative method of gas delivery at the ionization region of the needle, Teraoka *et al.* [63] could see only slight amount of field ion current in their first experiment. As stated in the reference [63], the further improvements in the ion sources

were needed. We believe that the impregnated type GFIS have not been studied widely for FIB applications.

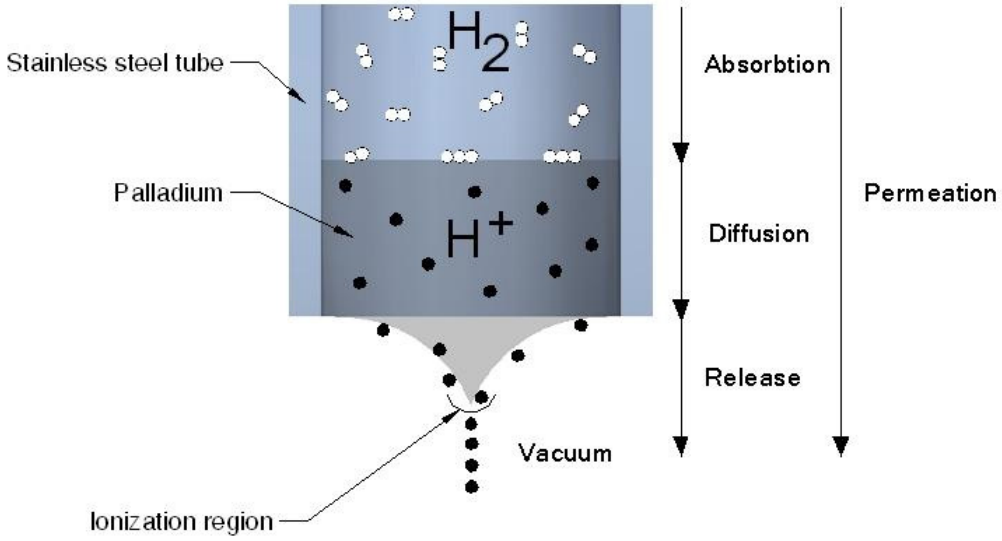

FIG. 6. (b) Impregnated type gas field ion sources. Adapted from Ref. [63].

1.3.1.3 Needle-in-capillary type GFIS

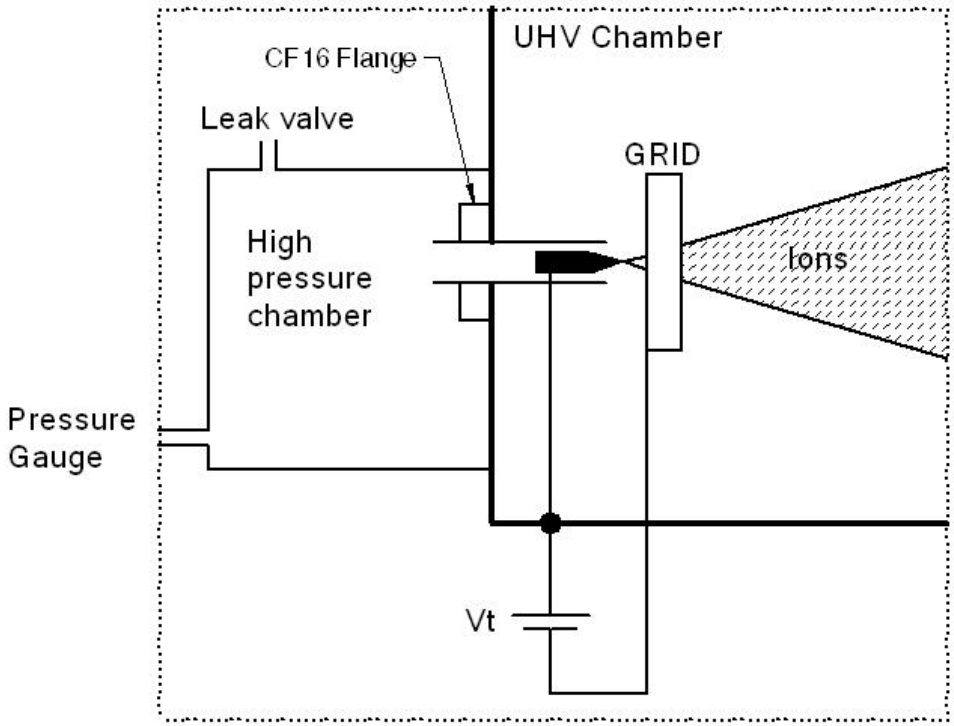

FIG. 7. Needle-in-capillary type gas field ion source. Adapted from Ref. [65].

Needle-in-capillary type GFIS [64] were designed for achieving a collimated gas jet towards the emitter tip. A high local pressure can be maintained in the vicinity of the tip. Konishi et al. [64] have operated their gas ion source with gas pressures up to 10^{-1} Pa. Recently, Salancon et al. [65] have used the same geometry (see Fig. 7) but used higher pressures, up to 10 Torr. The authors [65] also state the real need for a high-brightness noble gas ion source with room temperature operation for FIB applications. Their [65] first experimental results look quite encouraging. Energy-spread and brightness measurements have been proposed [65] and, of course, these should be the real test of their GFIS. It seems that this work [65] is the very recent development in GFIS research.

1.3.2 Plasma gas ion sources

The basic philosophy of plasma sources [66-87] proposed for FIB machines is to create plasma and extract ions through a small aperture (Fig. 8(a)). The smaller the extraction aperture is, the smaller the virtual source size. A plasma ion source can be used to generate positive-ion beams of the noble gases He, Ne, Ar, Kr, and Xe. Several types of gas ion species can be produced. An Ar beam can be useful for milling, whereas an O beam can be used for SIMS (Secondary Ion Mass Spectroscopy) and for ion implantation. The ion beam can be positive or negative, dependent on the polarity of the extraction electrodes. Actually, plasma ion sources are well known as broad beam ion sources and have a wide range of industrial applications, but are not often used for focused beams. There are vast number of plasma ion sources [34]. To review all those types of plasma ion sources given in reference [34] and compare them for their properties is out of scope of this article. Focused ion beams, as explained previously, require high-brightness, low-energy-spread ion sources. Obviously, field ionization sources have been widely studied for FIB applications and clearly, this chapter takes an extensive review of all the types of gas field ion source concepts.

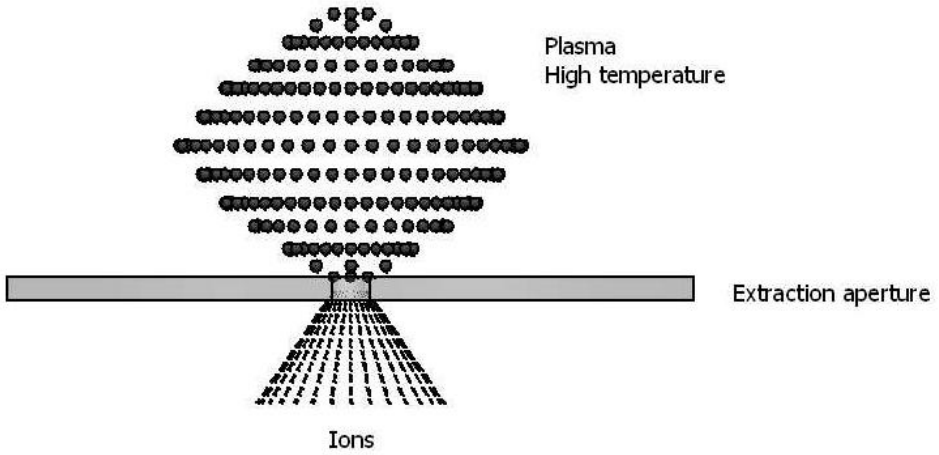

FIG. 8. (a) Plasma ion extraction process.

One of the main reasons that several researchers are working on plasma ion sources that could be used for focused beam applications is that the plasma ion sources

can be far more robust and reliable than GFIS, and particularly than supertips. The two types of plasma ion sources known as the Penning type [66-75] and the multicusp type [76-87] have been widely studied for focused beam applications. We will discuss these plasma ion sources and compare them with the LMIS. Figures 8(b) and 8(c) show both of these types of sources schematically.

1.3.2.1 Penning type plasma ion sources

Penning plasma ion sources are named after F.M. Penning, who invented the Philips ionization vacuum gauge [34]. The performance of a Penning type surface plasma source (see Fig. 8(b)) depends upon many parameters, such as the gas pressure, the magnetic field, the depth of the cell (*L*), the spacing between the anode A and cathode K, and the dimensions of the emission aperture [67]. Guharay et al. have operated penning plasma ion source in pulsed mode and have obtained negative ion beams with a reduced brightness of 10^5 A/m^{2}SrV with an energy spread of ~3 eV. This brightness is about three to four orders of magnitude higher than typical values for dc beams from duoplasmatron sources [66]. The typical pulse length in pulse-mode operation can be up to 1 ms with a repetition rate up to 12 Hz. According to Guharay et al. [66], the ion beams extracted from noiseless discharges can have a better quality. According to Guharay et al [70], the ion beam from their penning ion source follows Knauer model for energy broadening.

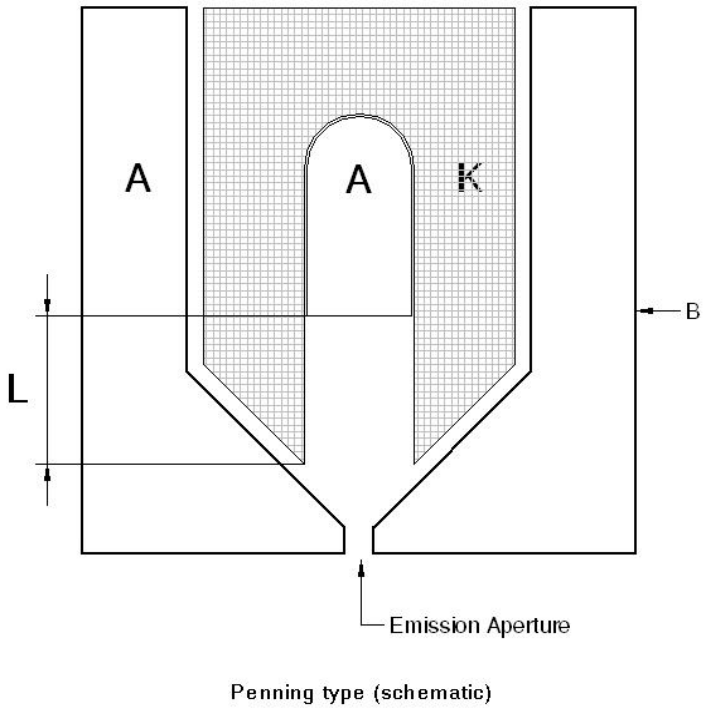

FIG. 8. (b) Penning type surface plasma ion source. Adapted from Ref. [67].

We have already stated that the Knauer model is valid for collisionless, high-brightness beams. This value (10^5) of the reduced brightness is just an order of magnitude smaller than that of LMIS, although in a pulsed mode. We also believe that it could be possible to operate Penning type plasma ion source in continuous mode for a long period of time, as in the year 1990, Bashkeev and Dudnikov demonstrated a continuously operated negative ion surface plasma source [72]. Bashkeev and Dudnikov showed that their ion source's life was longer than 100 hours [72]. They produced negative ion (H-,O-, OH-,NH-) beams [72]. Some further modification in the Bashkeev-Dudnikov surface plasma source are reported elsewhere [73]. To compare merits and demerits of the design geometries of penning ion sources from the different groups, for example, Penning ion source at Heidelberg [74] and the one at Rutherford Appleton Laboratory [75] is out of the scope of this article. To the best of our knowledge, the latest value of high brightness of this type of source is given by Guharay et al [66]. In brief, the penning type plasma ion source can produce several gas ion species and with the latest achieved value of high reduced brightness, the future of this type of plasma ion source looks promising.

1.3.2.2 Multicusp type plasma ion sources

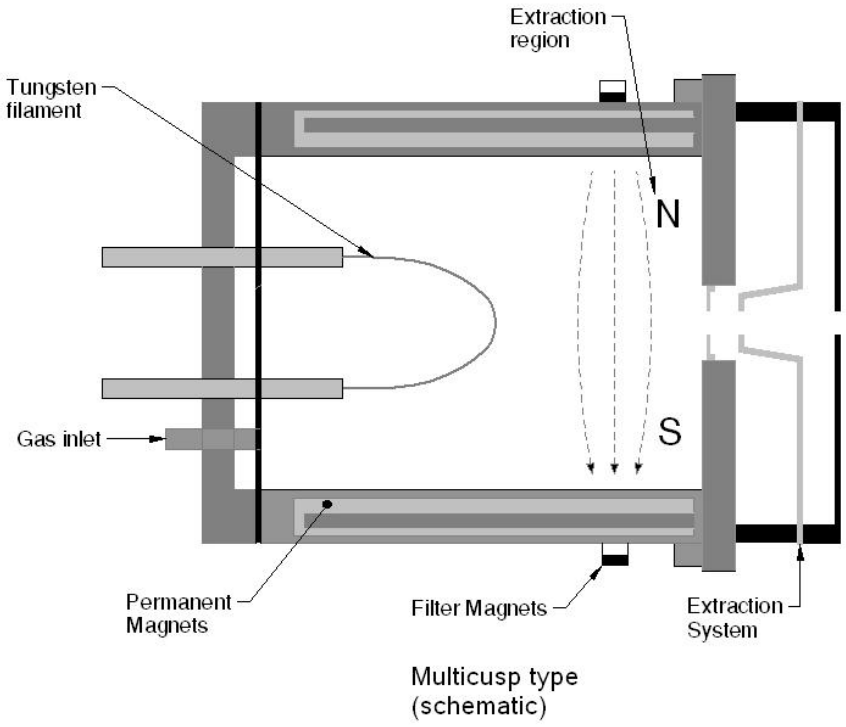

FIG. 8. (c) Multicusp type plasma ion source. Adapted from Ref. [80].

A multicusp ion source generates plasma by dc discharge or rf induction discharge [76-87]. The ion source uses permanent magnets around the cylindrical wall as well as on the opposite side of the extraction aperture (see Fig. 8(c)). The multicusp ion source is named this way because of the arrangement of the magnets that form magnetic

cusp fields to contain the plasma. A permanent magnetic filter is placed before the extraction electrodes. The magnetic filter improves the axial energy spread of the gas ions generated in the multicusp source.

In multicusp plasma ion sources, the ion current density J_i at the exit aperture is expressed by the following equation [80]:

$$J_i :: \sigma_i \, n_0 \, e \, (kT_e / m_i)^{1/2} \qquad (7)$$

Where σ_i is the ionization cross section, n_0 is the neutral gas density, k Boltzmann constant, T_e is the plasma electron temperature and m_i is the ion mass.

The maximum brightness ever reported for a multicusp rf plasma ion source is $1.5 \cdot 10^3$ A/m^{2}SrV and, according to Ji et al. [76], could be improved further if the rf power and source design is improved. The energy spread of a multicusp ion source can be maintained well within 1-3 eV because of the energy filters used in the ion source. Record low axial ion energy spread of 0.7 eV was reported by Lee et al. [83]. There are continuous efforts to achieve a high brightness as well as the lowest possible energy spread. Multicusp plasma sources can be operated in continuous mode as well as pulsed mode. In pulsed-mode operation, the current density can be higher, and therefore, this mode could be worth investigating, according to Scott et al. [77]. Apart from efforts to improve the ion source brightness, efforts to improve ion source lifetime can also be found in the literature. The life time of these multicusp plasma ion sources depends on the RF antennas or filament cathodes used for discharge. Normally, rf antennas have a longer life time than filament cathodes, which is 100-500 hr, depending upon antenna material and antenna arrangement [79].

There could be several other groups working on multicusp ion source apart from the group at Lawrence Berkeley National Laboratory (LBNL). However, to the best of our knowledge, the latest value of high brightness of this type of source is given by Ji et al of the LBNL group [76]. They have already shown that using their ion source they can make 50nm wide line spaces [82].

1.3.3 Other types of gas ion sources

It is clear from the above discussion that most of the ion source concepts studied by researchers for FIB applications are based on gas field ionization or ion extraction from gas plasma. It is also worthwhile to look at other types of gas ion sources, based on different working principles but designed for FIB applications.

1.3.3.1 Novel concept of a laser ion source

The conventional laser ion sources, in which lasers are used to create plasma, are well known [34]. Recently, Freinkman and co-workers [88] have proposed a novel ion source for focused ion beams. As shown in Fig. 9, a laser can be used to form a focused atomic beam, and subsequently that laser-collimated atomic beam can be ionized using another laser. According to Freinkman et al. [88], such an ion source can be used to generate gas ions as well as metal ions with an initial ion energy spread < 0.1 eV. This proposal is very recent and experiments are still awaited.

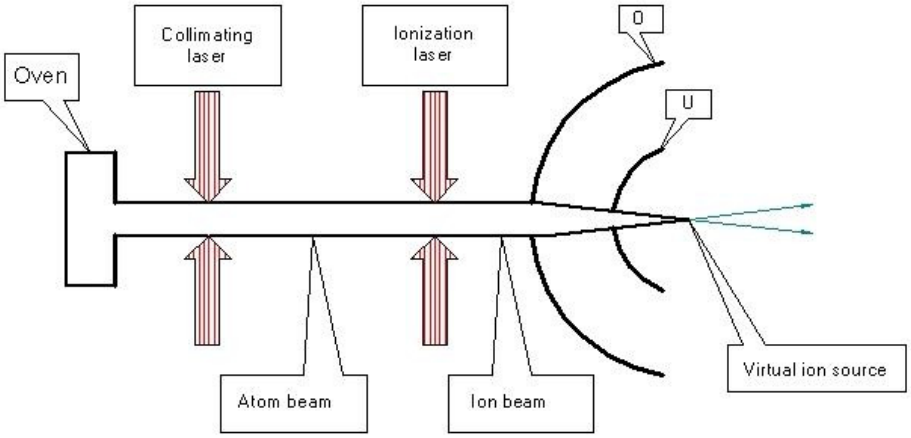

FIG. 9. Proposed novel laser ion source. Adapted from Ref. [88].

1.3.3.2 Electron-impact gas ion source (non-plasma mode)

In an electron-impact ion source, an electron beam is used to ionize the gas atoms or molecules by inelastic collisions [33]. Electron-impact ionization takes place at room temperature, and therefore, a non-plasma type electron-impact gas ion source is considered to be different from the plasma ion sources discussed above.

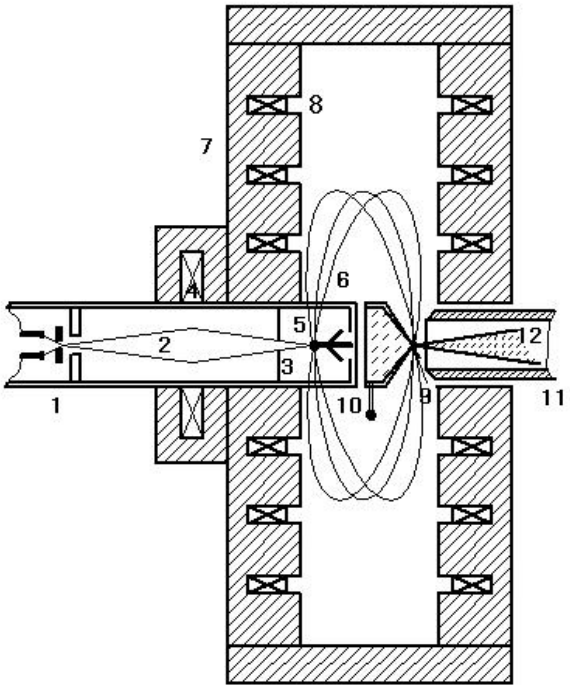

FIG. 10. Electron impact gas ion source operated in non plasma mode. (Conventional electron gun[1] gives a electron beam[2] that can be focused through an aperture[3] by a conventional magnetic lens[4] onto a tungsten sphere[5]. The thermionic electrons[6] emitted from the sphere are accelerated and focused by a magnetic mirror, consisting of an iron circuit[7] and coils[8] into the gas[9] streaming from the chamber[10]. Electrodes[11] accelerates the ions[12].). Adapted from Ref. [89].

In 1985, Barth and co-workers [89] suggested that if the ionization region is at micron scale, then the ion source brightness can be much larger than the conventional sources (see Fig. 10). They designed an electron gun-magnetic mirror system to deliver sufficient electron current to the ionization region. Their first ion source experiment with less than ideal experimental conditions showed a reduced brightness of 10^2 A/m^{2}SrV. According to Barth et al. [89], the reduced brightness of their gas ion source could be at least 10^4 A/m^{2}SrV, if more electron current was delivered to the gas ionization chamber. However, no further study has been reported by the authors [89] or other researchers.

1.3.3.3 Electron beam ion sources and traps

It could be worthwhile to briefly mention the ongoing efforts [90, 91] on electron beam ion sources and traps (EBIS/EBIT) at Lawrence Livermore National Laboratory (LLNL). According to Marrs [90], self-cooled ions can be obtained from EBIS/EBIT and the strong-self cooling effect observed by them might enable the development of the first high brightness source. The source would have applications in microanalysis and nanotechnology [90]. As we have already seen in equation 2, the term 'temperature', to reduce that temperature is one of the key for achieving high brightness. Indirectly, these efforts at LLNL also explains that, the conventional plasma ion sources are not good at producing high brightness beams because of the high temperature.

1.4 The Status of Gas Ion Source Research

Field ionization is an intrinsically wonderful way to produce high brightness ion beams. Unfortunately, GFIS are not reliable for FIB applications. However it does not mean that the new innovative developments will not occur in field ion sources or it does not mean that field ion sources are out dated and every one should work with conventional plasma ion sources.

Penning type of plasma ion source [66] has obtained high brightness (10^5A/m^{2}SrV), in pulsed mode. Using helium ions from a multicusp ion source, researchers [82] have made about 50 nm wide line spaces. We should also mention that NanoSIMS developed by Cameca [92, 93] has achieved a focused beam spot size of < 50nm. It shows that one can not say that if there is no noble gas ion source as bright as LMIS then, nothing can be done. However, one can also say that 50nm is not enough. The best image resolution obtained in FIB machines with Ga-LMIS can be <10nm. One can also argue that the quality of beam is determined by spot size as well as current density in it. In brief, the FIB user will always compare the properties of a gas ion source with those of LMIS.

We also appreciate the other efforts to fabricate noble gas ion sources in which, one does not want to follow the way of field ionization sources or conventional plasma ion sources.

As we saw in the section 1.3, some of the gas ion sources were studied widely and some not. There are a few review articles on the high-brightness gas ion sources [94-97]. However, we believe that we have reported most of the gas ion sources studied for FIB applications in this review article. We have considered their latest values of reduced brightness and energy spread and have commented on the present status and possible future of those ion sources from our own perspective. Clearly, none of the gas ion sources are as bright as (or as encouraging as) LMIS, and therefore, probably in the future new gas ion source concepts or improvements in the existing concepts will be seen in the literature. Table 2 compares the crucial properties of the most widely studied gas ion sources with respect to LMIS.

Table 2. Properties of gas ion sources as compared to LMIS

Ion sources	**Reduced Brightness (A/m^2SrV)**	**Energy Spread (eV)**	**References**
LMIS	$\sim 1 \cdot 10^6$	~ 5-10	[1]
GFIS-supertip	$\sim 3 \cdot 10^{11}$ *	~ 1	[50]
Multicusp	$\sim 1.5 \cdot 10^3$ **	~ 0.7	[76] and [83]
Penning	$\sim 10^5$ ***	~ 3	[66]

* The author remains skeptical about this super high value of reduced brightness (See Section 1.3.1.1. c). In any case, these gas ion sources are brighter than plasma gas ion sources.
** Operated in continuous mode.
*** Operated in pulsed mode.

1.5 Conclusions

Any noble gas ion source with at least similar properties (brightness, energy spread, current stability, and life time) as LMIS is extremely desirable, and there have been several efforts by various researchers to develop such noble gas ion sources. GFIS and plasma ion sources have been widely studied. There are several types of GFIS. However, can we obtain a working GFIS as reliable as LMIS? That still remains an open question. Plasma ion sources are more robust, easy to maintain, and more reliable than any GFIS (particularly, GFIS-supertip). They can also produce several gas species. Despite of several efforts plasma ion sources are not as bright as LMIS for FIB applications. To date, we know no plasma ion source that can have a reduced brightness as good as LMIS ~ $1 \cdot 10^6 A/m^2SrV$. The main reason that plasma ion sources cannot produce high-brightness ion beams is the high temperature, which is an inherent problem in plasma sources.

Therefore, it seems there is enough scope to work on high-brightness noble gas ion sources that have different types of geometry or even different working principles.

Acknowledgements

The author gratefully acknowledges prof. dr. ir. P. Kruit for useful discussions. Many thanks to P.J. Vetter for his help in reproducing figures. The author also thanks Dr. J. E. Barth and A.E. van Diepen for reading this manuscript. This work was part of the research program of the "Stichting voor Fundamenteel Onderzoek der Materie" (FOM), which is supported by the "Nederlandse Organisatie voor Wetenschappelijk Onderzoek"(NWO).

Note: -

Recently, while writing this chapter 1, we found a publication that can be considered in the section **1.3.3.1**.

B. J. Claessens, S.B. van der Geer, G. Taban, E. J. D. Vredenbregt and O.J. Luiten, Phy. Rev. Lett. **95**, 164801, (2005).

References

[1] As a review see:

L.A. Giannuzzi and F.A. Stevie, *Introduction to Focused Ion Beams: Instrumentation, Theory, Techniques and Practice* (Springer, New York, 2005).

J. Orloff, M. Utlaut, L. Swanson, *High Resolution Focused Ion Beams* (FIB and Its applications) (Kluwer Academic/Plenum Publishers, New York 2003).

M. Utlaut, in *Handbook of Charged Particle Optics*, Chapter 11, edited by J. Orloff (CRC Press, New York, 1997).

R.A.D. Mackenzie and G.D.W Smith. Nanotechnology **1**, 163 (1990).

J Melngailis. J. Vac. Sci. Technol. B **5(2)**, 469 (1987).

U.S. Tandon, Vacuum **43(3)**, 241 (1992).

J. Gierak, D. Mailly, P. Hawkes, R. Jede, L. Bruchhaus, L. Bardotti, B. Prevel, P. Melinon, A. Perez, R. Hyndman, J. P. Jamet, J. Ferre, A. Mougin, C. Chappert, V. Mathet, P. Warin, and J. Chapman, Appl.Phys.A **80**, 187 (2005).

http://dsa.dimes.tudelft.nl/usage/technology/FIB/index.html

[2] S. Khizroev and D. Litvinov, Nanotechnology **15**, R7 (2004).

[3] Z. Cui, P. D. Prewett, and J. G.Watson, J. Vac. Sci. Technol. B **14(6)**, 3942 (1996).

[4] P. D. Prewett, A. W. Eastwood, G. S. Turner, and J. G.Watson, Microelectron. Eng. **21**, 191 (1993).

[5] G. L. R. Mair, in *Handbook of Charged Particle Optics*, Chapter 3, edited by J. Orloff (CRC Press, New York, 1997).

[6] G. D. Alton, in *Experimental Methods in the Physical Sciences (Atomic, Molecular and Optical Physics: Charged Particles)*, Vol 29A, Chapter 3, edited by F.B. Dunning and R. G. Hulet (Academic Press, London, 1995).

[7] L.W. Swanson, Appl. Surf. Sci., **76/77** , 80 (1994).

[8] J.J. van Es, J. Gierak, R.G. Forbes, V.G. Suvorov, T. van den Berghe, Ph. Dubuisson, I. Monnet, and A.Septier, Microelectron. Eng. **73-74**, 132 (2004).

[9] L. Bischoff, Ultramicroscopy **103**, 59 (2005).

[10] V. E. Krohn and G. R. Ringo, Appl. Phys. Lett. **27(9)**, 479 (1975).

[11] P. D. Prewett and G. L. R. Mair, *Focused Ion Beams from Liquid Metal Ion Sources* (Research Studies Press, Taunton, U.K., 1991).

[12] R. G. Forbes, Vacuum **48(1)**, 85 (1997).

[13] As a review see:

J. Orloff, in, *Handbook of Surface Imaging Visualization*, Chapter 13, edited by Arthur T. Hubbard (CRC Press, Boca Raton, 1995).

E. W. Müller and T. T. Tsong, *Field-Ion Microscopy, Field Ionization and Field evaporation* (Pergamon Press, Oxford, 1973).

K. M. Bowkett and D. A. Smith, *Field-Ion Microscopy* (North-Holland Publishing Company, Amsterdam, 1970).

E. W. Müller and T. T. Tsong, *Field Ion Microscopy; Principles and Applications* (Elsevier, Amsterdam, 1969).

R. Gomer, *Field Emission and Field Ionization* (Cambridge: Harvard University Press, 1961).

[14] P.W.H. de Jager and L.J. Vijgen, Microelectron. Eng. **23**, 107 (1994).

[15] Y. Zou, Y. Cui, V. Yun, A. Valfells, R.A. Kishek, S. Bernal, I. Haber, M.Reiser, P.G. O'Shea and J.G. Wang, Physical Review Special Topics-Accelerators and Beams, **5**, 072801 (2002).

[16] A.V. Crewe, in, *Handbook of Charged Particle Optics*, Chapter 10, edited by J. Orloff (CRC Press, New York, 1997).

[17] P.W. Hawkes and E. Kasper, *Principles of Electron Optics*, Vol.1, 2, 3 (Academic Press, London, 1994).

[18] H.N. Slingerland, *A Fast Ion Beam Pattern Generator*, Wibro, Helmond, 1988.

[19] L. Didenko, S.K. Guharay, J. Orloff and J. Melngailis, Nucl. Instrum. Methods Phys. Res. A **427**, 121 (1999).

[20] S. Hirohata, T. Kosugi, H.Sawaragi, R. Aihara and K. Gamo, J.Vac. Sci. Technol B **10(6)**, 2814 (1992).

[21] G.H. Jansen, Nucl. Instrum. Methods Phys. Res. A **298**, 496 (1990).

[22] H. Boersh, Z. Phys. **139**, 115 (1954).

[23]G L R Mair, J. Phys.D:Appl.Phys. **29**, 2186 (1996).

[24] W.Knauer, Optik, **59(4)**, 335(1981).

[25] B. Zimmermann, Adv. Electron.Electron. Phys. **29**, 257 (1979).

[26] L.W. Swanson, Nucl. Instrum. Methods Phys. Res. **218**, 347 (1983).

[27] P. Kruit, L.J.Vijgen and J. Xinrong, Nucl. Instrum. Methods in Phys. Res. A **363**, 220 (1995).

[28] X.R. Jiang and P.Kruit, Microelectron. Eng. **30**, 249(1996).

[29] G.H. Jansen, Coulomb Interactions in Particle Beams, Advances in Electronics and Electron Physics, suppl.21 (Academic Press, London,1991).

[30] P. Kruit and G. H. Jansen, in *Handbook of Charged Particle Optics*, Chapter 7, edited by J. Orloff (CRC Press, New York, 1997).

[31] X.R. Jiang, J.E. Barth and P.Kruit,J.Vac. Sci. Technol. B **14(6)**, 3747 (1996).

[32] M.T. Postek, in, *Handbbok of Charged Particle Optics*, Chapter 9, edited by, J. Orloff (CRC Press, New York, 1997).

[33] L. Valyi, *Atom and Ion Sources* (Wiley and Sons, London and Budapest, 1977).

[34] See for example, *Handbook of Ion Sources*, edited by B. Wolf (CRC Press, Boca Raton, 1995).

[35] R. Levi-Setti, Proceedings of Seventh Annual SEM Symposium (IITRI, Chicago, 1974), p. 125;

[36] J. H. Orloff and L. W. Swanson, J. Vac. Sci. Technol. **12(6)**,1209 (1975).

[37] J. H. Orloff and L. W. Swanson, J.Appl. Phys. **50(9)**, 6026 (1979).

[38] S. Sato, T. Kato, and N. Igata. Proc.11th Symp. on ISIAT 87, Tokyo ,1987, p.91

[39] T. Itakura, K. Horiuchi, and H. Ishikawa, Proc.11th Symp. on ISIAT 87, Tokyo ,1987, p.211

[40] K. Horiuchi, T. Itakura, and H. Ishikawa, J. Vac. Sci. Technol. B **6(3)**, 937 (1988).

[41] M. Sato, Jpn. J.Appl. Phys. Vol **31**, Part 2(3A), L291 (1992).

[42] T. Sakata, K. Kumagai, M. Naitou, I. Watanabe, Y.Ohhashi, O. Hosoda, Y. Kokubo, and K. Tanaka, J. Vac. Sci. Technol. B **10(6)**, 2842 (1992).

[43] G. L. Allan, G. J. F. Legge, and J. Zhu, Nucl. Instrum. Methods Phys. Res. B **34**, 122 (1988).

[44] G. R. Hanson and B.M. Siegel, J. Vac. Sci. Technol. **16(6)**, 1875 (1979).

[45] G. R. Hanson and B.M. Siegel, J. Vac. Sci. Technol. **19(4)**, 1176 (1981).

[46] P. Schwoebel and G. Hanson, J. Appl. Phys **56(7)**, 2101 (1984).

[47] P. R. Schwoebel and G. R. Hanson, J. Vac. Sci. Technol. B **3(1)**, 214 (1985).

[48] S. Kalbitzer, Appl. Phys. A **79**, 1901 (2004).

[49] S. Kalbitzer and A. Knoblauch, Appl. Phys. A **78**, 269 (2004).

[50] S. Kalbitzer, Nucl. Instrum. Methods Phys. Res. B **158**, 53 (1999).

[51] S. Kalbitzer and A. Knoblauch, Rev. Sci. Instrum. **69(2)**, 1026 (1998).

[52] Th. Miller, A. Knoblauch, and S. Kalbitzer, Mater. Sci. Forum **248-249**, 433 (1997).

[53] Ch. Wilbertz, Th. Maisch, D. Huttner, K. Bohringer, K. Jousten, and S. Kalbitzer, Nucl. Instrum. Methods Phys. Res. B **63**, 120 (1992).

[54] R. Borret, K. Bohringer, and S Kalbitzer, J. Phys. D : Appl. Phys. **23**, 1271 (1990).

[55] K. Jousten, K. Bohringer, R. Borret, and S. Kalbitzer, Ultramicroscopy **26**, 301 (1988).

[56] R. Borret, K. Jousten, K. Bohringer, and S. Kalbitzer, J. Phys. D: Appl. Phys. **21**, 1835 (1988).

[57] M. K. Miller and S. J. Sijbrandij, Ultramicroscopy **79**, 225 (1999).

[58] K. Edinger, V. Yun, J. Melngailis, J. Orloff, and G. Magera, J. Vac. Sci. Technol. B **15(6)**, 2365 (1997).

[59] A. E. Bell, K. Jousten, and L. W. Swanson, Rev.Sci. Instrum. **61(1)**, 363 (1990).

[60] S. T. Purcell, V. T. Binh, and P. Thevenard, Nanotechnology **12**, 168 (2001).

[61] S. T. Purcell and V. T. Binh, J. Vac. Sci. Technol. B **19(1)**, 79 (2001).

[62] C. A. Spindt, Surf. Sci. **266**, 145 (1992); http://ssl.mit.edu/publications/theses/SM-2001-AndringaJason.pdf

[63] T. Teraoka, H. Nakane, and H. Adachi, Jpn. J.Appl. Phys. Vol. **33**, Part 2(8A), L1110 (1994).

[64] M. Konishi, M. Takizawa, and T. Tsumori, J. Vac. Sci. Technol. B **6(1)**, 498 (1988).

[65] E. Salançon, Z. Hammadi, and R. Morin, Ultramicroscopy **95**, 183 (2003).

[66] S. K. Guharay, S. Douglass, and J. Orloff, Appl. Surf. Sci. **231-232**, 926 (2004).

[67] S. K. Guharay, E. Sokolovsky, and J. Orloff, J. Vac, Sci. Technol. B **17(6)**, 2779 (1999).

[68] S. K. Guharay, E. Sokolovsky, and J. Orloff, J.Vac. Sci.Technol. B **16(6)**, 3370 (1998).

[69] S. K. Guharay and M. Reiser, IEEE, 1998, p. 2681

[70] S. K. Guharay, E. A. Sokolovsky, M. Reiser, J. Orloff, and J. Melngailis, Microelectron. Eng. **35**, 435 (1997).

[71] S. K. Guharay, W. Wang, V. G. Dudnikov, M. Reiser, J. Orloff, and J. Melngailis, J. Vac, Sci. Technol. B **14(6)**, 3907 (1996).

[72] A.A. Bashkeev and V.G. Dudnikov, AIP conference proceedings, **210(1)**, 329(1990).

[73] V. Dudnikov, C.W. Schmidt, R.Hren and J. Wendt, Rev. Sci. Instrum.**73(2)**, 989 (2002).

[74] S.Scheloske, W.Durr, M. Maetz, R. Pfahler, R. Repnow, H. Schiebler and K. Traxel, Nucl. Instrum. Methods Phys. Res. B **161-163**, 302 (2000).

[75] J.W.G. Thomason, R.Sidlow and M.O. Whitehead, Rev. Sci. Instrum. **73(2)**, 896 (2002).

[76] Q. Ji, X. Jiang, T. J. King, K. N. Leung, K. Standiford, and S. B. Wilde, J. Vac, Sci. Technol. B **20(6)**, 2717 (2002).

[77] K. L. Scott, T. J. King, K. N. Leung, and R. F. Pease, J. Vac. Sci. Technol. B **19(6)**, 2602 (2001).

[78] L. Scipioni, D. Stewart, D. Ferranti, and A. Saxonis, J. Vac, Sci. Technol. B **18(6)**, 3194 (2000).

[79] K. N. Leung, Rev. Sci. Instrum **71(2)**, 1064 (2000).

[80] Y. Lee, Q. Ji, K. N. Leung, and N. Zahir, Rev. Sci. Instrum. **71(2)**, 722 (2000).

[81] K. N. Leung, J. Vac. Sci. Technol B **17(6)**, 2776 (1999).

[82] Y. Lee, K. N. Leung, M. D. Williams, W. H. Bruenger, W. Fallmann, H. Loschner, and G. Stengl, Proceedings of the 1999 Particle Accelerator Conference, NewYork, IEEE, 1999, p.2575

[83] Y. Lee, R. A. Gough, K. N. Leung, J. Vujic, M. D. Williams, N. Zahir, W. Fallman, M. Tockler, and W. Bruenger, J. Vac. Sci. Technol. B **16(6)**, 3367 (1998).

[84] Y. Lee, R. A. Gough, W. B. Kunkel, K. N. Leung, J. Vujic, M. D. Williams, D. Wutte, and F.L. Yang, Microelectron. Eng. **41/42**, 241 (1998).

[85] Y. Lee, R. A. Gough, W. B. Kunkel, K. N. Leung, L. T. Perkins, D. S. Pickard, L. Sun, J. Vujic, M. D. Williams, D. Wutte, A. A. Mondelli, and G. Stengl, Nucl. Instrum. Methods Phys. Res. A **385**, 204 (1997).

[86] Y. Lee, L. T. Perkins, R. A. Gough, M. Hoffmann, W. B. Kunkel, K. N. Leung, M. Sarstedt, J. Vujic, M. Weber, and M. D. Williams, Nucl. Instrum. Methods Phys. Res. A **374**, 1 (1996).

[87] K. N. Leung, P. Herz, W. B. Kunkel, Y. Lee, L. Perkins, D. Pickard, M. Sarstedt, M. Weber, and M. D. Williams, J. Vac. Sci. Technol. B **13(6)**, 2600 (1995).

[88] B. G. Freinkman, A. V. Eletskii, and S. I. Zaitsev, Microelectron. Eng. **73-74**, 139 (2004).

[89] J. E. Barth, C. B. de Gruyter, E. Koets, P. Kruit, P. E. van der Leeden, J. B. Le Poole, and K. D. van der Mast, Microelectron. Eng. **3**, 147 (1985).

[90] R. E. Marrs, Nucl. Instrum. Methods Phys. Res. B **149**, 182 (1999).

[91] J.W.McDonald, R.W. Bauer and D.H.G. Schneider, Rev. Sci Instrum. **73(1)**, 30 (2002).

[92] F.J. Stadermann, Goldschmidt Conference Abstracts 2002 published in, Geochimica et Cosmochimica Acta , **66(15A)**, A734(2002).

[93] http://www.cameca.fr/html/application_note.html

[94] J. Melngailis, Proceedings of 2001 Particle Accelerator Conference, Chicago, IEEE, 2001, p. 76

[95] V.G. Dudnikov, Rev. Sci. Instrum **67(3)**, 915 (1996).

[96] R. Muhle, Rev. Sci. Instrum.**63(5)**, 3040 (1992).

[97] R.F.Welton, Proceedings of LINAC 2002, Gyeongju, Korea.

Chapter 2

*Thermal field electron impact noble gas ion source**

V. N. Tondare and P. Kruit

Abstract

From Chapter 1, it has become clear that even after a few decades of attempts by several researchers to fabricate a noble gas ion source for FIB applications, which meets minimum standards as LMIS, has not been yet realized. This is mainly because while designing those ion sources researchers did not consider all the requirements of an ion source for FIB applications simultaneously.

In this Chapter 2, we have proposed a novel ion source concept 'thermal field electron impact noble gas ion source' for FIB applications, by considering (i) high brightness (ii) low energy spread (iii) ion emission stability (iv) ion source lifetime (v) minimum ion current from the source and (vi) room temperature operation etc. simultaneously.

The electron impact ionization chamber in this concept consists of two closely spaced (~100nm) parallel conducting plates each with a small aperture (~100nm) on the axis. The plates are electrically isolated from each other. The space between the two plates is filled with noble gas in the molecular flow regime. At such a small device scale (of the double-aperture gas ionization chamber), a relatively high pressure of gas in the molecular flow regime can be maintained in the ionization region, while the gas particle density along the optical axis, outside the chamber can be kept extremely small. Electrons from a thermal field electron gun (Schottky electron gun) enter through one of the apertures and ionize the gas in non-plasma mode, which means at room temperature (~ 293 K). The ions can be extracted through the second aperture under influence of the electric field.

We have estimated the ion source performance. The thermal field electron impact gas ion source can have a high-reduced brightness ($\geq 10^6$ A/m^{2}srV) with minimum 1 nA ion current at the source and a low energy spread (< 1 eV). The reliability and lifetime of this ion source is also discussed in comparison with LMIS.

***** P. Kruit and V.N. Tondare, European Patent (applied on 22-02-06), "Particle-optical apparatus equipped with a gas ion source", Application No.: 06110257.0-

2.1 Introduction

Focused ion beam (FIB) machines have tremendous applications in material sciences, in the semiconductor industry, and for nanotechnology in general [1-5]. One of the main drawbacks of current commercial FIB machines is that contamination is inevitable [6]. This is because the only ion source that meets the requirements for beam brightness and reliability is a liquid metal ion source (LMIS), in which typically gallium is used [6]. Implanted Ga metal ions not only change the electric properties but can also change the magnetic properties of the device under fabrication or inspection in a FIB machine [6]. Gallium staining due to deposition of gallium ions in the quartz substrate during FIB repair of a photo-mask is another important issue [6].

Therefore, in FIB machines, noble gas ion sources are favorable [6]. However, the noble gas ion source to be used for FIB applications should have at least similar properties (reduced brightness [6] ~ $1 \cdot 10^6$ A/m^2SrV, energy spread ~ 5-10 eV, ion emission current stability ~ ± 2% on a minute scale and lifetime ~ > 2000 h with ion current ~2 μA) as LMIS for better performance of a FIB machine [6]. Actually, the energy spread ~ 5-10 eV of a Ga LMIS is too high, which is a disadvantage [6]. Ion sources with small intrinsic energy spread (< 1 eV) to maintain minimum chromatic aberration in the FIB machine are desirable [6]. The lifetime of the Ga LMIS and its emission current at the source are satisfactory. The emission current of a noble gas ion source to be used for FIB applications should be at least 1 nA with lifetime of ~ 2000 h, comparable to LMIS [6]. Besides the demands on brightness of the ion source, there is also the need of ion emission current stability, because unstable emission at the source results in modulation of the dose with which the specimen is illuminated. An ion emission current stability of ~ ± 2% on a minute scale is acceptable or at least should be aimed at while fabricating a noble gas ion source. The reduced brightness of ~ $1 \cdot 10^6$ A/m^2SrV of a Ga LMIS is not very high, but at least this value should be aimed at when fabricating a noble gas ion source. The importance of high-reduced brightness and low initial ion energy spread for achieving a high quality ion beam (smallest spot on specimen with high current in it) can be found elsewhere [6].

There have been several efforts by various researchers to develop such noble gas ion sources [6]. Gas field ion sources (GFIS) and plasma ion sources have been widely studied [6]. Actually, GFIS (point sources) can generate high brightness, low energy spread noble gas ion beams [6]. However, these sources are not at all reliable (ion emission current stability and lifetime) [6]. Also, for an effective ionization these sources need to be operated at low temperature (≤ 77K). Room temperature operation of ion sources is favorable (as with Ga LMIS) as far as industrial applications are concerned [6]. Small change in temperature or impurity atoms in the noble gas can cause current fluctuations in GFIS [6]. An example that illustrates the futile efforts in the research of GFIS is the so-called 'super tip GFIS' [6]. The claimed high-reduced brightness (~ $3 \cdot 10^{11}$ A/m^2SrV) for super tip GFIS is not only questionable [6] but also the lifetime of the supertip GFIS cannot match that of LMIS [6]. Can we obtain a working GFIS as reliable as LMIS? That still remains an open question [6]. In brief, the progress in this direction is not very encouraging as far as the actual fabrication of the device is concerned [6]. The two types of plasma ion sources, the Penning type plasma ion source and the multicusp type plasma ion source have been widely studied. Plasma ion sources can produce several

gas species [6]. Plasma ion sources are more robust, easy to maintain, and more reliable than any type of GFIS [6]. However, despite several efforts, plasma ion sources are not as bright as LMIS for FIB applications because of the high temperature, which is an inherent problem in plasma sources [6]. The latest values of reduced brightness and energy spread for Penning and multicusp type plasma ion sources have been cited in Ref. [6]; for a Penning ion source operated in pulsed mode these are ~10^5 A/m^{2}SrV and 3eV, respectively, and for a multicusp ion source operated in continuous mode ~$1.5 \cdot 10^3$ A/m^{2}SrV and 0.7 eV [6]. The value of reduced brightness for the Penning source is not obtained in continuous mode, while a 3-eV energy spread is still too high. Although the low energy spread of 0.7 eV achieved with an energy filter in a multicusp ion source is impressive, the reduced brightness for this source is too low compared to LMIS.

Recently, a few researchers [7, 8] have recognized the problem of plasma ion sources and have come with proposals to extract ions from ultracold plasma or laser collimated atomic beams. We believe that experimental work in this direction is certainly more desirable than trying to improve the reduced brightness and energy spread of conventional plasma ion sources such as the Penning or multicusp types. However, at this moment we do not know how practical it would be to maintain and operate these ion sources [7, 8] on a daily basis for common FIB users. As mentioned earlier, a noble gas ion source that can be operated at room temperature (as with Ga LMIS) and is easy to maintain, while also having at least similar properties as LMIS is needed.

In this chapter, it is proposed to fabricate a miniaturized electron impact ionization chamber for a reliable noble gas ion source with high brightness and low energy spread that can be operated at room temperature [9]. Conventional electron impact ion sources operated in plasma as well as non-plasma mode have been known since long time [10]. However, to the best of our knowledge, electron impact ion sources operated in non-plasma mode at sub-micron scale [9] have not yet been studied. The following sections describe its concept, predict its properties, and compares its properties with the properties of LMIS.

2.2 Electron impact ionization process

Inelastic collisions between gas atoms and electrons can lead to electron impact gas ionization, provided that the minimum energy required for the removal of an electron from a gas atom (in its ground state or excited state) is smaller than the electron impact energy [11]. An attractive feature of this process is that the ionization occurs at room temperature [11]. Not all electrons passing through the gas ionization chamber may collide with or ionize the gas atoms, and therefore, one needs to talk about electron impact ionization cross sections [11-13]. The term 'absolute partial cross section' [14, 15] is used for expressing the production of single or multiple charged individual gas ion species. The absolute partial cross section can be described (see Fig. 1) as follows [14, 15] with the condition that very few incident electrons produce ions,

$$\sigma(X) = \frac{N_i(X)}{N_e nl} \tag{1}$$

where $\sigma(X)$ is the partial cross section for charge production by electrons (m^2), $N_i(X)$ is the number of produced ions of the particular ion species X, N_e is the number of

electrons, n is the gas particle density (number of gas atoms/m^3) and l is the distance over which the electron passes in the gas medium (m).

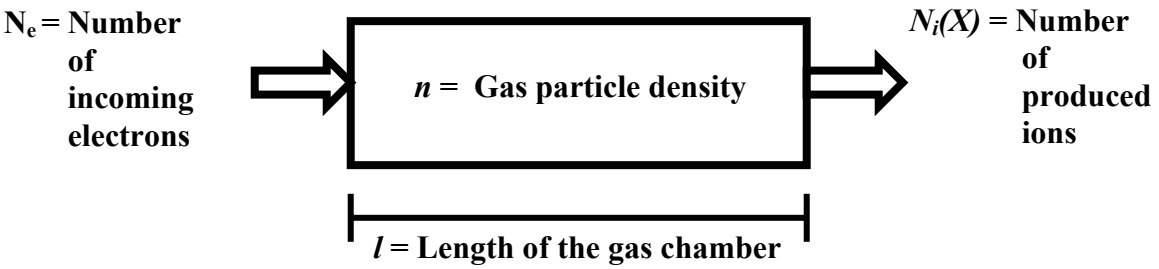

Figure 1: Definition of the absolute partial cross section $\sigma(X)$.

The ratio of ion to electron current can be estimated using Eq. (1). Rejoub *et al*. and many others [14 and references therein] have experimentally measured electron impact partial ionization cross sections for various noble gases of our interest. In this chapter, we will consider argon gas as an example. If one plots a single graph of the absolute partial ionization cross sections for Ar^+, Ar^{++}, Ar^{+++}, and Ar^{++++} for incident electron energies of 17 to 1000 eV with the data from Ref. [14], one can understand that for this range of electron energies the ion current largely consists of Ar^+ (single-charge) ions and the contribution due to Ar^{++}, Ar^{+++}, and Ar^{++++} can be ignored. Figure 2 shows the experimentally measured absolute partial cross section of Ar^+ ions due to electron bombardment [14].

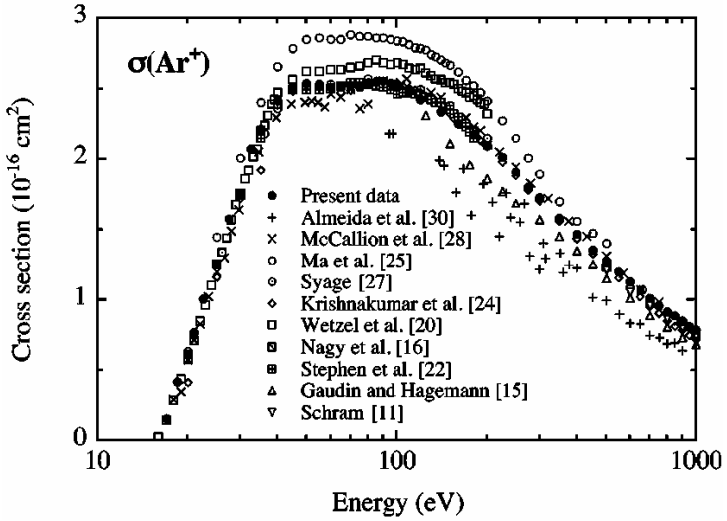

Figure 2: Experimentally measured absolute partial cross section of Ar^+ ions due to electron bombardment. Adapted from reference [14]. (In the above figure, 'the present data' is of the Ref. 14 of this chapter and other references shown in this figure are the references given in the Ref. 14 of this chapter.)

The experimental set up of Ref [14] is described in Ref [15]. The chamber has dimensions of 19 cm × 15 cm and the gas pressure is such that the mean free path (atom-atom) is ~ 20 cm, which is in the molecular flow regime. This is for keeping the charge transfer cross section small and the ionization cross-section measurement precise [15].

2.3 Concept of a thermal field electron impact ion source

The electron impact ionization chamber (see Fig. 3) in this concept [9] consists of two closely spaced (sub-micron) parallel conducting plates each with a small hole on the axis. The plates are electrically isolated from each other. The space between the two plates is filled with noble gas (for example, argon gas) in the molecular flow regime. At such a small device scale (of the double-aperture gas chamber), a relatively high pressure of gas in the molecular flow regime can be maintained [16] in the ionization region, while the gas particle density along the optical axis, outside the chamber can be extremely small [16]. Electrons from a thermal field electron gun (Schottky electron gun) enter through one of the apertures and ionize the gas in non-plasma mode, which means at room temperature (~ 293 K). The ions can be extracted through the second aperture under influence of the electric field.

Although ions do not start from a single plane, one can approximately estimate the reduced brightness for this ion source from Eq. (2), assuming that particle interactions (ion-neutral or ion-ion) outside the ionization region and near the ion exit aperture are extremely small [6],

$$B_r = \frac{eI_i}{\pi^2 r^2 kT_i} \tag{2}$$

where B_r is the reduced brightness (A/m^{2}SrV), e is the electric charge, I_i is the ion current, r is the radius of the aperture (hole), k is Boltzmann's constant, and T_i is the ion temperature.

In our case, considering T_i is 293K and by substituting the values of the other constants in Eq. (2), we get,

$$B_r \approx 4.013 \frac{I_i}{r^2} \approx 12.607 J_i \tag{3}$$

where J_i is the ion current density.

The energy spread of this ion source is mostly dependent on the applied voltage across the double aperture, as charge transfer or ion formation outside the ionization region and near the ion exit aperture is assumed to be extremely small. A maximum voltage should be applied to extract ions in order to avoid space charge problems and to avoid ion current loss to the second aperture. To keep the energy spread ≤ 1eV, the ions should be extracted by ≤ 1volt because the energy spread will be mainly due to the amount of voltage applied to the second aperture. The maximum applied voltage should not exceed the electric field of 10^6 V/m to avoid field-induced discharges.

The ion emission current stability of this ion source is dependent on the stability of the electron current, the stability of the incident electron energy, and the stability of the gas flow rate in the ionization region. Focusing of the maximum electron current in a

small spot (in our case, electron entrance aperture) requires an electron gun with high-reduced brightness and low initial energy spread [6]. Schottky electron sources are known as high-brightness and reliable electron sources [17, 18].

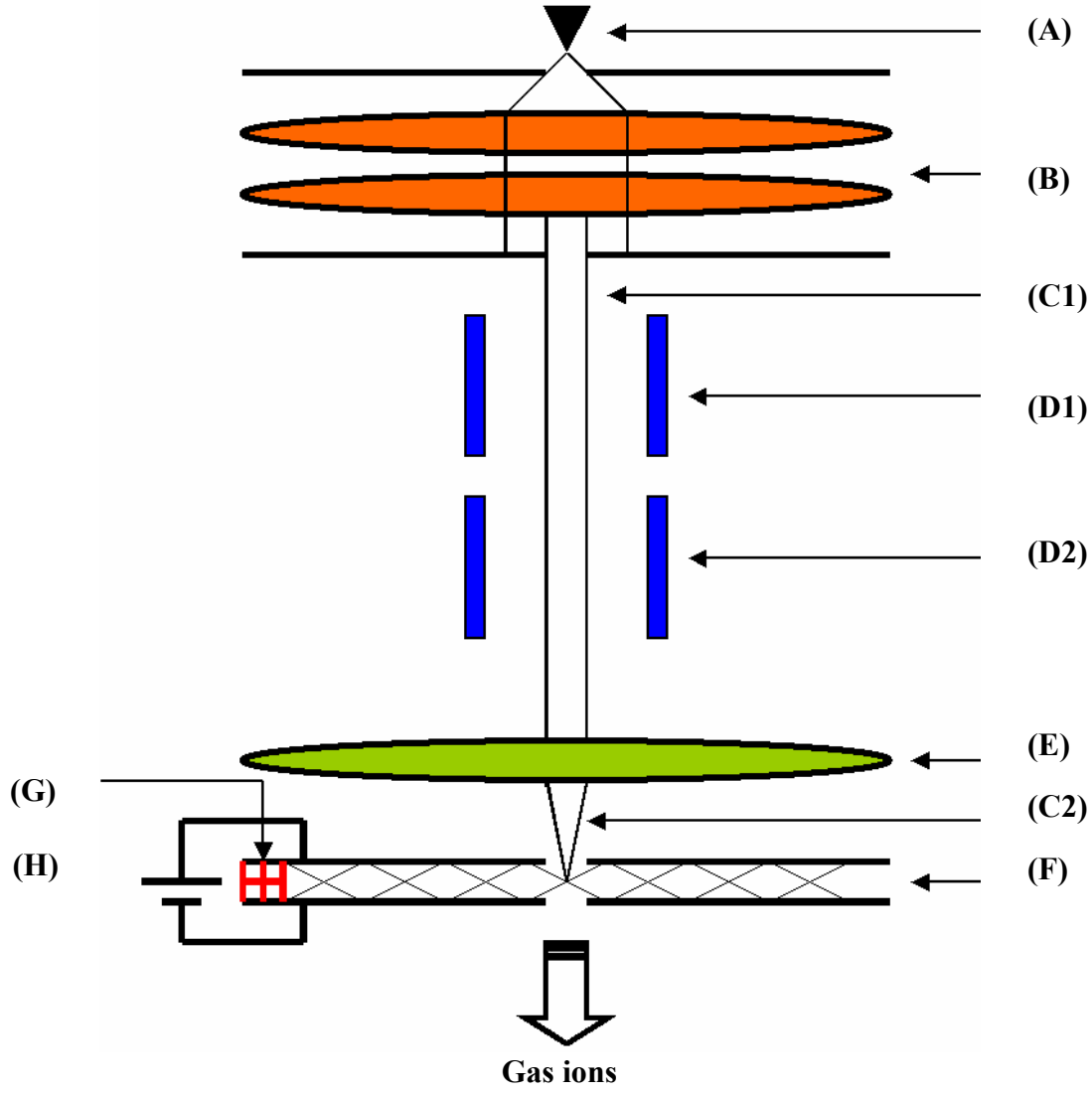

Figure 3: The concept of a high-brightness, monochromatic thermal field electron impact ion source. The letters in the figure indicate (i) A is the Schottky source (ii) B is the electron gun lens (iii) C1 is the electron beam of energy ~5 keV (iv) D1 and D2 are the deflectors to scan the beam (v) E is the final probe forming lens (retarding lens) (vi) C2 is the electron beam of energy < 1 KeV (vii) F is the gas target, gas is kept in the molecular flow regime (viii) G is the electric insulator to isolate the parallel plates and (ix) H is where voltage is applied. (The figure is not to the scale. The sub-micron size of the gas target is exaggerated. The total length of this ion source can be around 10 to15cm)

Furthermore, the stability of the gas flow rate can be much better than that of GFIS [6] as we do not have to depend significantly on the surface properties of a material. The lifetime of this ion source is mainly dependent on the lifetime of the electron gun and the sub-micron gas ionization chamber itself. The lifetime of the Schottky source is acceptable and the electron current can be delivered directly into the chamber without damaging the chamber.

The advantage of this kind of construction is that all parameters, such as reduced brightness, energy spread, ion current stability, and lifetime can be designed and maintained reliably.

2.4 Estimation of the reduced brightness and energy spread of the ion source

To meet the same experimental conditions as described in Ref. [15] we estimate the ratio of the ion current to the electron current (or ion current density to electron current density) for two different gas pressures using Eq. (1):

For $l = \lambda$, $$\frac{J_i}{J_e} = \frac{I_i}{I_e} \approx 0.016 \times 10^{20} \sigma(X) \quad (4)$$

For $l/\lambda = 0.1$, $$\frac{J_i}{J_e} = \frac{I_i}{I_e} \approx 0.016 \times 10^{19} \sigma(X) \quad (5)$$

As shown in Fig. 4, $l = \lambda$ is where the spacing of the double aperture l is equal to the mean free path λ (mean free path of gas particles in gas, $\lambda = kT/\pi pD^2(2)^{1/2}$, where k =is Boltzmann's constant, T is the gas temperature, p is the pressure, and D is the effective diameter of collision of atoms or molecules [19]) At $l/\lambda = 0.1$, the spacing of the double aperture l is ten times smaller than the mean free path λ.

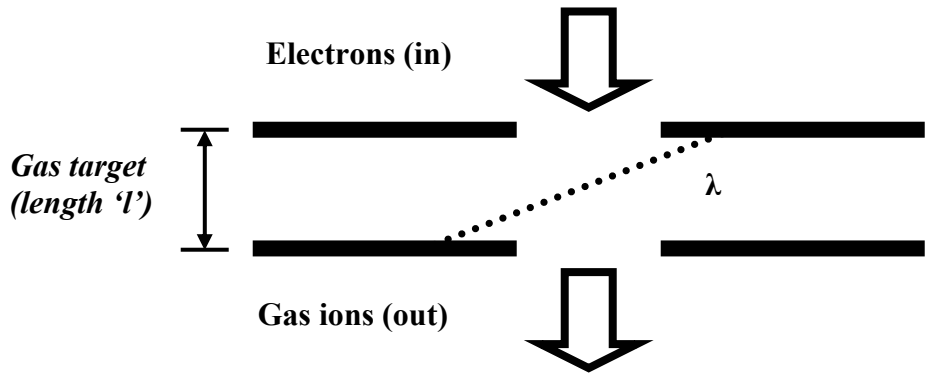

Figure 4: Definition of λ and l.

It should be noted that according to a Monte Carlo simulation study by Peatross and Meyerhofer [16], outside the double aperture, along the optical axis the gas particle density is extremely small (in the molecular flow regime, *i.e.* $l = \lambda$), and this trend remains almost the same even for a higher pressure (up to $l/\lambda = 10$) [16]. Therefore, we can certainly expect that for very low pressure ($l/\lambda = 0.1$) the gas particles density along the optical axis and outside the double aperture must be extremely small.

It is clear from Eq. (5) that to extract the same amount of ion current, more electron current is necessary at low pressures. As one can see in Ref [14], the cross section for the production of Ar^+ (single charge) ions can be high for electron energies ~ 100eV. However, first of all, we should plot a graph of the electron current density versus the spot size (in our case aperture diameter) to find the maximum value of Eq. (3). Kruit and co-workers [18] have used the experimental data from Ref. [17] for a Schottky source and by optimizing various parameters in an optical system, such as the accepted half-angle at the emitter and the half-angle at the probe, have obtained a current- probe size relation for the Schottky electron emitter [18]. They have also obtained a few analytical equations by optimizing the accepted half-angle at the emitter and the half-angle at the probe, as follows.

If the chromatic aberration C_c of the probe lens dominates a system with emitter brightness B_r, V the accelerating voltage and emitter FW50 energy spread δU, the current in a probe of FW50 size d_p is

$$I_p = 1.71 \frac{d_p{}^4 B_r V^3}{C_c{}^2 \delta U^2} \tag{6}$$

If the spherical aberration C_s of the probe lens dominates a system with emitter brightness B_r, the current in a probe of FW50 size d_p is

$$\mathrm{I_p} = 2.44 \frac{\mathrm{d_p}{}^{8/3} B_r V}{C_s{}^{2/3}} \tag{7}$$

If the brightness does not play role, but the chromatic aberration of the gun lens needs to be balanced with the chromatic aberration of the probe lens, then with parameters such as angular current density J_Ω, chromatic aberration coefficient of gun lens C_{cg} and the extractor voltage V_e one writes,

$$\mathrm{I_p} = 2.18 \frac{\mathrm{d_p}{}^2 J_\Omega V_e{}^{1/2} V^{3/2}}{C_c C_{cg} \delta U^2} \tag{8}$$

If the spherical aberration of the gun lens needs to be balanced with the spherical aberration of the probe lens then with the parameter, spherical aberration coefficient of gun lens C_{sg} one writes,

$$\mathrm{I_p} = 6.77 \frac{\mathrm{d_p}{}^{2/3} J_\Omega V^{1/4}}{C_s{}^{1/6} C_{sg}{}^{1/2} V_e{}^{1/4}} \tag{9}$$

Using these equations (6,7,8 and 9) and by substituting the values from the Ref. 17, one can plot a graph of the electron current density versus spot size.

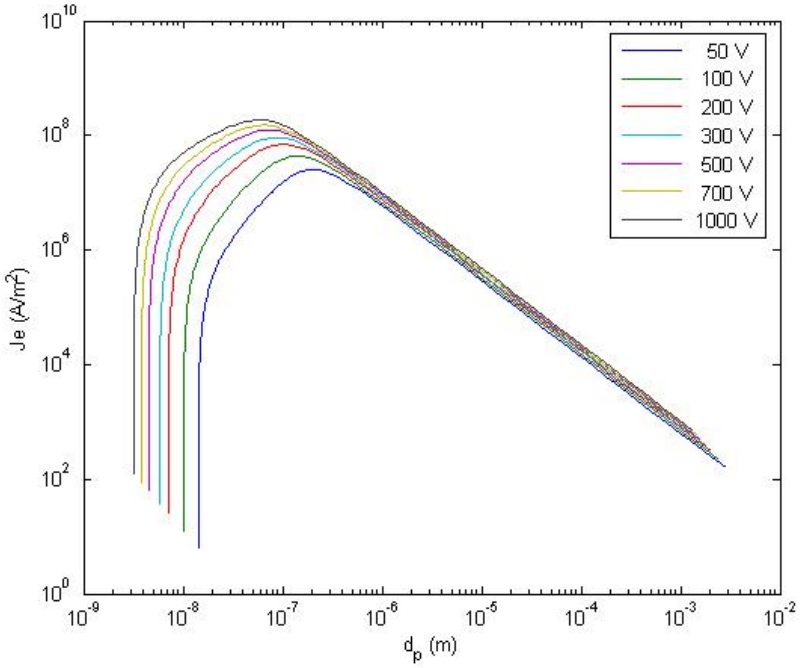

Figure 5: Electron current density vs. spot size for incident electron energies of 50 eV, 100 eV, 200 eV, 300 eV 500 eV, 700 eV, and 1000 eV.

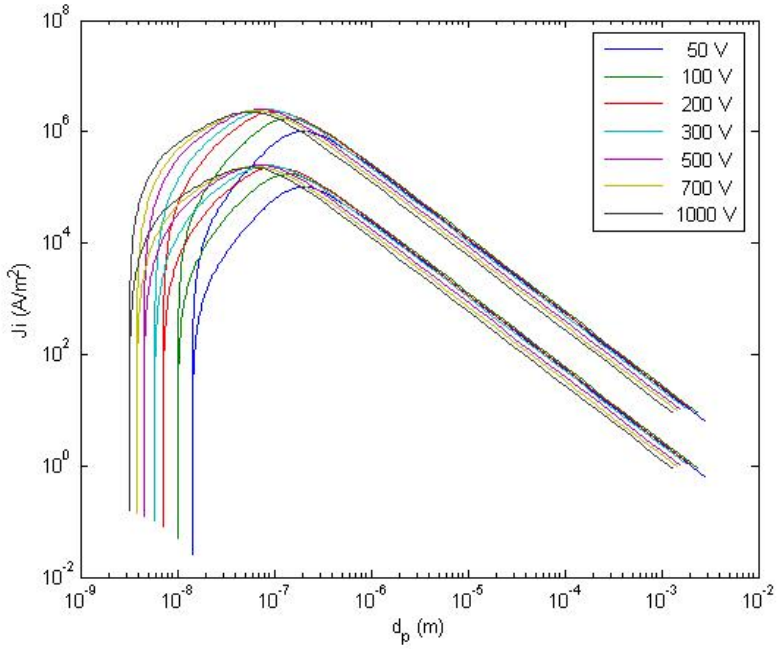

Figure 6: Ion current density vs. spot size for two different pressure conditions [l/λ = 1 (upper curves) and l/λ =0.1 (lower curves)] at incident electron energies between 50 and 1000 eV.

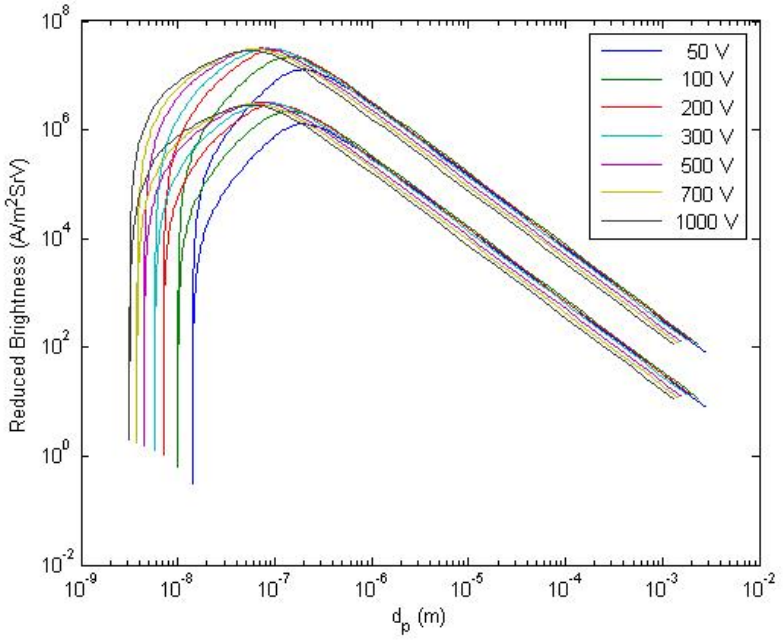

Figure 7: Reduced brightness vs. aperture diameter for two different pressure conditions [l/λ = 1 (upper curves) and l/λ =0.1 (lower curves)].

In Ref. [18], Kruit and co-workers used an electron acceleration voltage of 1000 V. One can also plot the graph or graphs considering lower values of acceleration voltage V.

Using the optimization method described in ref [18], we have plotted Figure 5. Because, here we are also considering lower electron acceleration voltages, we have taken the values of spherical aberration coefficients C_s and chromatic aberration coefficients C_c dependent on the acceleration voltage V (that means not from reference 17 for V < 1000 V, for instance, we have considered 1mm for 1000V and 0.3 mm for 100V). One thing to note is that the value of $B_r = 5\times10^7 A/m^2SrV$ [in Ref. 17] is quite moderate (and therefore acceptable to avoid overoptimistic estimates), as higher values have been reported elsewhere [20]. The figure 5 shows the graph of electron current density versus spot size, plotted for different values of the electron acceleration voltage, ranging from 50 to 1000 V. It is clear that with electron acceleration of 1000 V, the electron current density (about $10^8 A/m^2$) can be obtained. The spot size at higher electron acceleration voltage can be smaller than that at lower electron acceleration voltage.

We can use Eqs. (4) and (5) to calculate ion current density J_i at two different pressures (see Fig. 6) by substituting values obtained from Fig. 5 and considering $\sigma(X)$ [from Ref. 14] . One can obtain the corresponding values for the ion current density versus spot size at the two different pressure conditions (l/λ = 1 and l/λ =0.1). It is important to note that the spot size in our case is the diameter of the aperture.

Obviously, using these values of ion current density versus spot size at different incident electron energies and using Eq. (3), one can obtain Fig. 7, which shows the reduced brightness versus aperture diameter plotted for two different pressure conditions (l/λ = 1 and l/λ =0.1). Even for a pressure l/λ =0.1 we can obtain reduced brightness

better than that of LMIS (10^6 A/m^{2}SrV). It is clear from Fig. 7 that the aperture diameter should be about 100 nm to achieve maximum brightness.

We assume the spacing between the two apertures to be also ~100 nm. To maintain an electric field at < 3×10^6 V/m across the double aperture spacing a voltage of < 0.1 volt should be enough. As stated earlier, the energy spread is mainly dependent on this voltage. We expect the energy spread of this ion source to be ~ 0.1 eV. The fabrication of a 100-nm double aperture cannot be difficult, as one knows that 100-nm double-gated field emitter arrays exist [21]. From Fig. 7 and Eq. (2) it is clear that an ion current of 1 nA can be extracted.

The spacing across the double aperture (see Fig. 8) can be written as

$$l = \frac{2eEt^2}{m} \tag{10}$$

Where, e is the electric charge, E is the electric field across the double aperture, t is the time of ion flight for the full length of the double aperture and m is the mass of the ion. By substituting $m = 6.6 \times 10^{-26}$ kg (Ar^+ gas ion), $e = 1.6022\times10^{-19}$ C, $E = 3\times10^6$ V/m and $l = 100$ nm we get the ion time-of –flight $t = 0.083 \times 10^{-9}$ s.

That means that up to about 1-nA ion current can be extracted literally without ion-ion collision out of the 100-nm spacing, or in other words, one ion at a time extraction through ion chamber. This current level (1 nA) through a 100-nm spacing at the applied electric field of about 3×10^6 V/m is in the pencil- beam regime as the average axial distance between the particles and the average distance between the neighbor particles is comparable [22]. We can safely assume that the ion-ion collisions outside the chamber are negligible. Because of the low gas pressure, interactions between ion and gas particles outside the chamber should be negligible.

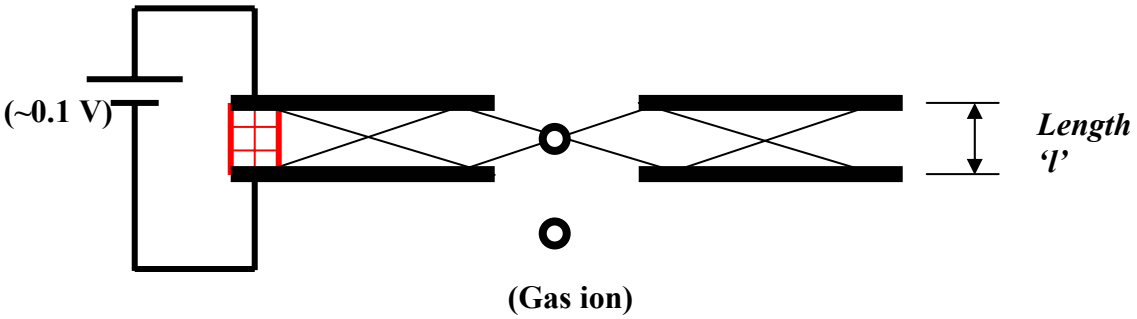

Figure 8: Almost only one ion exits at any given time inside the chamber or near the exit.

An interesting question arises: can one try to deliver electrons directly into the first aperture with a cold field emission tip [23, 24] (high electric field across the tip and the electron entrance aperture)? As we know [23, 24], cold field emitters require ultra-high vacuum (10^{-12} torr) for stable operation and in the case of our ion source the tip has to be very close to the first aperture for sufficient electron throughput. We will try to answer this question in the Chapter 3.

However, we strongly believe that the well-proven reliable Schottky electron source [17] can illuminate the total aperture uniformly, with stable electron current at stable incident energy. We believe that a dual beam instrument with a noble gas ion source and an electron probe of low energy (1000 V) can be fabricated in future.

2.5 Conclusion

We believe that if this ion source is fabricated using a Schottky electron gun, it will have similar properties as LMIS or better. Even if we are wrong by one or two orders of magnitude in the estimation of the reduced brightness (~10^6 A/m^{2}SrV), this ion source is better than any known plasma ion source (reduced brightness < 10^4 A/m^{2}SrV in continuous mode [6]). The low energy spread of ~ 0.1eV achieved without energy filter is promising. As explained above one can expect a reliability and lifetime of this ion source comparable to the LMIS, as this ion source does not significantly depend on the material's surface properties.

Acknowledgements

This work was part of the research program of the "Stichting voor Fundamenteel Onderzoek der Materie" (FOM), which is supported by the "Nederlandse Organisatie voor Wetenschappelijk Onderzoek"(NWO).

References

[1] L.A. Giannuzzi and F.A. Stevie, *Introduction to Focused ion beams: instrumentation, Theory, Techniques and Practice* (Springer, New York, 2005).

[2] J. Orloff, M. Utlaut, and L. Swanson, *High Resolution Focused ion beams (FIB and its applications)* (Kluwer Academic/Plenum, New York, 2003).

[3] M. Utlaut, *in Handbook of Charged Particle Optics,* Chap 11, edited by J. Orloff (CRC Press, New York , 1997).

[4] R.A.D. Mackenzie and G.D.W. Smith, Nanotechnology **1**, 163 (1990).

[5] J. Melngailis, J. Vac. Sci. Technol., **B 5**, 469 (1987).

[6] See for an example the critical review on high brightness, monochromatic noble gas ion sources. V. N. Tondare, J. Vac. Sci. Technol., **A 23**, 1498 (2005).

[7] See sections III.C.1 and III.C.3 in Ref. [6].

[8] B. J. Claessens, S.B. van der Geer, G. Taban, E. J. D. Vredenbregt and O.J. Luiten, Phy. Rev. Lett. **95**, 164801, (2005).

[9] P. Kruit and V.N. Tondare, European Patent (applied on 22-02-2006), "Particle-optical apparatus equipped with a gas ion source", Application No.: 06110257.0-

[10] See, for example, *Handbook of Ion Sources*, edited by B. Wolf (CRC press, Boca Raton, 1995).

[11] L Valyi, *Atom and Ion Sources* (Wiley, London, 1977).

[12] Massey and Burhop, *Electronic and Ionic Impact Phenomenon* (Oxford at the Clarendon Press, 1952).

[13] See, for example, *Electron Impact ionization*, edited by T.D Mark and G.H. Dunn, (Springer-Verlag Wien, New York, 1985).

[14] R. Rejoub, B.G. Lindsay and R.F. Stebbings, Phys. Rev. A, **65**, 042713 (2002).

[15] H. C. Straub, P. Renault, B.G. Lindsay, K. A. Smith and R.F. Stebbings, Phys. Rev. A, **52(2)**, 1115 (1995).

[16] J. Peatross and D.D. Meyerhofer, Rev. Sci. Instrum., **64(11)**, 3066 (1993).

[17] L.W. Swanson and G.A. Schwind, *Handbook of Charged Particle Optics*, Ch.2, Edited by J. Orloff, (CRC press LLC, 1997).

[18] P. Kruit, M. Bezuijen and J.E. Barth, J.Appl. Phys., **99**, 024315 (2006).

[19] A. Roth, *Vacuum Technology*, (Elsevier Science BV, The Netherlands, 1990).

[20]http://www.htiweb.com/Product_Infor/SEM/SUPRA/SUPRA_Adv_Schottky_FE_Source.htm (the reduced brightness of a Schottky electron gun is given $B_r = 10^8$ A/m^{2}SrV).

[21] Jo Choi, A.I. Akinwande and H.I. Smith, J. Vac. Sci. Technol.B, **19(3)**, 900 (2001).

[22] P. Kruit and G.H. Jansen, *Handbook of Charged Particle Optics*, Chapter 7, Edited by J. Orloff, (CRC press LLC, 1997).

[23] F. Charbonnier, Appl. Surf. Sci, **94/95**, 26 (1996).

[24] V.N. Tondare, N.J. van Druten, C.W. Hagen and P. Kruit., J. Vac. Sci. Technol., **B 21**, 1602 (2003).

Chapter 3

*Cold field electron impact noble gas ion source**

V. N. Tondare, N. J. van Druten, C. W. Hagen, and P. Kruit

Abstract

This chapter describes the concept of the cold field electron impact noble gas ion source. The main difference with the concept of the thermal field electron impact ion source (proposed in Chapter 2) is the cold electron gun used and avoiding the lenses. Cold field electron emitter can deliver electrons directly into the gas chamber. This ion source can have a simple and compact design and more importantly, avoiding lenses means avoiding aberrations and putting higher electron current density into the gas chamber and therefore, achieving higher reduced brightness than the thermal field electron impact ion source. However, it is a fact that cold field emitters require ultra-high vacuum (10^{-12} torr) for the successful operation that means to achieve a stable current for a long period of time. It is impossible to maintain such an ultra-high vacuum around the cold field electron emitter in this ion source concept. If electron current is not stable or electron emitter has too short lifetime then, this would seriously affect the performance of this ion source. Obviously, this ion source concept can satisfy all the ion source requirements described in Chapter 2 and that is only if one shows a successful operation of a cold field emitter in poor vacuum conditions.

The experiments reported in this chapter were designed to understand the behavior of a cold field electron emitter when placed in front of the gas target, that means not in ultra high vacuum conditions.

We have obtained encouraging experimental results that may be also useful for the field emission or vacuum microelectronics community. Further experimental work has been proposed.

***** The part of this chapter has been published as a research article; V.N. Tondare, N.J. van Druten, C.W. Hagen, and P. Kruit; J. Vac. Sci. Technol. B **21(4)**, (2003) 1602. The concept of the cold field electron impact noble gas ion source has been applied for the patent [P. Kruit and V.N. Tondare, European Patent (mentioned in Chapter 2)].

3.1 Concept of the cold field electron impact noble ion source

The concept of cold field electron impact noble gas ion source is shown in Fig. 1. The cold field emission tip (a sharp metal tip) can be held directly in front of the submicron gas ionization chamber using a piezo motor or tip and the double aperture gas ionization chamber can be fabricated as one assembly using lithographic techniques. Besides miniaturization, another advantages of cold field electron impact noble gas ion sources are that they can be cost effective and can have higher reduced brightness than thermal field electron impact ion source (proposed in Chapter 2). This is because avoiding lenses can reduce the cost as well avoiding lenses means avoiding aberrations and putting more electron current density into the gas ionization chamber.

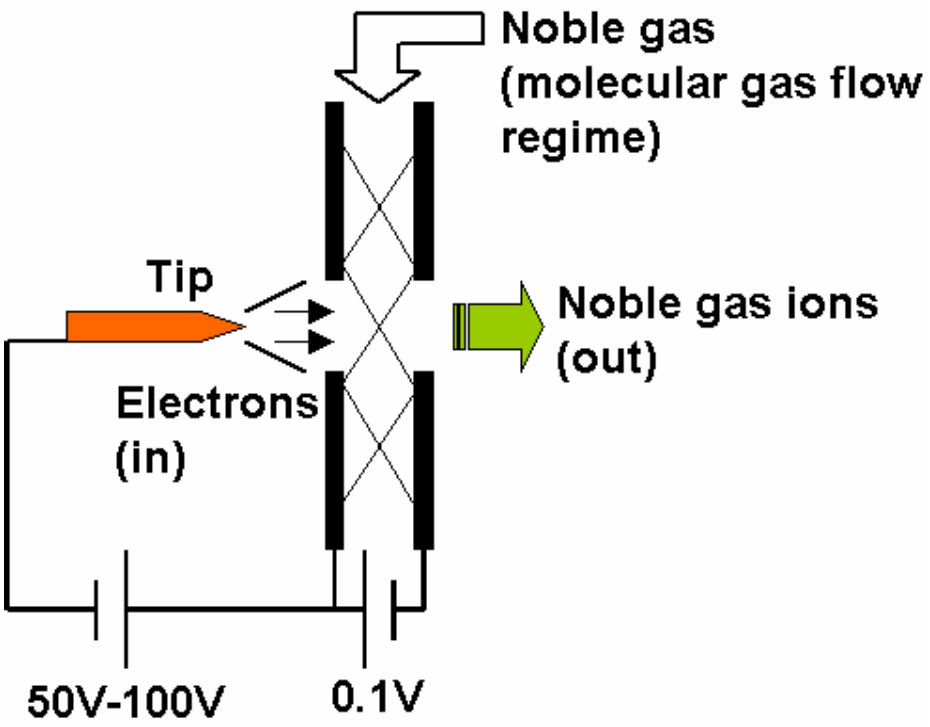

Figure 1: Concept of cold field electron impact noble gas ion source.

As we know from Chapter 2, for a better performance of our electron impact ion source the electron source must deliver a stable electron current, the incident electron energy must be constant, the source should have a lifetime as good as LMIS, and the electron source should be able to deliver electrons into the gas ionization chamber without damaging it.

All these issues of the reliability of the ion source are extremely important; one can understand from Chapter 1 that there would hardly have been a need for an extensive search for noble gas ion sources if the reliability of an ion source was not an issue at all. Gas field ion sources can have a better reduced-brightness and smaller energy spread than LMIS.

The success of a cold field electron impact noble gas ion source is mainly dependent on its electron source. The cold field emission vacuum requirements are more stringent than that of thermal field electron sources. The cold field emission tip has to be very close to the aperture of the gas ionization chamber. There is no guarantee that cold field emitters will behave reliably as it can be understood from the next Section 3.2.

3.2 About cold field electron emitters

The history of the development of cold field electron emitters for industrial applications shows that achieving a better current stability in relatively poor vacuum conditions (or industrial vacuum conditions, pressure > 10^{-7} mbar) is one of the big challenges that remains yet unsolved [1,2,3]. The nature of field emission (FE) current fluctuations has been well studied by various researchers [4,5 and references therein]. Tungsten field emitters were extensively studied by Dyke and coworkers [2,6] and they concluded that for stable operation a system pressure of 10^{-12} torr or lower (ultra-high vacuum) is needed, which is not practical in commercial devices. The conditions for a stable FE current at a fixed applied voltage are well known [2].

First of all, there should not be any change in work function of the emitter material. In recent years, there has been a considerable amount of research on different materials, such as diamond thin films and carbon nanotubes, which are more chemically inert than metals and are potential candidates for FE cathodes [1,3]. Despite considerable progress for these new materials, they do not exhibit an excellent FE current stability [1,7-10].

Secondly, the shape of the emitter tip should be constant on an atomic scale during emission. Since positive ion bombardment of the tip is one of the main causes for FE current instability [2], we believe that the device must be operated at voltages less than the first ionization potential of the ambient gas molecules. But even then the FE current may not be stable [11].

Therefore, we believe that for the ultimate success of FE-based devices, it is not going to be enough to rely only on new materials, which are just better than metal emitters. Instead, it seems that there should be some active mechanism in devices, which corrects and controls the applied voltage to stabilize the FE current. This idea is not new as a feedback mechanism to stabilize near-axial emission was used by Cleaver and Smith [12] in a scanning electron microscope. Kanemaru *et al.* [13] showed that stable emission at pressures up to 10^{-5} torr could be achieved from metal-oxide-silicon field-effect-transistor (MOSFET)-structured silicon field emitters, which was not possible with conventional silicon FE tips. There have been many attempts by Baptist and coworkers to use a resistive sheet as a passive element to improve the FE current stability [14,15]. However, it did not emerge as a final solution. Py and Baptist [14] have shown the problems of a resistive sheet and recommended to avoid it as far as possible. There have been excellent efforts by Chang and coworkers [16-18] to use feedback on tip-anode distance to improve the FE current stability. They operate a scanning tunneling microscope (STM) in constant field emission current mode.

3.3 Experiments for developing stable cold field emitters for elevated vacuum conditions

As it is clear from the above-mentioned brief history of cold field emitters, it is necessary to develop stable field emitters at elevated vacuum conditions for their use in cold field electron impact noble gas ion sources.

The aim of the experiments presented in this chapter is to investigate a number of factors that are of interest for the use of cold field emitters in field electron impact gas ion sources. Questions that have been addressed are a) Use of sharp tungsten tips? b) How does an unclean tungsten field emission pattern look? c) Can we achieve a stable field emission current at stable voltages (~ 90 eV) in poor vacuum conditions using a current regulator circuit? d) Which material is better for field emitters? e) Does the field emission tip pull the gas target under influence of electric field? f) What should be the material of the gas target? and g) Does erosion occur on the gas target? etc…

Interestingly, if the cold field electron source satisfies all the requirements of a cold field electron impact ion source, then it will automatically be acceptable for focused electron beam systems (for example a cold field emission gun (CFEG) in an electron microscope without assistance of an ion pump!). In fact, from a gas ion source point of view a high current density at elevated pressure is desirable for the CFEG and from an electron microscope point of view a high current density in vacuum (~ 10^{-7}- 10^{-3} mbar) is also an achievement.

We report our attempts to stabilize the field emission current at stable voltages for a long time. Our approach to stabilize the field emission current is to vary the tip voltage at sub-millisecond to maintain the FE current constant. In our results, the FE current stability is much better than that reported previously [16, 17]. Our circuit bandwidth can be better than what was reported in references [16, 17].

Furthermore, we might use our approach for multitip arrays easily, whereas in the approach of Chang and coworkers an equal number of STMs is required to operate many tips simultaneously [18]. In this chapter, we present our encouraging results that might well be of interest for the field emission or vacuum-microelectronics community in general.

3.3.1 Fabrication of sharp metal tips (tungsten tips)

Sharp single tungsten (W) FE tips were prepared from W-wire of 0.16-mm diameter by electrochemical etching in a 3 N NaOH solution. A detailed procedure for making sharp W-tips can be found elsewhere [19, 20].

A scanning electron microscope (Philips XL30S, DIMES, TU Delft) was used to determine the radius of the W-tips. Typical tungsten tips that can be prepared with our setup and have been used in the experiments are shown in Fig. 1.

(a)

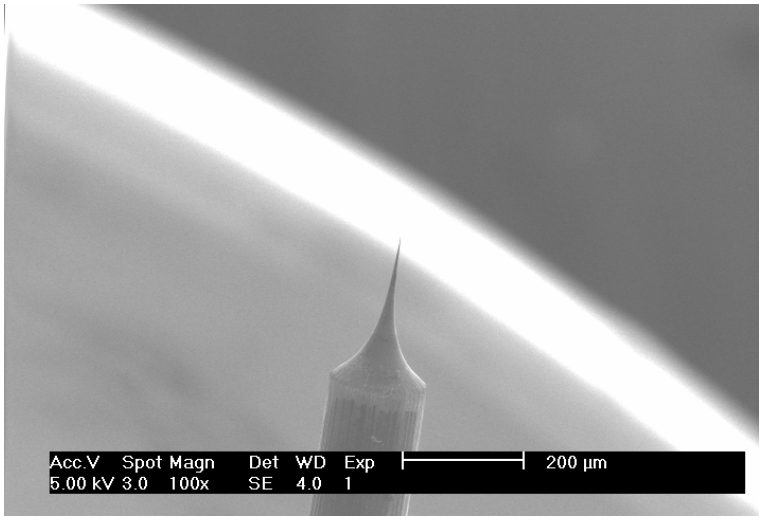

(b)

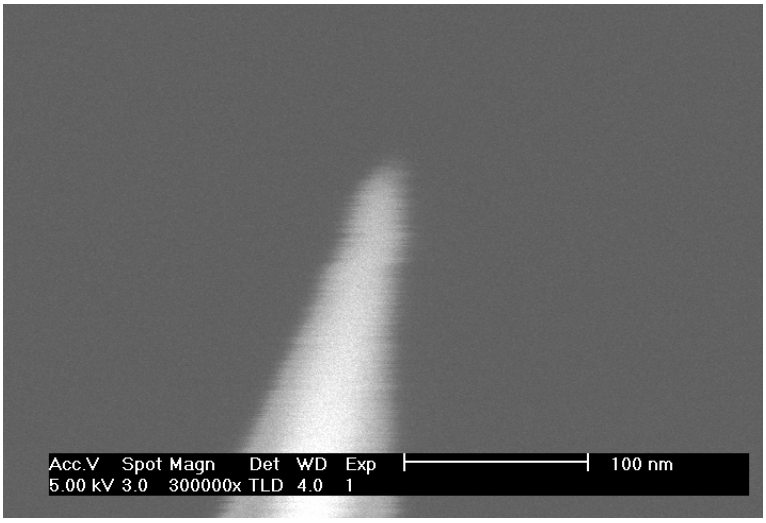

Figure 1: Scanning electron micrograph of tungsten tip with (a) low magnification and (b) high magnification shows that the tip radius is ~ 10 nm.

3.3.2 Looking at unclean field emission patterns

A small vacuum system was fabricated. The phosphor-coated screen was prepared by a decantation method [21] on top a of thin gold layer coated by a sputtering technique. The tip-phosphor screen assembly is shown in Fig. 2.

Figure 2: Field emission microscope. The figure shows the emitter tip (left side) and the screen (right side).

The scanning electron micrograph of the apex of the tip is shown in Fig. 3(a). The system was evacuated down to 1×10^{-9} mbar. The field emission pattern was observed on the screen with minimum negative high voltage without disturbing the first image and it recorded with Nikon digital camera. Figure 3 (b) shows the field emission patterns originating from the unclean tungsten tip. One can observe a few bright patches. However, these bright patches (a sort of supertips formed on the regular tungsten tip) can change their place and shape if the vacuum deteriorates.

(a)

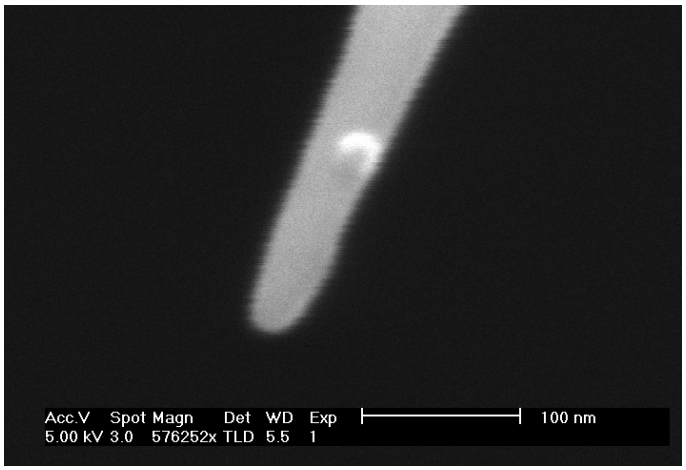

(b)

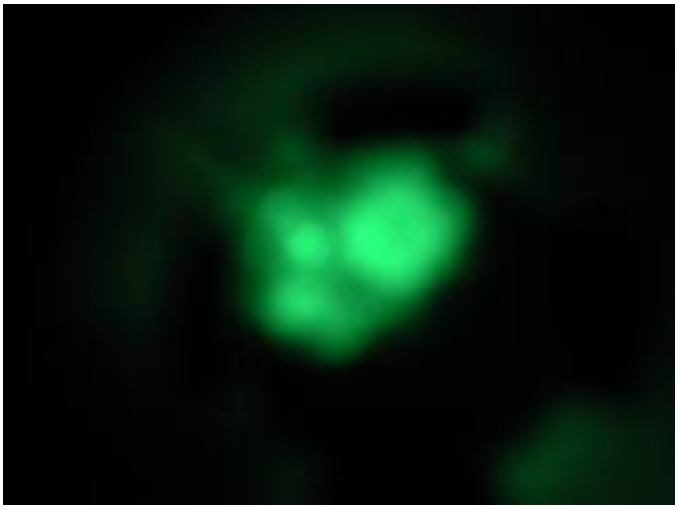

Figure 3: (a) Field emission tip used for this experiment; (b) Field emission micrograph of unclean tungsten tip.

3.3.3 Experiments with a tip-sphere assembly

This section describes the field emission experiments performed in a simple experimental setup using a current regulator circuit (bandwidth ~ 1.6 kHz). A sharp tungsten tip and a spherical counter electrode are used with a spacing of a few tens of micrometers. The feedback is on the tip voltage.

The aim of this study was to verify if we could really develop a cold field emitter that delivers a stable field emission current at almost fixed voltage in poor vacuum

conditions. The experimental results also give insight into the metal tip erosion process due to sputtering, and the death of the emitter. Section 3.3.3.1 describes the experimental setup, Section 3.3.3.3 describes the current regulator circuit, and Sections 3.3.3.2 and 3.3.3.4 describe the experiments.

3.3.3.1 The experimental setup

FE measurements were carried out in a glass tube (see, Fig. 4a and Fig. 4b) connected to the ultra high vacuum (UHV) system. A gold-coated stainless steel sphere (diameter ~ 1 cm) was used as counter electrode, which could be moved manually with a precision of 20 μm towards the tip to adjust the spacing between W-tip and anode. The system was also equipped with the high-precision Ar gas leak valve (VG, England) to pass argon gas into the system, a convectron gauge (Granville-Phillips), and a cold cathode gauge (Balzers, Germany). The tip-sphere spacing could be directly observed through the glass tube using an optical microscope (Leitz Wetzler, Germany) with a magnification *M* of 50 (see, Fig. 5). The current stability measurements were carried out using a high voltage power supply (Heinzinger, Germany) and a digital oscilloscope (Lecroy, LT 262, Japan).

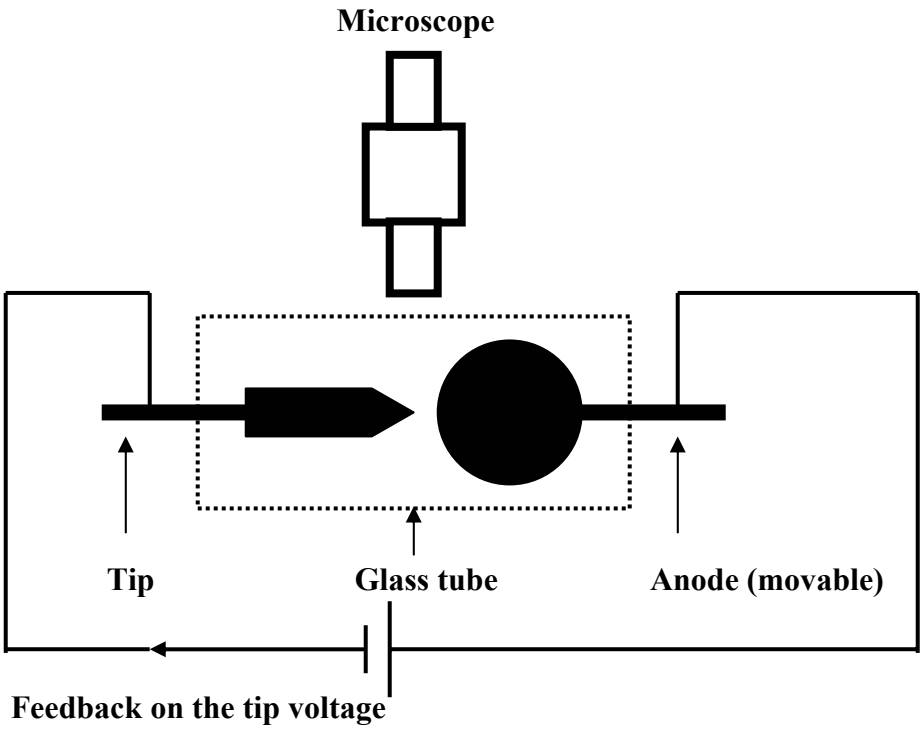

Figure 4(a): Schematic of the tip and metal sphere (anode) assembly

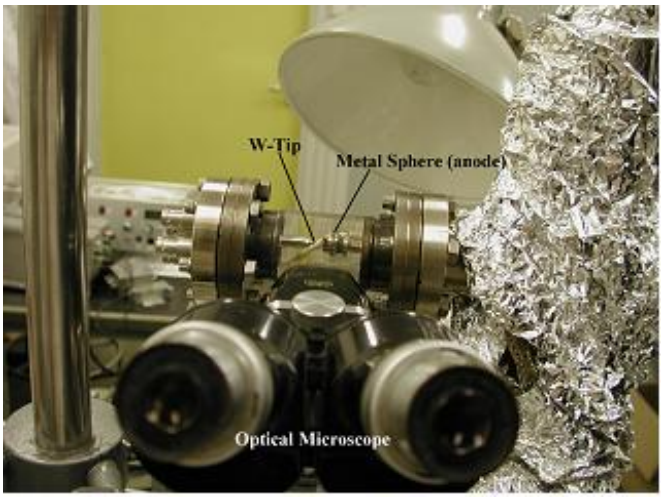

Figure 4 b: Tip and metal sphere (anode) assembly, optical microscope (M = 50).

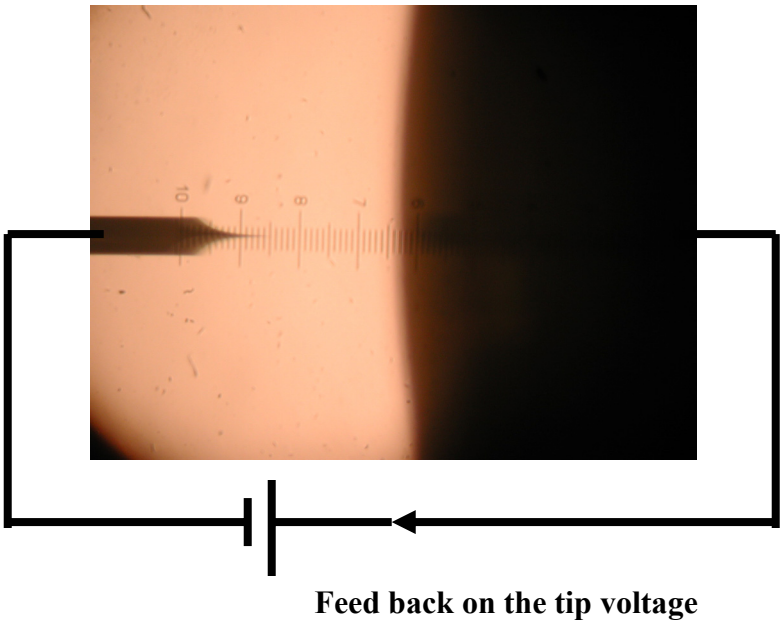

Figure 5: The tip (left side) and the metal sphere anode (right side) seen through the microscope.

3.3.3.2 Field emission current fluctuations at constant voltage (in high vacuum conditions)

It was observed that both with and without argon gas (noble gas environment) in high vacuum conditions up to 10^{-3} mbar with typical tip voltages (~ 100-120 V) and a cathode-

anode spacing of ~ 40-60 μm, the field emission current from tungsten tip was not at all stable. More than 100% random fluctuations were observed at currents of 1 nA or larger. We have also operated a few tungsten tips around ~70-80 V with and without argon gas at a pressure up to 10^{-3} mbar, but the required < 1-2 % fluctuation in the field emission current was far beyond reach.

The essential conditions for field emission current stability [2] are: (i) the applied voltage must be constant while operating the emitter (ii) the geometry of the emitter should remain rigid at atomic scale, and (iii) the work function of the emitter should remain unaltered. For tungsten field emitters these three requirements can be satisfied in 10^{-12} torr, which is difficult to maintain in practical devices [2]. Various surface phenomena [21] such as adsorption, desorption, and diffusion at the tip surface occur, causing a change in tip geometry at atomic scale as well as changes in the work function of the tip material and field emission current fluctuations Moreover, the sputtering threshold of tungsten is ~ 20 eV, and at voltages above this value sputtering due to positive ion bombardment may occur.

3.3.3.3 Current regulator circuit

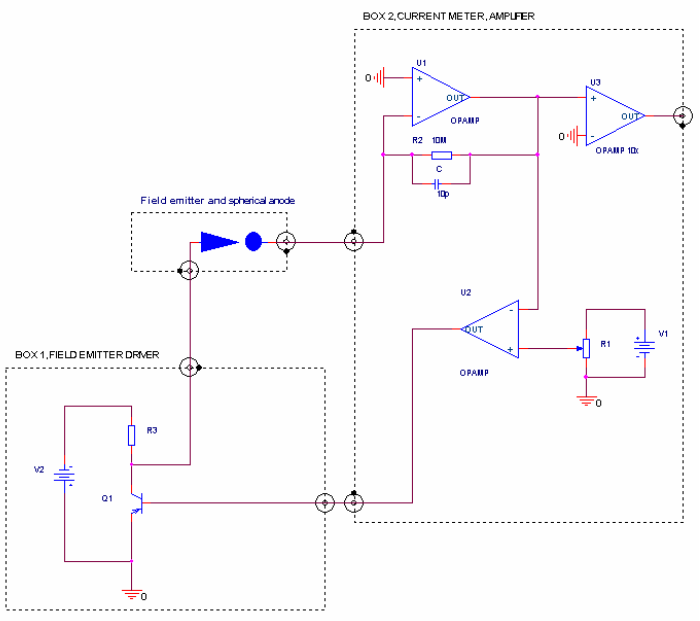

Figure 6: Feedback circuit connected to the system (bandwidth~1.6 kHz).

A current regulator circuit (bandwidth ~ 1.6 kHz) has been built in order to control the emission current fluctuations. This was easily possible because of the low voltage requirements (< 100 V). The current regulator circuit (feedback circuit) corrects and controls the applied voltage according to the measured emission current. The schematic of the current regulator circuit connected to the experimental setup is shown in Fig. 6. It

can be used up to 500-V tip voltage, but in these experiments only tips were used that emit a few nA at around 120 V or lower.

3.3.3.4 Field emission current stability (in high vacuum conditions with feedback circuit on)

We performed short-term current stability measurements to observe the current regulating action and long-term (one week) current stability measurements to understand the overall behavior of the current regulator circuit and field emitter tip.

3.3.3.4a Short-term current fluctuations

The tungsten tips used in the experiments were not cleaned or flashed before or during the experiment. It was found that tips with radii of typically 10-15 nm can emit a few nA at around 120 V and a 60-μm electrode spacing with more than 300% fluctuation in the current. Then, the current regulator circuit was connected to the tip and counter electrode. It improved the FE current stability drastically. It was observed that at a current level of ~ 3.5 nA and at a regulation voltage of ~ 120 V, the fluctuations in the FE current were ~ 5 % (see Fig. 7(a)). Stable operation of the W-FE tip was recorded (see Fig. 7(b)) in this experiment for more than 90 minutes before measuring the short-term stability at different Ar gas pressures.

We emphasize here that with a W-FE tip at this pressure, it is impossible to achieve FE current stability without current regulator circuit. The current regulating action can be seen clearly in Fig. 7(b) in the time interval from 60 to 80 minutes, when the current tries to increase due to some unknown change on the tip surface causing the current regulation circuit to lower its voltage in order to maintain the FE current constant.

(a)

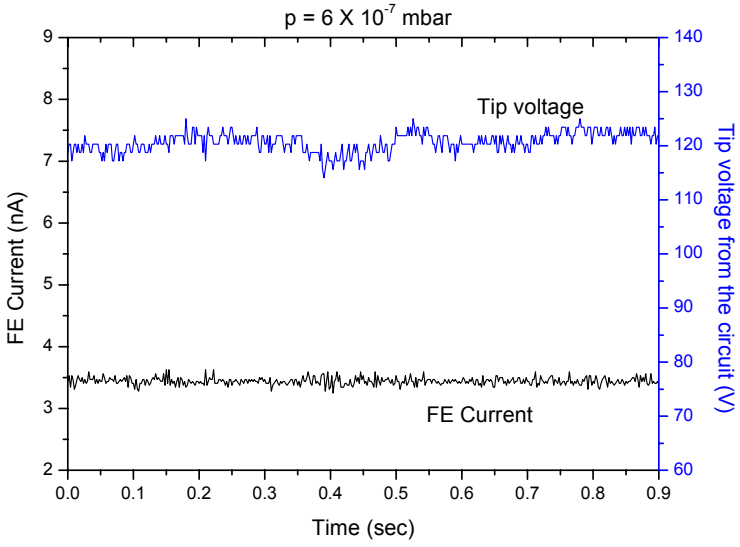

(b)

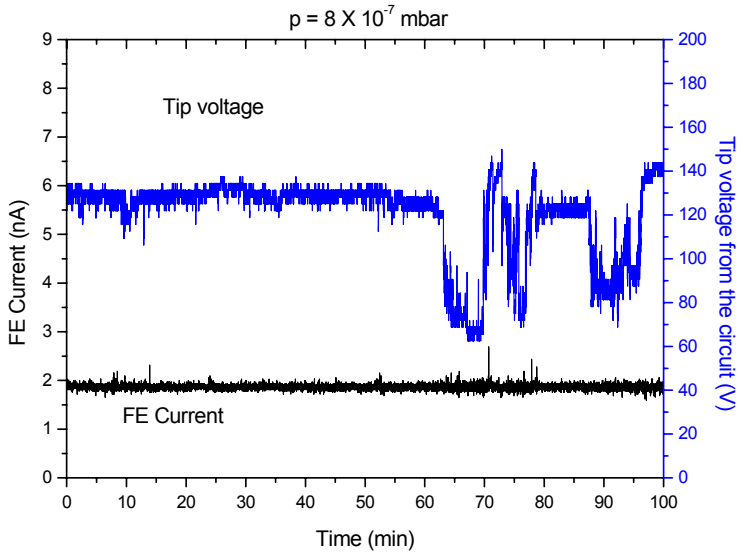

Figure 7: FE current stability and tip voltage fluctuations at unbaked W-tip; (a) short-term, $p = 6\times10^{-7}$ mbar; (b) long-term, $p = 8\times10^{-7}$ mbar.

Subsequently, the system pressure was increased to up to 10^{-3} mbar Ar and it was observed that the current regulator circuit worked with almost the same efficiency, as shown in Fig. 8 (a)-(c). At around 10^{-2} mbar of Ar gas pressure, larger short-term fluctuations started appearing (see Fig. 8(d)) and at around 10^{-1} mbar, the current regulator circuit failed to regulate the current.

(a)

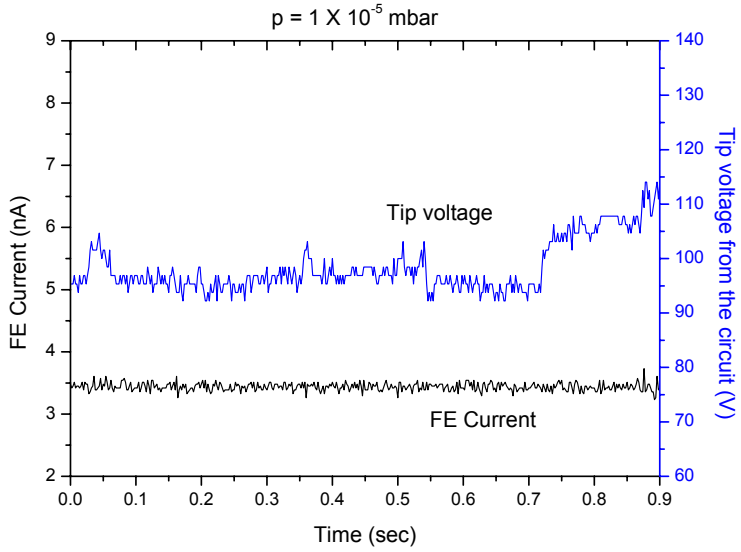

(b)

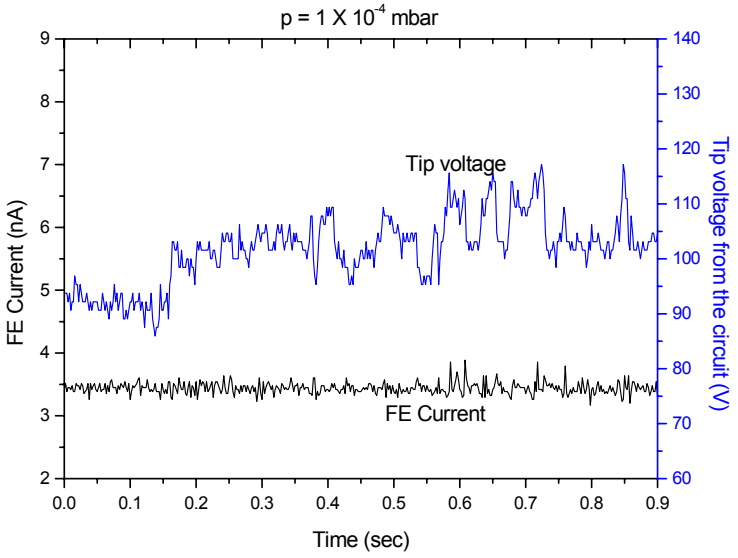

Figure 8: Short-term FE current stability and tip voltage fluctuations at unbaked W-tip; (a) $p = 1\times10^{-5}$ mbar, (b) $p = 1\times10^{-4}$ mbar, (c) $p = 1\times10^{-3}$ mbar, (d) $p = 1.3\times10^{-2}$ mbar.

(c)

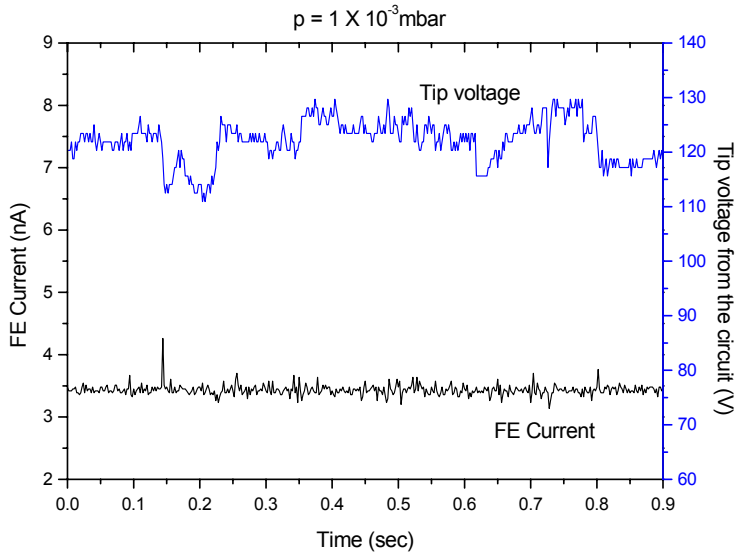

(d)

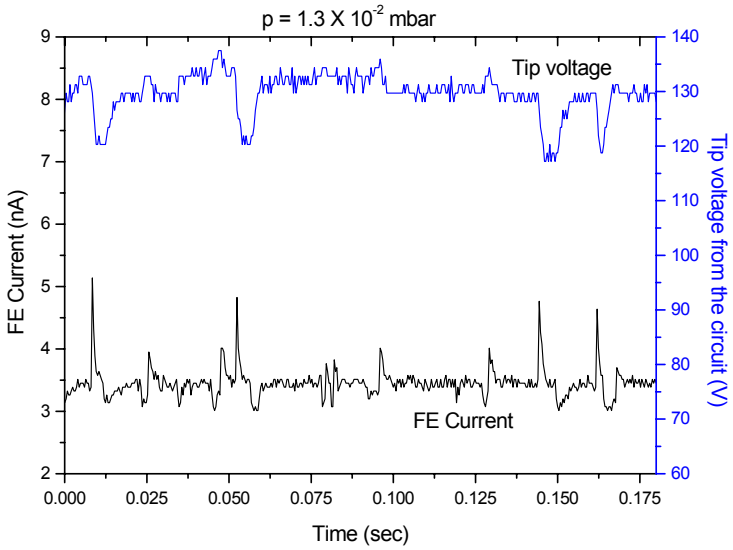

Figure 8 continued: Short-term FE current stability and tip voltage fluctuations at unbaked W-tip (c), (d)

3.3.3.4b Long-term field emission current fluctuations

The first long-term experiment was a current stability measurement at a current of 1.5 nA and an Ar pressure of 10^{-3}mbar during about 50 hours of operation over a period of four days. It was observed that after switching off the emission current at night, it returned to the same value when switched on the next morning (Fig. 9). Interestingly, we saw that the tip voltage gradually decreased (see Fig. 9). This means that the tip had become sharper and sharper and a lower voltage (~40-50 V) was sufficient to maintain the same amount of current.

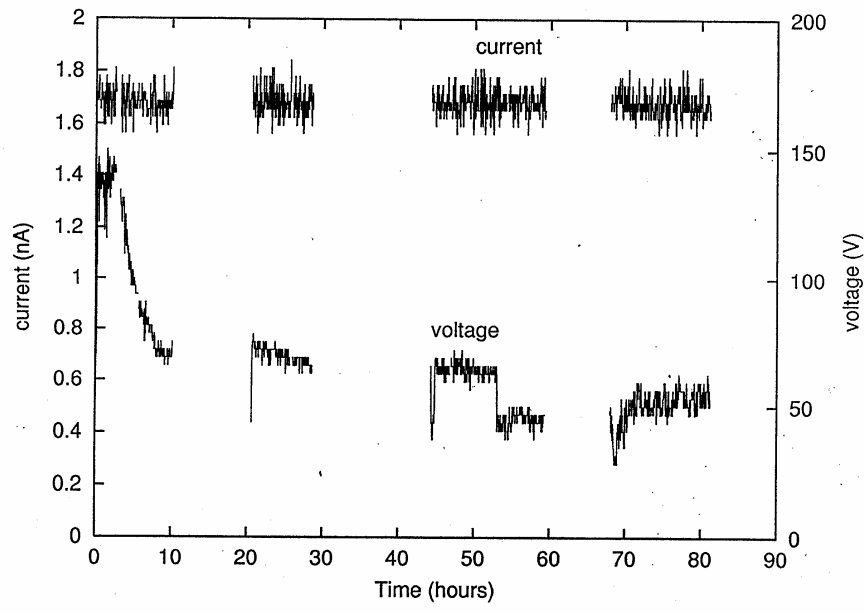

Figure 9: Long-term FE current (~1.5 nA) stability and tip voltage fluctuations at unbaked W-tip; $p = 1\times10^{-3}$ mbar.

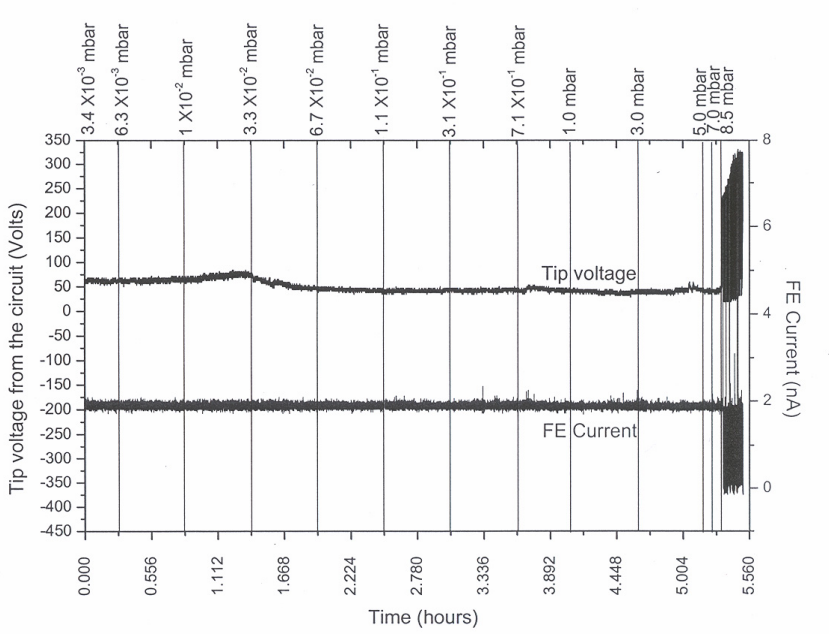

Figure 10: Long-term FE current stability and tip voltage fluctuations at higher pressures.

Then the same tip we used to perform high-pressure field emission experiments and the tip and current regulator circuit worked up to at least 3-mbar pressure. Then, after the pressure was increased to 5 mbar, the tip crashed (see Fig. 10) because we could not maintain the pressure and we had to close the valve fully. The pressure was gradually increasing up to 7 mbar and then with a faster rate till 8.5 mbar where the stability broke. We should mention that the pressure measurement was done with a common convectron gauge (not calibrated for Ar).

We should also mention that we have not performed an energy analysis of this electron current and we believe that part of the electron current could be due to gas ionization at high pressures.

The long-term stability experiments were repeated again at 10^{-3} mbar at current levels of 2 nA and 25 nA. At higher current levels, ~ 25 nA, and a W-tip voltage of ~ 80 V, almost one week of stable FE was recorded (see Fig. 11 (a) and (b)).

Large fluctuations in voltage were observed. It is believed that the tip went through cyclic changes and became sharp and blunt several times till the experiment was stopped on day seven. However, the continuous drop in voltage as observed in Fig 9, was not observed. We suspect that the initial field emitter shape and the value of the FE current can play an important role here. It was clear that many experimental parameters, such as tip shank, crystal orientation, and sputtering angle could not be reproduced exactly. For general information we refer to papers on tungsten tip sharpening by ion bombardment [22, 23].

(a)

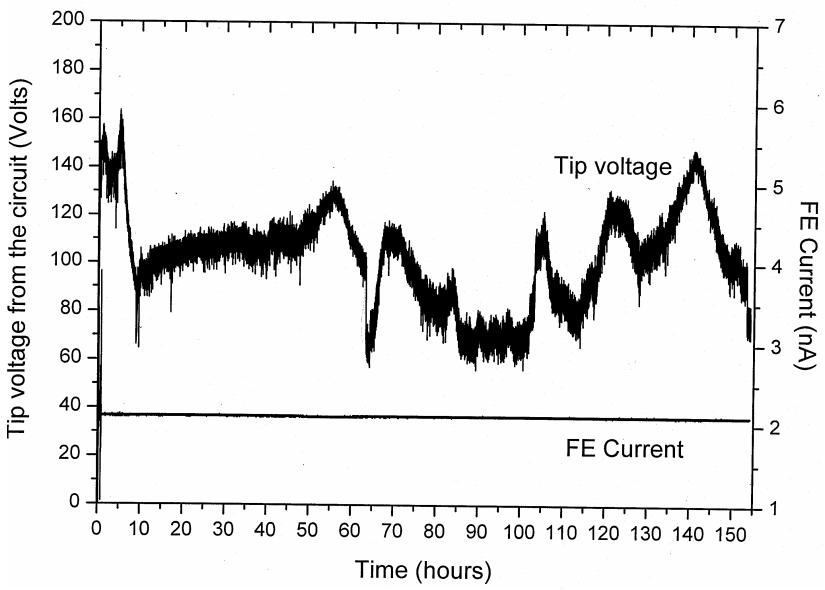

(b)

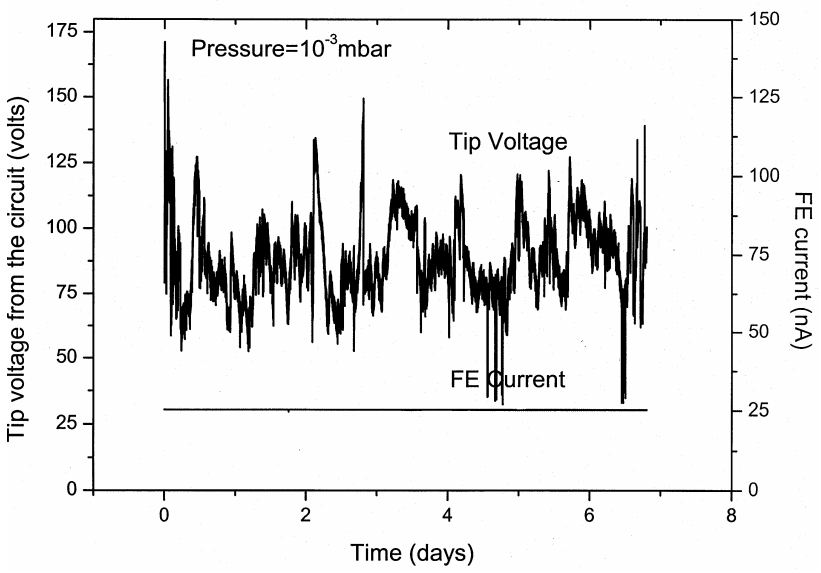

Figure 11: Long-term FE current stability and tip voltage fluctuations at p = 1×10^{-3} mbar; (a) ~ 2nA, (b) ~ 25 nA.

We also operated the field emission tip (see Fig. 12) at higher current level (~96 nA). It could run for more than one hour before the tip became blunt. The tip voltage increased to > 200 V. From Figs. 11 and 12 it was very clear that we could maintain a constant current for a long time, but that the voltage fluctuations are undesirable and unavoidable. For higher current levels, the frequency of voltage fluctuations increased (compare Figs. 11 (a) and (b)).

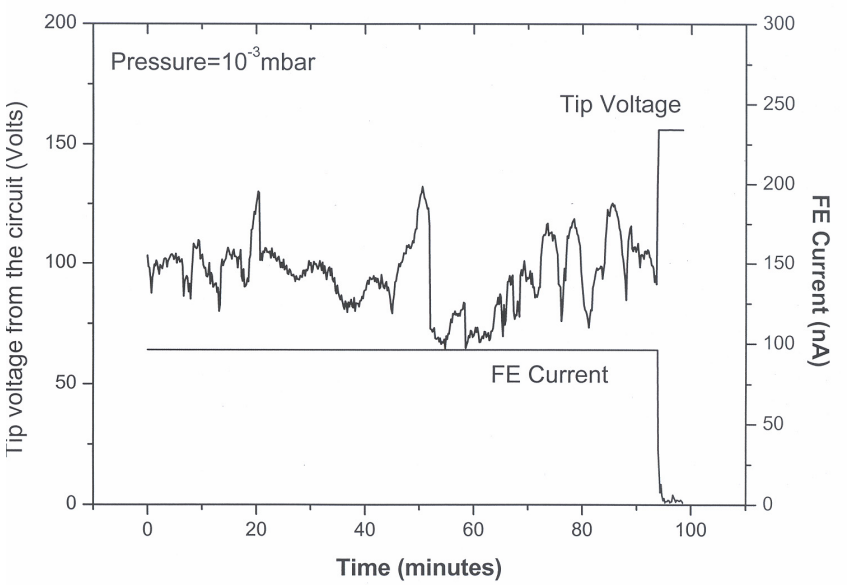

Figure 12: Long-term FE current (~ 96 nA) stability and tip voltage fluctuations at $p = 1\times10^{-3}$ mbar.

We have to consider two effects in voltage fluctuations. The first is the change in voltage to take care of a change in geometry at atomic scale, which is the cause of a change in electric field due to gas adsorption. The current regulator circuit takes care of that. In this case, we assume that the overall shape of the metal tip does not change. The second is the change in voltage due to tip erosion as a result of positive ion bombardment.

The voltage fluctuations will affect the stability of the ionization cross-section, and therefore, the stability of the ion current. Overall voltage variation at large time scale is due to sputtering and that we wish to avoid. Therefore, we must operate the tip below the sputtering threshold to maintain the voltage reasonably stable for the entire operation time. Different materials have different sputtering thresholds. The tip should not be damaged at all by positive ion bombardment. We may have to try other robust carbon-based materials such as diamond thin film, which hopefully would not erode as much as tungsten at ~ 50 V. To operate tungsten below the sputtering threshold (~ 20 eV) is not very useful for our electron impact gas ion source (for the ionization cross section, see Chapter 2, Fig. 2).

Fluctuations in electron energy due to changes in tip voltage are not desirable even for a cold field emission gun in an electron microscope. Voltage fluctuations due to surface phenomena like adsorption, desorption, and surface diffusion are unavoidable. The small unavoidable voltage change at the anode in such a system would obviously lead to a fluctuating virtual source size, which is highly unwanted. The voltage fluctuations at small time scale are expected to be really small in amplitude. If voltage fluctuations are well below 1-2 V, this would be acceptable. If it is required, we can also introduce another aperture to correct the virtual source size with feedback of the corrected voltage from the first aperture.

3.3.4 Experiments in a shadow microscope

The above experimental results show that FE current stability in poor vacuum can be much better than what is shown in literature [16,17]. These studies were performed with a tip in front of an anode that stopped the beam. For practical applications (for example, use in a microscope or our electron impact gas ion source) we need to form a beam behind the anode.

3.3.4.1 Introduction to shadow microscopy

When charged particle point sources such as field electron emitters and field ion emitters are brought close to a semi transparent object (for example, a grid), the transmitted beam can create a highly magnified image if the distance between source and object is small enough [24]. The magnification (see Fig. 13) of a shadow microscope is given by $M = (R/r)$, where R is the distance between object and screen and r is the distance between object and point source. We have performed field emission experiments in a shadow microscope to understand how a field emission tip will behave in front of a gas target (cold field electron impact ion source).

A shadow microscope was built. The same shadow microscope can be used to mount a gas target and perform proof-of-concept experiments of cold field electron impact ion source experiments. The system essentially consists of a scanning tunneling microscope to position a field emission tip in front of an aperture. It also has a gas delivery system, argon pressure gauge, residual gas analyzer etc. The gas target or a TEM grid can be mounted at the middle of the chamber and the shadow image can be viewed on the phosphor screen.

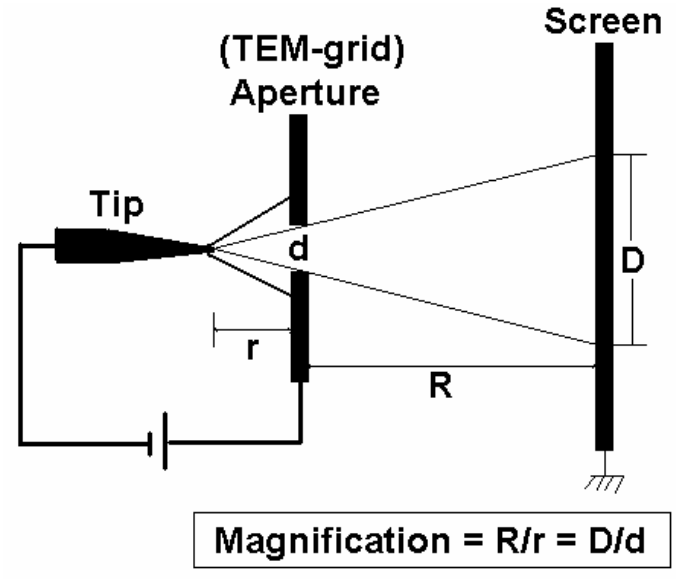

Figure 13: The magnification in shadow microscope.

3.3.4.2 A new current regulator circuit

A new current regulator circuit with improved bandwidth (~ 1 MHz) was developed, which can be operated at < 150 V. The main changes are the values of the resistance and capacitors in the old circuit. The tip can be at a voltage of + Ve or – Ve. Figure 14 shows a schematic of the feedback circuit connected to the shadow microscope (in Fig. 9, a Faraday cup is shown instead of the screen).

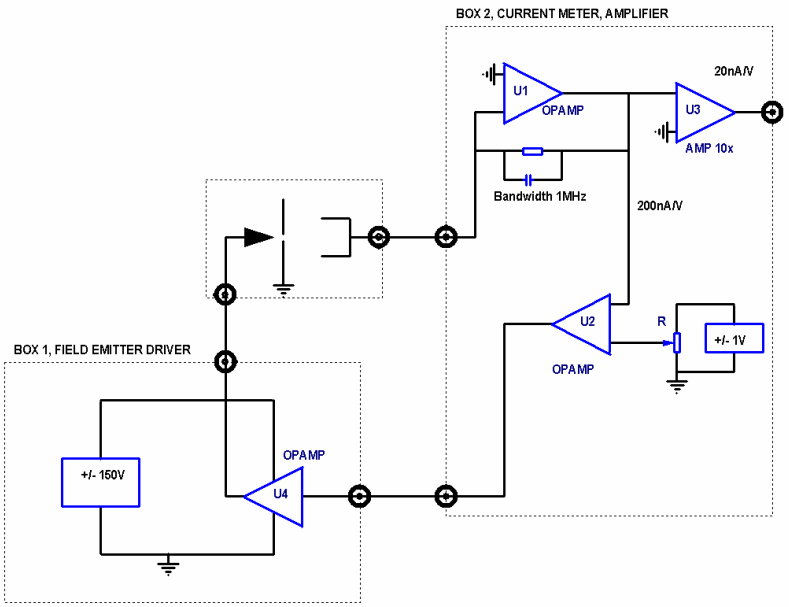

Figure 14: New feedback circuit with improved bandwidth (~ 1 MHz).

3.3.4.3 Field emission experiments with a very thin grid

In the shadow microscope, TEM-grid (Quantifoil) was used as object [25, 26]. The grid was observed in a scanning electron microscope (SEM) before mounting it in the shadow microscope. The scanning electron micrographs (see Fig. 15) of the grid show that the grid is 40 μm × 40 μm with a bar size of ~15 μm. It has well defined circular holes with a diameter of ~ 1.8 μm. The grid is basically a carbon-coated plastic foil [25]. The foil thickness as observed in the SEM is ~ 30 nm. The type of TEM-grid used here has been previously used for shadow microscopy purposes by others [26].

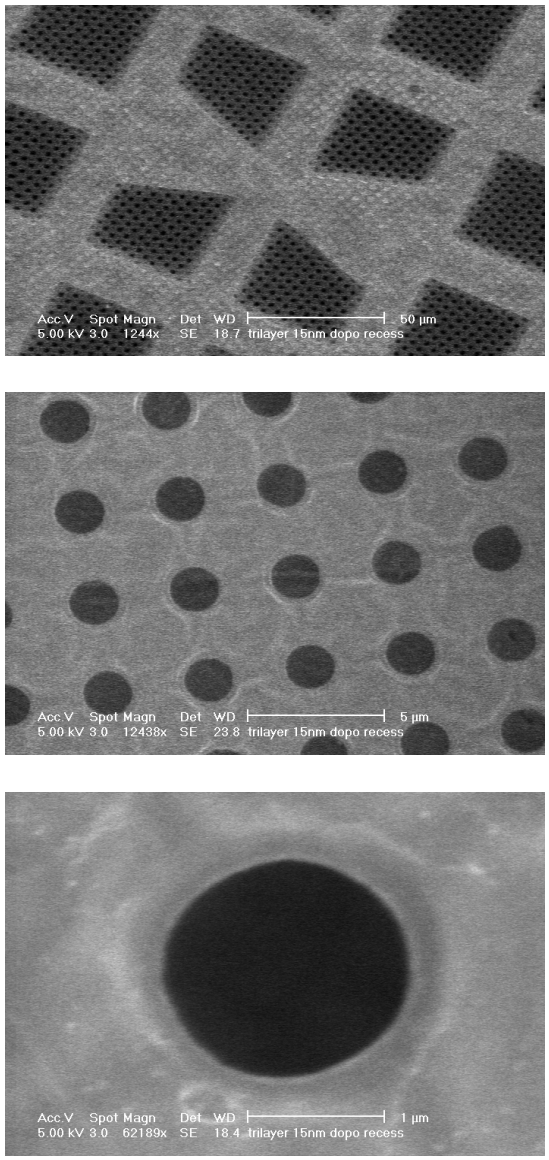

Figure 15: SEM images at different magnification of the TEM grid used for the shadow microscopy (Quantifoil) experiment. Top: M = 1244; middle: M = 12438, bottom: M = 62189.

3.3.4.4 The shadow image of the grid and its single aperture

Using the scanning tunneling microscope's positioning system, the tip can be brought closer towards the grid. Figure 16 (a) shows a typical shadow image at sufficiently close distance. The electrons come through the small apertures of the grid, making the shadow image. The tip can be brought much closer and positioned in front of a single aperture of the grid. Figure 16 (b) shows the shadow image of a single aperture of the grid. The magnification is ~ 10^4 (calculated from the size of the image on the screen divided by the

actual aperture size, see Fig. 17). The screen-to-object distance is ~ 10 cm, and therefore, the tip-to-grid distance should be ~ 10 μm.

(a)

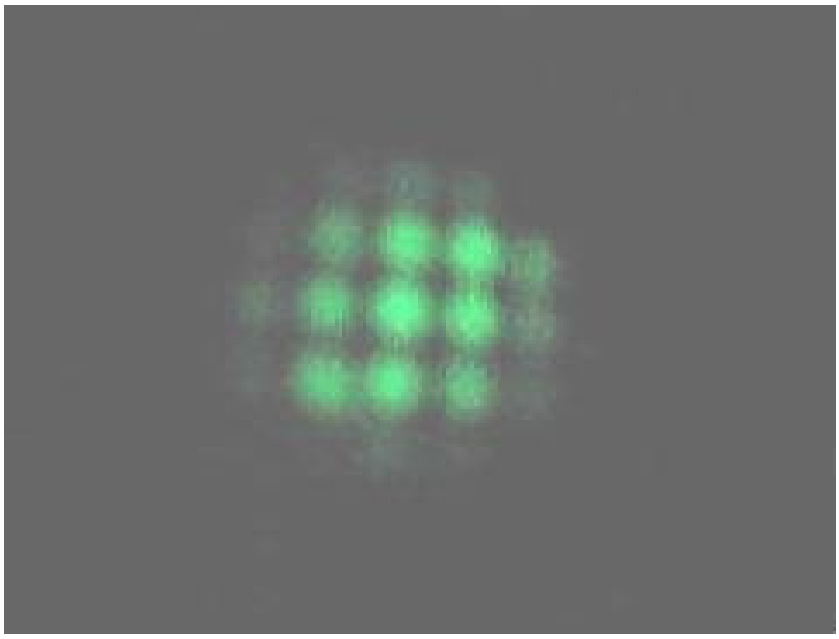

(b)

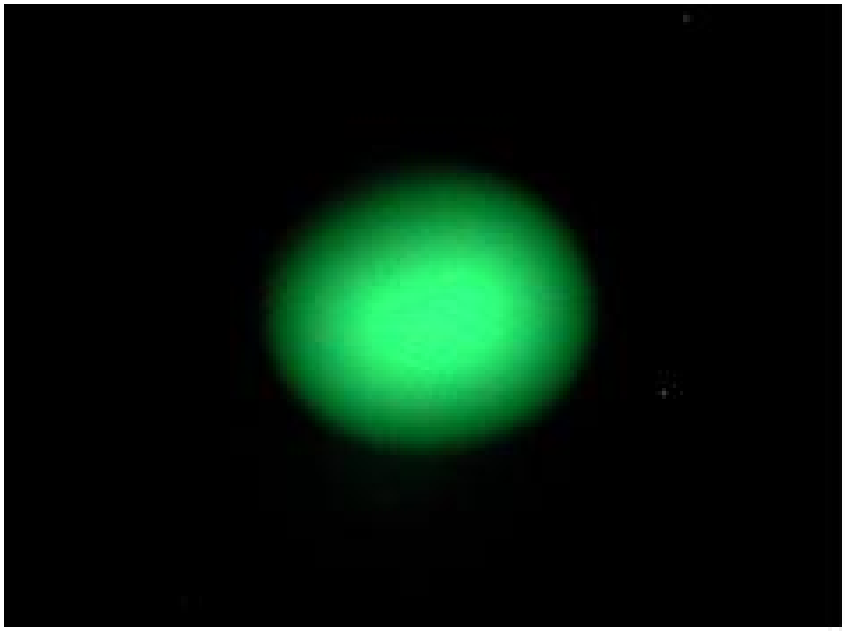

Figure 16: Shadow image (a) at sufficiently close distance (emission coming through many apertures) and (b) after bringing tip too close (emission coming through single aperture).

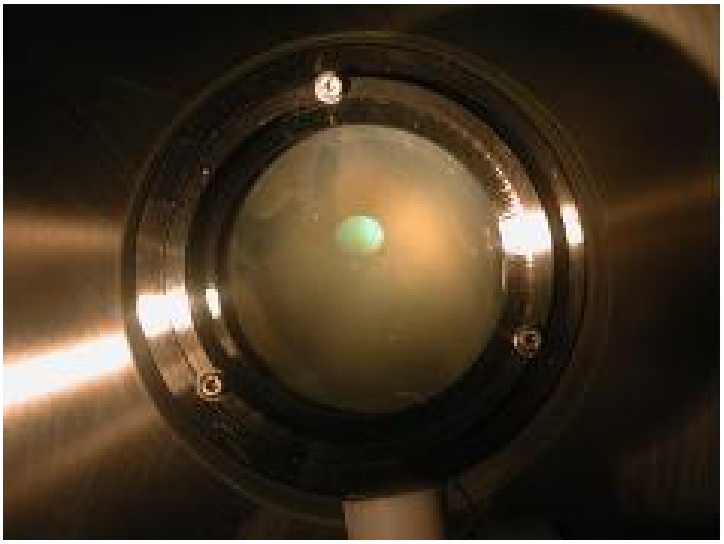

Figure 17: The same image as shown in Fig. 16(b). The screen dimensions with respect to the spot size are required for calculation of the magnification of the system.

3.3.4.5 Current stability and limitation on effective feedback

An experiment was performed at 5×10^{-8} mbar vacuum for more than 150 minutes. The current stability was measured at two places, at the grid and at the screen. The grid current of ~ 7.5 nA was used for feedback. The screen current, that is the emission through a single aperture of the TEM grid, was ~ 2 nA.

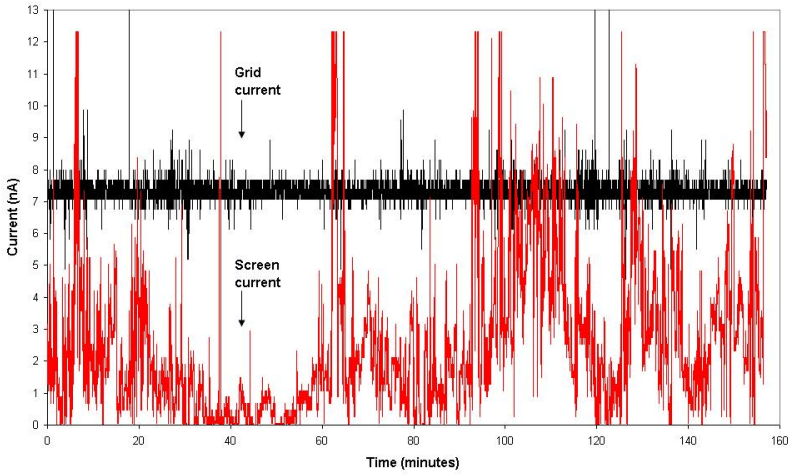

Figure 18: Field emission current stability; upper part is grid current, lower part is screen current.

As shown in Fig. 18, the grid current was fairly stable, but the screen current was not. This can be explained by considering several factors such as a) the ratio of the screen current to the grid current is >1 and therefore, there is no effective feedback b) the emission could be non-uniform (the field emission image was also observed to vary its

intensity) c) the thin plastic foil might not be stable during field emission. It could have melted or sputtered out as observed later.

3.3.4.6 Inspection of the used grid

The used TEM grid was observed through an optical microscope. The grid shows a considerable amount of irreversible damage (see Fig. 19). It also shows permanent and local bending towards the tip side (see figure 19(b)). This could have happened because of tip-foil attraction. It seems that the foil could have melted locally and also sputtered out. Therefore, the field emission current stability results shown in Section 3.3.4.5 cannot be considered as final or decisive.

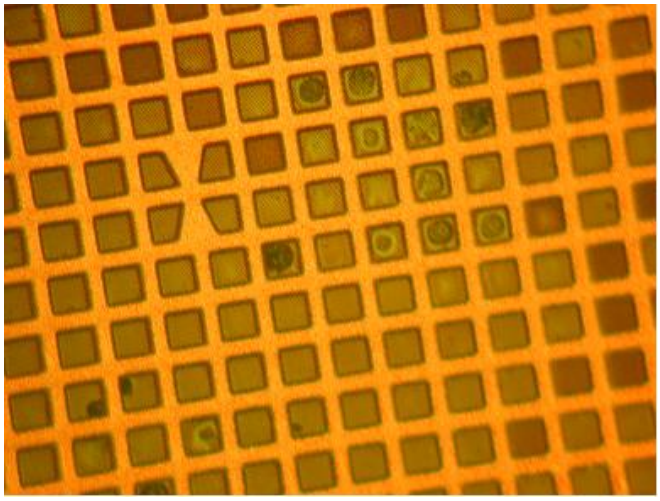

(a)

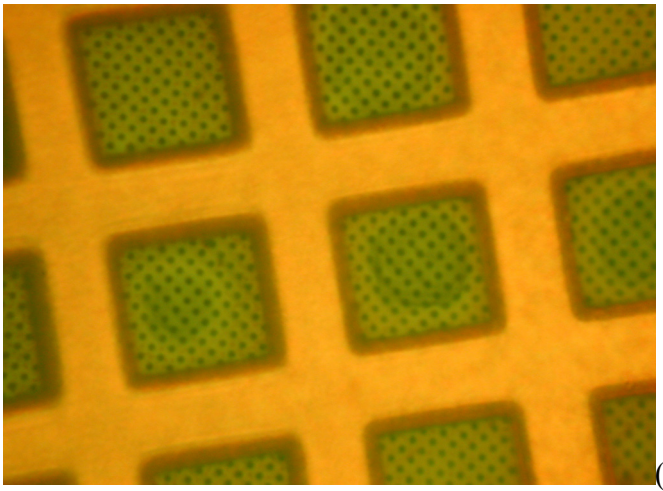

(b)

Figures 19: The used TEM-grid as observed through an optical microscope at two different magnifications.

The properties of the foil should not affect the current stability experiments. However, this suggests that the thickness of and material of the gas target in electron

impact gas ion sources are important parameters. A slightly thicker (~ 1-2 μm) foil made of silicon nitride should be used.

3.4 Discussion

As we are applying feedback on tip voltage, in order to maintain a constant electric current, voltage fluctuations will occur. We know that as far as useful cold electron guns are concerned, we do not want to vary the voltage and thus introduce an energy spread.

As discussed in section 3.3.3.4b., voltage fluctuations are due to two reasons the small fluctuations at very small time scale is to control current fluctuations, which are caused by local and temporary geometry change due to gas adsorption and desorption. Overall voltage variation at large time scale is due to sputtering and that we want to avoid. Therefore, one must operate the tip below sputtering threshold to maintain the voltage reasonably stable for overall period.

The small time scale voltage fluctuations are expected to be really small in amplitude. If voltage fluctuations are well below 1-2 volts, it may be acceptable. Different materials have different sputtering threshold. We hope that at < 50 Volt for carbon based materials; the sputtering should not be the problem. The tip should not be damaged at all by positive ion bombardment.

As we saw in Section 3.3.4.5, there was a problem of effective feedback. At least a few things can be improved. As shown in Fig. 20, a single assembly (of a cold field emission tip and a submicron gas ionization chamber) may form a rigid construction. The feedback on the tip voltage should be comprehensive, which means that even with this new construction the electron current (or the information) that is not collected by gate (1) or gate (2) must be fed back to the tip.

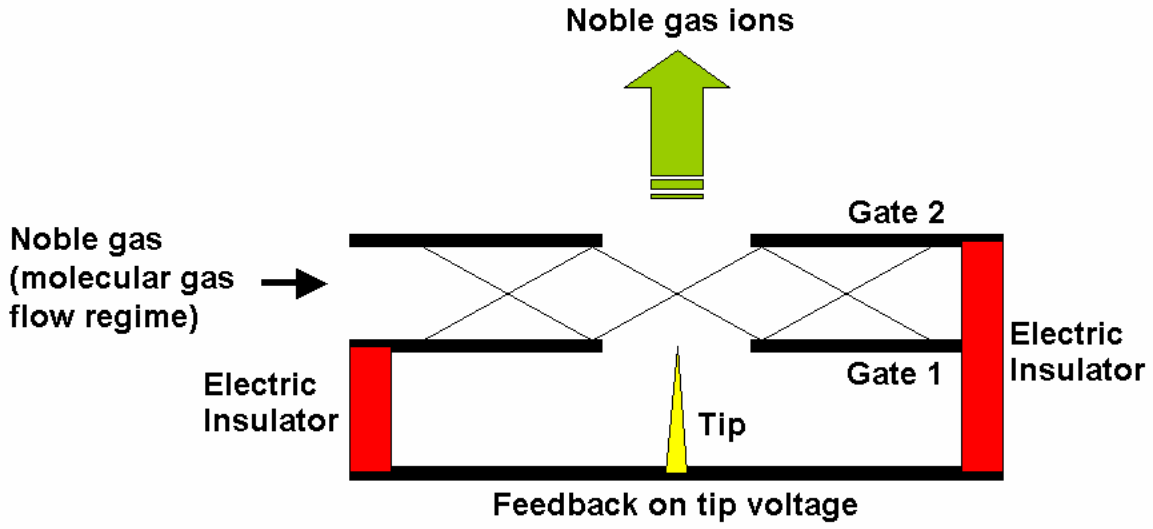

Figure 20: Cold field emission tip and submicron gas ionization chamber as one assembly.

3.5 Conclusion

Cold field emitters are notorious for their poor electron current stability. We believe that field electron impact noble gas ion source experiments should be performed with under the following three conditions:
a) Fabricate the tip and the gas ionization chamber as one assembly using lithographic techniques. The system would look like a double-gated field emitter array with a gas delivery system in between the two gates,
b) Operate the tip below the sputtering threshold of the tip material (as far as possible use carbon-based materials) and expect a good lifetime for the tip and
c) Use a comprehensive feedback on the tip voltage to have stable emission of electron current at extremely small voltage fluctuations (as we want the incident electron energy to be constant).

Acknowledgements

We thank J. Nonhebel, J.de Looff, R.Radhoe, S. van Berloo and P.W. van Harrewijn, for their technical assistance in building the experimental setup. This work was part of the research program of the "Stichting voor Fundamenteel Onderzoek der Materie" (FOM), which is supported by the "Nederlandse Organisatie voor Wetenschappelijk Onderzoek"(NWO).

References

[1] Wei Zhu, *Vacuum Microelectronics*, John Wiley & Sons, Inc., USA, (2001).

[2] F. Charbonnier, Appl. Surf. Science, **94/95**, 26 (1996).

[3] D. Temple, Mater. Sci. Eng., **R24**, 185 (1999).

[4] Ch. Kleint, Surf. Science, **200**, 472 (1988).

[5] L.W. Swanson, Surf. Science, **70**, 165 (1978).

[6] W.P. Dyke and W.W. Dolan, Advances in Electronics and Electron Physics, Edited by L. Marton, Academic Press Inc, Publishers, NY, **Vol. VIII**, 89 (1956).

[7] A. Lamouri, Y. Wang, G.T. Mearini, I.L. Krainsky, J.A. Dayton, Jr. W. Mueller, J. Vac. Sci. Technol. B, **14**, 2046 (1996).

[8] V.V. Zhirnov, A.B. Voronin, E.I. Givargizov and A.L. Meshcheryakova, J. Vac. Sci. Technol. B, **14**, 2034 (1996).

[9] W.B. Choi, D.S. Chung, J.H. Kang, H.Y. Kim, Y.W. Jin, I.T. Han, Y.H. Lee, J.E. Jung, N.S. Lee, G.S. Park and J.M. Kim, Appl.Phys.Lett., **75 (20)**, 3129 (1999).

[10] R. Collazo, R. Schlesser, Z. Sitar, Diamond and Related Materials **11**, 769 (2002).

[11] A.A.G. Driskill-Smith, D.G. Hasko and H. Ahmed, Appl.Phys.Lett, **71(21)**, 3159 (1997).

[12] JRA Cleaver and KCA Smith, Proc. Fifth Europen Congress on Electron Microscopy, p.18, Manchester 1972.

[13] S.Kanemaru, T.Hirano, K.Honda, J. Itoh, Appl. Surf. Science, **146**, 198 (1999).

[14] C. Py and R. Baptist, J. Vac. Sci. Technol. B, **12**, 685 (1994).

[15] J.D. Levine, R. Meyer, R. Baptist, T.E. Felter and A.A. Talin, J. Vac. Sci. Technol. B, **13**, 474 (1995).

[16] T.H.P. Chang, D.P. Kern, M.A. McCord and L.P. Muray, J. Vac. Sci. Technol, **9(2)**, 438 (1991).

[17] L.P. Muray, U. Staufer, E. Bassous, D.P. Kern and T.H.P. Chang, J. Vac. Sci. Technol, **9(6)**, 2955 (1991).

[18] T.H.P. Chang, D.P. Kern and L.P. Muray, J. Vac. Sci. Technol, **10(6)**, 2743 (1992).

[19] A. J. Melmed, J. Vac. Sci. Technol. B, **9(2)**, 601 (1991).

[20] J.P. Ibe, P.P. Bey, Jr. S.L. Brandow, R.A. Brizzolara, N. A. Burnham, D. P. DiLella, K.P. Lee, C.R.K. Marrian and R.J. Colton, J. Vac. Sci. Technol. A, **8**, 3570 (1990).

[21] R.Gomer, Field emission and field ionization, American vacuum society classics, 1993, NY, USA.

[22] P. Hoffrogge, H. Kopf and R. Reichelt, J. Appl. Phys, **90(10)**, 5322 (2001).

[23] C. Schiller, A.A. Koomans, T.L. Vanrooy, C. Schonenberger, H.B. Elswijk, Surf. Sci., **339 (3)**: L925-L930 OCT 1 1995.

[24] G.M. Shedd, H. Scmid, P. Unger, HW Fink and AD Dubner; Rev. Sci. Instrum. **64 (9)**, 2579 (1993).

[25] E. Ermantraut, K. Wohlfart and W. Tichelaar, Ultramicroscopy, **74**, 75(1998).

[26] H.W. Fink and C. Schonenberger, Nature, **398**, 407 (1999).

Chapter 4

Fabrication of sub-micron scale gas ionization chamber

A. H. M. Coppens, V. N. Tondare and P. Kruit

Abstract

Chapter 2 is about the thermal field electron noble gas ion source and Chapter 3 is about the cold field electron impact noble gas ion source, both the ion sources have been proposed for FIB applications. However, it was decided to fabricate the thermal field electron noble gas ion source to prove the concept.

The thermal field electron noble gas ion source needs a sub-micron scale (~100nm) gas ionization chamber. This chapter describes the fabrication process of the gas ionization chamber. The two apertures of the ionization chamber are made of a ~ 100-nm thick Si_3N_4 membrane, covered with a 10-nm thick molybdenum layer, and supported by a Si wafer. Both apertures are electrically isolated by electron beam resist (PMMA950K). We have made a gas ionization chamber of an aperture diameter of ~ 400 nm a spacing of ~ 400 nm. The results also show that it is possible to fabricate a gas ionization chamber with an aperture diameter of ~ 100 nm and a spacing of ~ 100 nm. The main advantage of the reported fabrication process is that several gas ionization chambers can be fabricated simultaneously.

4.1 Introduction

Thermal field electron impact ion sources consist of two components: 1) a Schottky source and 2) a sub-micron scale gas ionization chamber. The Schottky source has been well proven, which means that the degree of success of thermal field electron impact ion sources is manly dependent on the sub-micron scale gas ionization chamber.

There is a report of the fabrication of sub-millimeter scale gas ionization chambers for use in laser harmonic generation [1]. However, to the best of our knowledge, there is no published report on or proposal for the fabrication of sub-micron scale gas ionization chambers. Fabrication of sub-micron scale devices obviously involves lithographic fabrication steps.

The two apertures of the ionization chamber can be made of ~ 100-nm Si_3N_4 film, covered with a 10-nm thick molybdenum layer, and supported by Si wafer. Both apertures are electrically isolated by electron beam resist (PMMA950K).

Several clean-room instruments and techniques [2,3], such as spin coating, low-pressure chemical vapor deposition, wet etching, plasma etching, and magnetron sputtering deposition have been used in this fabrication process. An electron beam pattern generator machine and a dual (electron and ion) focused beam machine have also been used.

It is possible to fabricate several gas ionization chambers simultaneously. We can also choose the desired spacing and aperture diameter of the ionization chamber.

4.2 Fabrication process

The steps below describe the fabrication process of a sub-micron scale gas ionization chamber.

Step 1: - *Wafer with Si_3N_4*

A four inch Si <100> wafer with a thickness of ~ 450 μm was used to make 19 mm × 19 mm square pieces. As shown in Fig. 1, on both sides of the Si wafer, a ~ 100-nm thick layer of Si_3N_4 was deposited using the low-pressure chemical vapor deposition method.

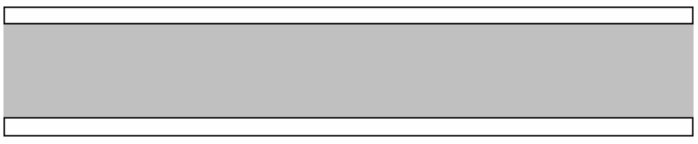

Figure 1: Si wafer with Si_3N_4 layer; ▭ is the Si wafer and ▭ is the Si_3N_4 layer.

Step 2: - *Etch window and alignment marks in Si_3N_4*

On both sides of this Si_3N_4-covered Si wafer, electron beam resist PMMA (thickness ~ 1 μm) was coated by a spin coating technique. The resist was baked at 175 ^oC for 30 minutes. An electron beam pattern generator machine was used to write pattern as well as

break lines at a size of 9.5 mm × 9.5 mm, so that four samples can be prepared in one process flow. A dose of 1300mc/cm^2 was used. As shown in Fig. 2, the middle pattern was a square of ~ 657 μm × ~ 657 μm and the others were squares of ~ 687 μm × ~687 μm. The electron beam resist (PMMA) was developed by putting the sample in a mixture of methylisobutylketone and isopropanol (ratio 1:3) for 70 seconds. It was rinsed in isopropanol and dried in a nitrogen gas jet. Then the exposed Si_3N_4 area was removed by using a CHF_3/O_2 plasma etch. The electron beam resist on both sides were removed using an acetone bath at 40 ^oC in an ultrasonic cleaner for about three minutes.

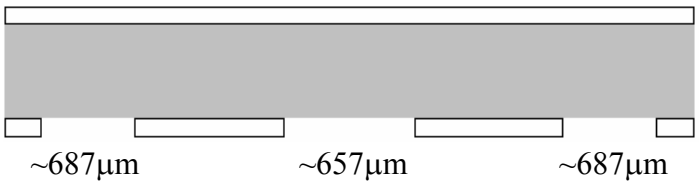

Figure 2: Pattern in Si_3N_4 layer (Si wafer size: 9.5 mm × 9.5 mm; ▭ is the Si wafer and ▭ is the Si_3N_4 layer).

Step 3: - *Wet etch Si*

To etch the exposed Si wafer (see step 2), a 40% KOH solution at 80 ^oC was used. Etching was carried out during approximately eight hours at an etch rate of ~ 1 μm/minute. This anisotropic etch resulted in pyramidal holes (Fig. 3), because Si is etched faster in the <100> direction than in the <111> direction. The middle square ended as a square with a size of ~ 25 μm × ~ 25 μm. The others ended as squares with a size of ~ 50μm × ~ 50 μm. So, in the middle of the wafer, we have a Si_3N_4 membrane (~25 μm × ~ 25 μm) supported by the Si wafer. Etching can be continued somewhat longer, as the KOH solution does not etch Si_3N_4. The over-etching helps to remove residues of Si on the membrane. The sample was cleaned (removing traces of KOH) using HCl and then by using demineralized water and then the sample was rinsed in isopropanol again and carefully dried in a nitrogen gas jet. Two of such a samples were used to make a double aperture.

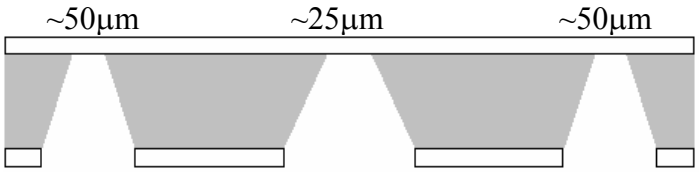

Figure 3: Anisotropic wet etching of Si; ▭ is the Si wafer and ▭ is the Si_3N_4 layer.

Step 4: - *For top sample open alignment windows*

The middle pyramidal hole was covered with (easily removable) photoresist, as shown in Fig. 4. It was baked at 90 ^{o}C for 30 minutes. Then the exposed Si_3N_4 area was removed by using a CHF_3/O_2 plasma etch. The photoresist was removed using an acetone bath at 40 ^{o}C for about three minutes.

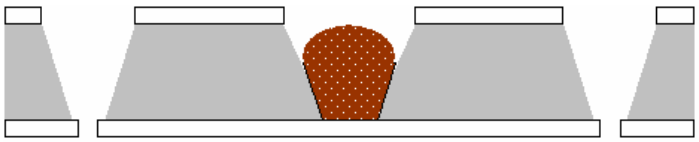

Figure 4: CHF_3/O_2 plasma etch of the exposed Si_3N_4 area; is the Si wafer, is the Si_3N_4 layer, and is the photoresist.

Step 5: - *Deposition of metal layer on the top as well as the bottom sample*.

As shown in Fig. 5, a metal layer (molybdenum) with a thickness of 10 nm was deposited on both the top and bottom samples by a magnetron sputtering deposition technique.

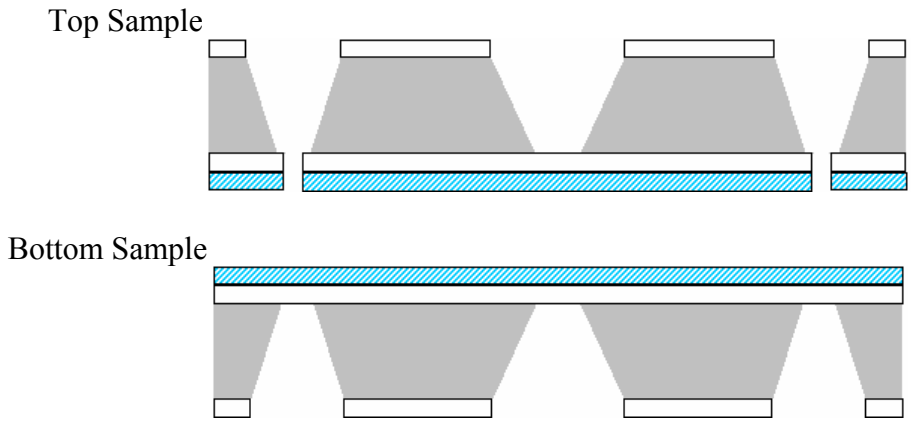

Figure 5: Deposition of metal layer; is the Si wafer, is the Si_3N_4 layer and is the molybdenum metal layer).

Step 6: - *Resist spin and patterning of bottom sample*

The electron beam resist (PMMA950K) was deposited on the bottom sample using a spin coating technique. The layer thickness, ~ 400 nm, was optimized using alpha step measurement. An electron beam pattern generator machine was used to write a pattern in the electron beam resist as shown in Fig. 6. A dose of 1300mc/cm^2 was used. The electron beam resist was developed by putting the sample in a mixture of

methylisobutylketone and isoprpanol (ratio 1:3) for 70 seconds. Finally, the sample was rinsed in isopropanol and dried in a nitrogen gas jet.

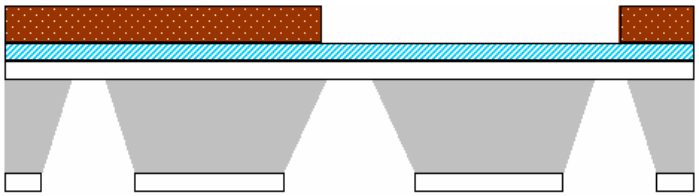

Figure 6: Pattern in the electron beam resist (is the Si wafer, is the Si_3N_4 layer, is the PMMA950K, and is the molybdenum metal layer)

Using an optical microscope without backlight, the patterns created in the electron beam resist can be seen (Fig. 7) as follows. The square structure is the middle pyramidal hole, which supports the Si_3N_4 membrane (~ 25 μm × 25 μm). The structure that looks like a test-tube is the gas line (~ 100 μm × 4 mm). The gas line perfectly covers the whole Si_3N_4 membrane (~ 25 μm × 25 μm). The rest of the area is the electron beam resist (with a thickness of ~ 400 nm) without pattern.

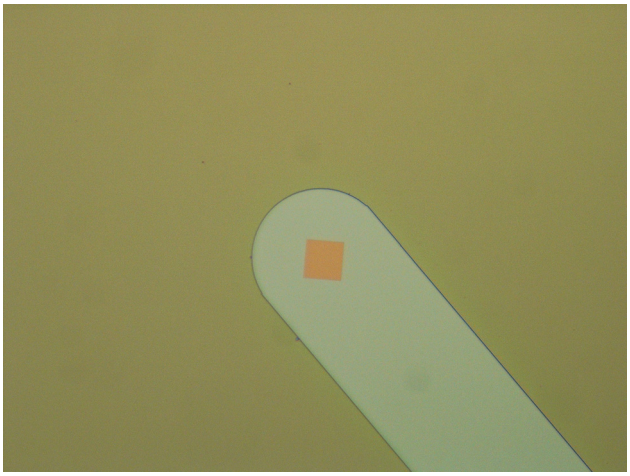

Figure 7: Optical micrograph of the pattern, made in the PMMA950K.

Step 7: - *Align both samples - bond samples together with resist*

In step 7, the top sample (see step 4 + molybdenum metal layer) was put on the bottom sample (see step 6) under an optical microscope using its backlight.

It can be seen in the optical micrograph (Fig. 8) that light passes through the top and bottom sample, and that is through the Si_3N_4 membrane (~ 100 nm) plus molybdenum metal layer (~10 nm) of the top as well as the bottom sample. The alignment of these top and bottom samples was done manually using the optical microscope. Figure 8 shows the first attempt of such an alignment. It is clear that the

middle pyramidal holes (~ 25 μm × 25 μm) are not perfectly aligned. However, as stated in step 6, the gas line covers a wider area than this ~ 25 μm × 25 μm.

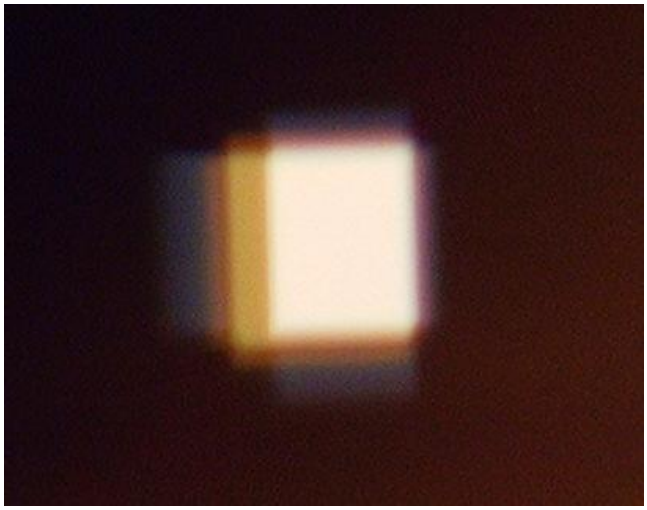

Figure 8: Optical micrograph using the backlight. The middle bright square shows that light is coming through the Si_3N_4 membranes of both the top and bottom sample, which were aligned together.

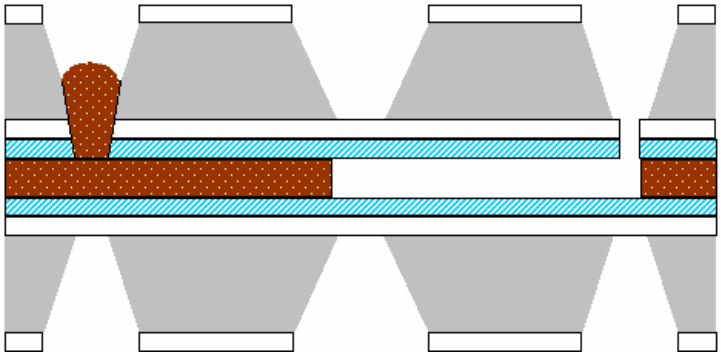

Figure 9: Bonding the two samples with PMMA950K; is the Si wafer, is the Si_3N_4 layer, is the PMMA950K, and is the molybdenum metal layer.

As shown in Fig. 9, the pyramidal hole (without the gas line) was covered with the electron beam resist and then the structure was baked at 90 ^{o}C for 30 minutes. This holds the top and bottom samples together.

Step 8: - *Focused ion beam work*

In step 8, a dual beam machine (an electron beam + a Ga ion beam) was used to observe the sample (prepared up to step 7) as well as to drill a sub-micron hole through the middle pyramidal holes (~25 μm × 25 μm).

First of all, a few tests were carried out on a test sample to find out whether there are really two separate thin films – both consisting of a Si_3N_4 membrane plus a molybdenum metal layer – separated by the ~ 400-nm thick electron beam resist. A high-energy (20 keV) electron beam was used to observe the sample (prepared up to the step 7). The scanning electron micrograph is shown in Fig. 10. It matches with the optical micrograph shown in Fig. 8, as one can see there is a little misalignment. However, it also shows that there are indeed two separate thin films.

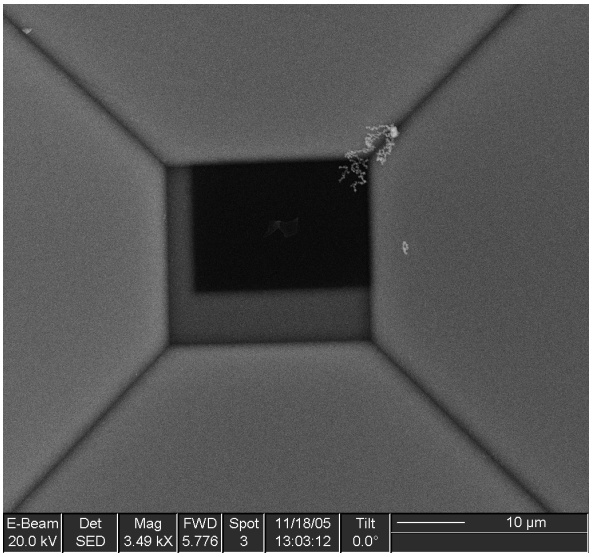

Figure 10: Scanning electron micrograph. A high-energy electron beam (~ 20 keV) was used. The misalignment of the top and bottom sample seen in Fig. 8 can be seen here more clearly.

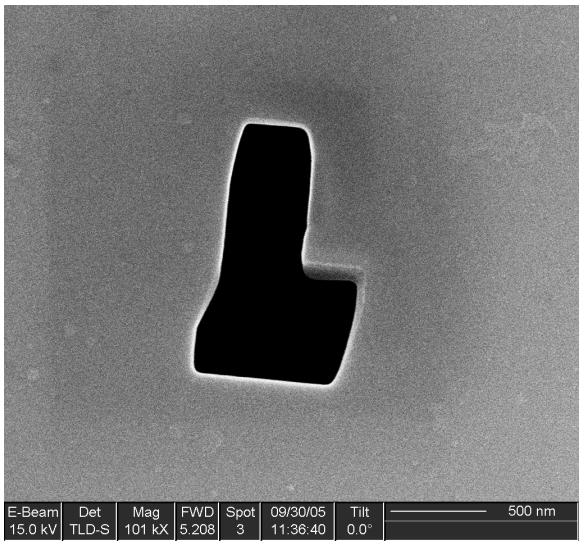

Figure 11: An arbitrary shape made (from the top side) through both layers using a Ga ion beam.

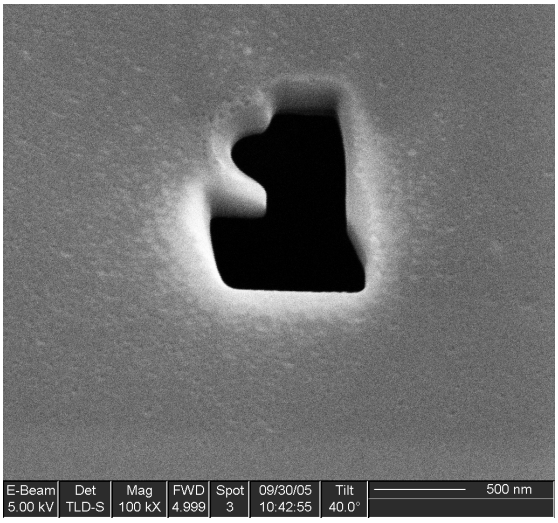

Figure 12: Another arbitrary shape made from the bottom side, approximately at the same coordinates as in Fig. 11, in such a way that the ion beam did not touch the top side of the sample.

To further confirm the presence of two separate layers, an arbitrary shape was made (from the top side) through both layers of the sample using a Ga ion beam (see Fig. 11). Then, from the bottom side, approximately at the same coordinates another arbitrary shape was made in such a way that the ion beam did not touch the topside of the sample (see Fig. 12).

The image made in the scanning electron microscope (SEM) from the top side (Fig. 13) shows that indeed there are two thin films with spacing in between.

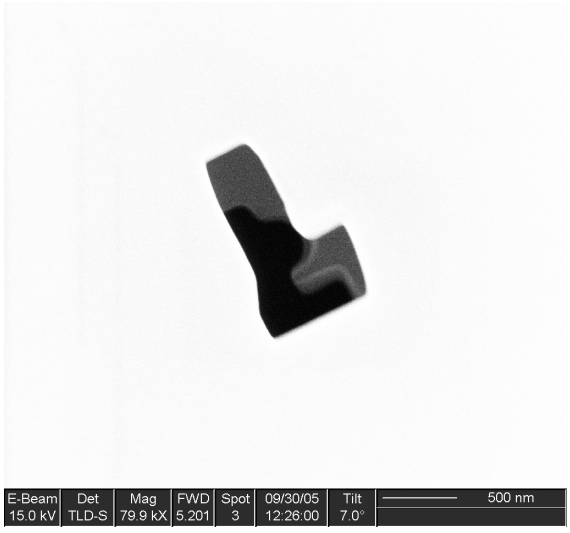

Figure 13: The scanning electron micrograph shows that indeed there are two thin films with spacing in between.

After we carried out the experiments on a test sample, a fresh sample was used (prepared up to step 8, see Fig. 9) to drill ~ 400-nm holes through both Si_3N_4 membranes in one line, as shown in Fig. 14.

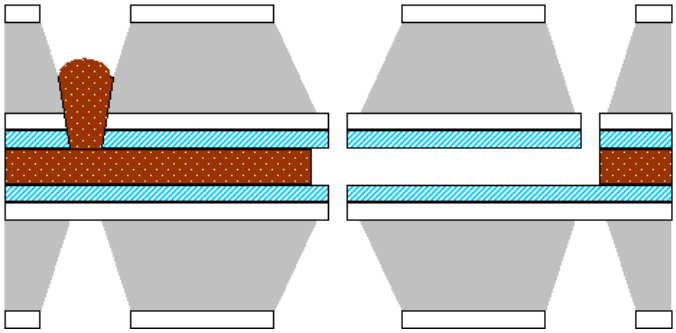

Figure 14: Holes drilled through membranes; is the Si wafer, is the Si_3N_4 layer, is the PMMA950K, and is the molybdenum metal layer.

Step 9: - *Deposition of a metal layer on both sides*

As shown in Fig. 15, in step 9 a metal layer (molybdenum) with a thickness of 10 nm was deposited on both the top and bottom sides of the sample (prepared up to step 8, see Fig. 14) by a magnetron sputtering deposition technique. The outer edges of the wafers were covered during deposition to avoid metal deposition on these edges and to prevent electrical contact of the membranes.

Thus one can fabricate a gas ionization chamber that consists of two sub-micron apertures electrically isolated from each other by sub-micron spacing. A different spacing can be created by adjusting the thickness of the electron beam resist (see step 6). Furthermore, different aperture sizes can be made using a focused ion beam. We have chosen the diameter of the aperture and spacing approximately same.

For very small aperture sizes (< 100 nm), it would be advantageous to have a Si_3N_4 membrane thinner than 100 nm.

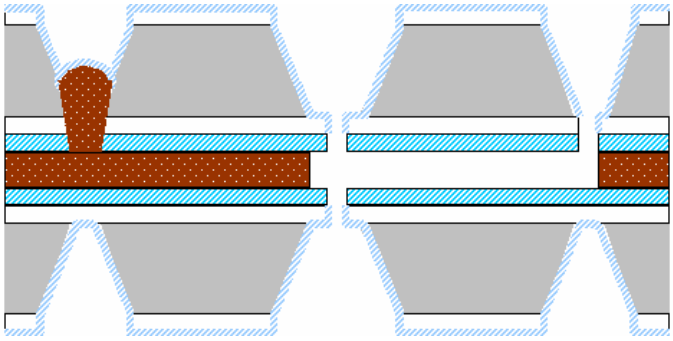

Figure 15: Metal layer deposited on top and bottom; is the Si wafer, is the Si_3N_4 layer, is the PMMA950K and is the molybdenum metal layer.

4.3 Results and Conclusion

(a)

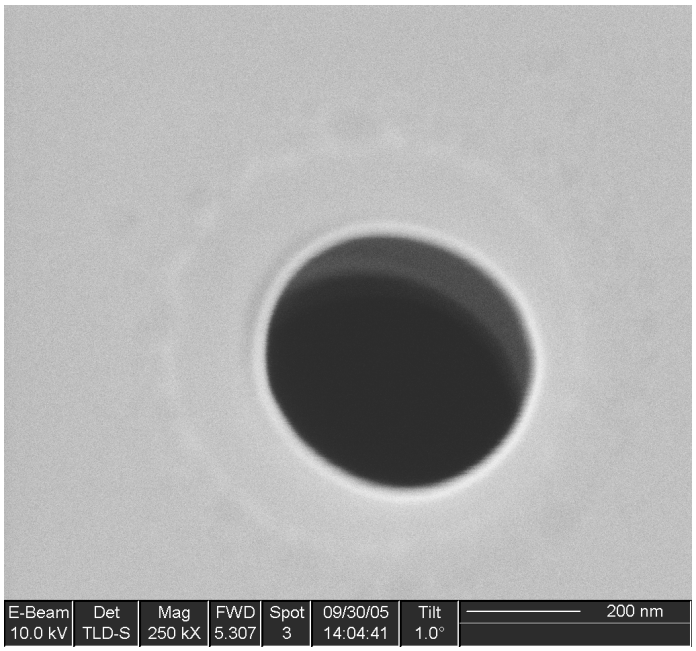

(b)

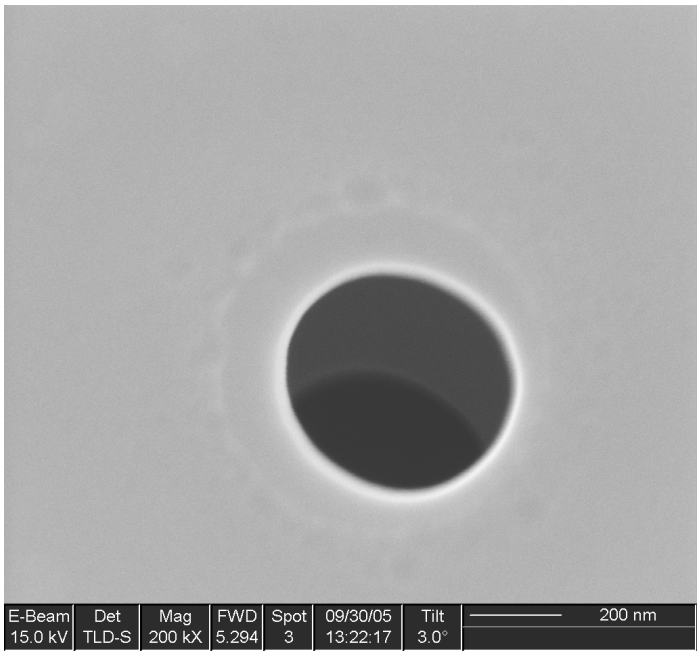

Figure 16: Scanning electron micrograph of the gas ionization chamber (aperture diameter is the same as spacing ~ 400 nm). Both top and bottom apertures can be distinguished. (a) one-degree-tilt, (b) three-degree tilt.

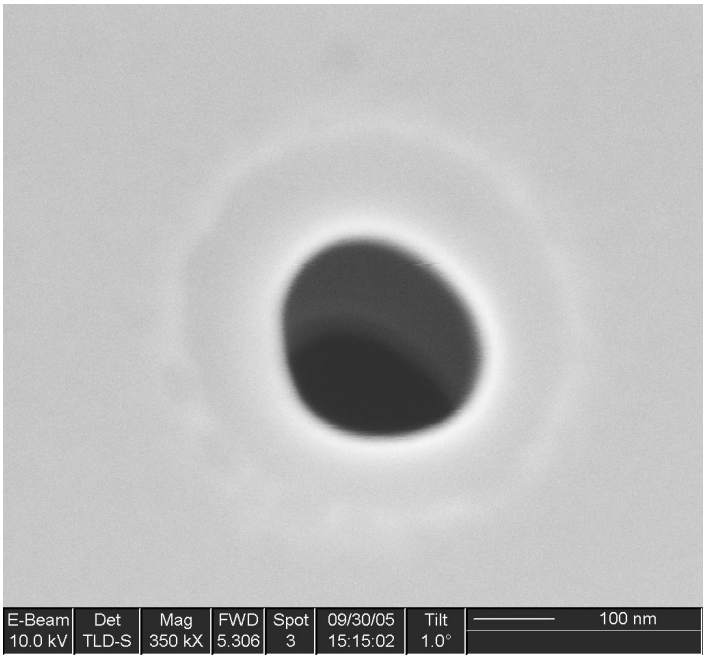

Figure 17: Scanning electron micrograph of the gas ionization chamber (aperture diameter is ~ 200 nm and spacing is ~ 400 nm). Both top and bottom apertures can be distinguished.

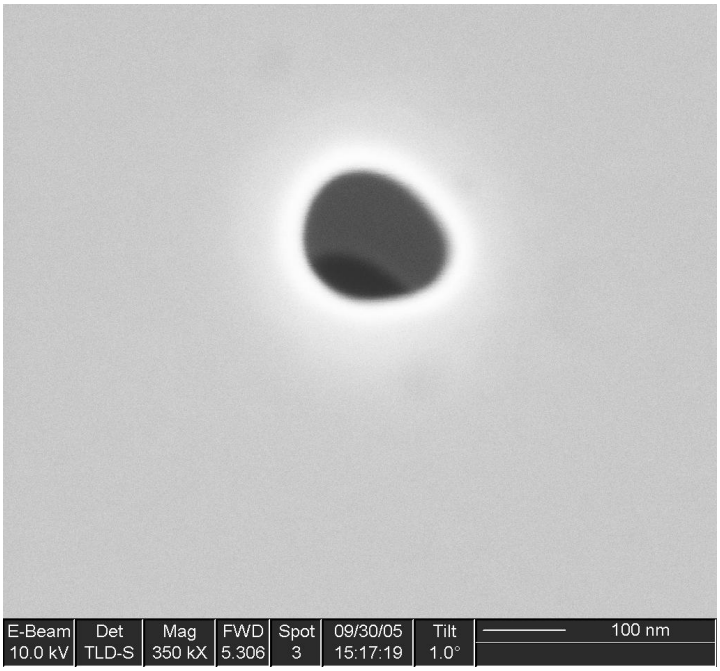

Figure 18: Scanning electron micrograph of the gas ionization chamber (aperture diameter is ~100 nm and spacing is ~ 400 nm). Both top and bottom apertures can be distinguished.

For the first ion source experiment, we have made a gas ionization chamber with an aperture diameter of ~ 400 nm, approximately the same as the spacing. The SEM image (see Fig. 16 (a)) shows the top aperture as well as the bottom aperture at a tilt of one degree. The bottom aperture can be seen more clearly with a tilt of three degrees (see Fig. 16 (b)). Two separate membranes can be distinguished.

The experiments on the test sample also showed that the entire gas line can remain opened and the entire structure can support the two membranes.

On a sample, which had a spacing of ~ 400 nm (electron beam resist), we have also tried to make apertures with a diameter of 200 nm (see Fig. 17) and 100 nm (see Fig. 18) .

One of the advantages of this fabrication process is that several gas ionization chambers can be made in one batch. Later on they can be inspected and can be used for the ion source experiments.

Acknowledgements

We thank DIMES, TU Delft, The Netherlands for providing the clean-room micro-fabrication facilities. This work was part of the research program of the "Stichting voor Fundamenteel Onderzoek der Materie" (FOM), which is supported by the "Nederlandse Organisatie voor Wetenschappelijk Onderzoek"(NWO).

References

[1] J. Peatross and D.D. Meyerhofer, Rev. Sci. Instrum., **64(11)**, 3066 (1993).

[2] N. Maluf and K. Williams, *An Introduction to Microelectromechanical Systems Engineering* (Boston: Artech House 2004).

[3] M.J. Madou, *The Fundamentals of Microfabrication : The Science of Miniaturization,* (Boca Raton : CRC Press, 2002).

Chapter 5

Experimental setup of thermal field electron impact noble gas ion source

V. N. Tondare, M. S. Bronsgeest and P. Kruit

Abstract

This chapter describes the experimental setup of the thermal field electron impact gas ion source for focused beam applications. The ion source mainly consists of an electron delivery system into the double aperture at energies <1000eV. The sub-micron gas ionization chamber is attached to the gas delivery system. The extracted ion beam can be focused on a target. The focusing of electron beam into the gas ionization chamber as well as the focusing of the extracted ion beam onto the target can be done with the help of four sets of quadrupole deflectors and two separate secondary electron detectors. An energy analyzer can be introduced in the same system. The system should be able to perform a proof-of-concept ion source experiment.

5.1 Introduction

As stated in chapter 2, a thermal field electron impact noble gas ion source needs incident electron energy < 1000eV for effective ionization. Most of the commercial electron microscopes are designed for high-energy electron beams. Therefore, the first task was to build a low-voltage electron optical system equipped with a Schottky source. As the Schottky source is far away from the gas ionization chamber, it should function in a normal way in ultra high vacuum ($p \leq 1\times10^{-9}$ mbar). As there is a facility to scan the electron beam over the gas ionization chamber as well as to detect secondary electrons, the whole construction of electron delivery system is equivalent to a low-voltage scanning electron microscope. The gas ionization chamber attached with gas delivery system can be inserted at the right place. Although we will use noble gas (argon) for the proof-of-concept experiment, in principle, other gases can be also used. There is also a facility to focus, scan and detect the extracted ion beam over a target and that means an ion optical column has also been built.

The whole system has been designed using ELD [1] and SIMION-3D electron optical simulation software [2].

5.2 Design of Schottky electron gun for the gas ion source

For the operation of the gas ion source an electron beam is required to focus into the double aperture. The electron beam will be generated by extracting electrons from a Schottky source. Behind the extractor there is a gun lens that is used to decrease the half opening angle of the beam, a set of deflectors, and finally a probe-forming lens that focuses the electron beam onto the gas containing double aperture. Some of the components of the probe-forming lens had been already designed and manufactured for a different purpose and a Schottky source with a tip radius of 0.5 μm was ready for use. To reduce manufacturing time it was desirable to use Schottky gun components that are available within the group and adjust these to meet the requirements. A disadvantage of the gun components available was that the alignment was not very robust. Furthermore a beam-limiting aperture was lacking: the current passing the extractor (typically a few μA's) had to be reduced to ~100 nA before hitting the double aperture.

The gun geometry was largely determined by the components that had already been manufactured for different projects. Changes to improve robustness and to incorporate a beam-limiting aperture should preferably be as small as possible. A beam-limiting aperture close to the tip is desirable to cut the current as soon as possible and thus reduce trajectory displacement. The voltage on the first electrode of the probe forming lens is the same as that on the last electrode of the gun lens and should be ~5 kV. To prevent electrical breakdown the potential difference between electrodes in the gun lens or probe forming lens should not exceed 8 kV. The distance between gun and this probe-forming lens was unknown and estimated to be 50 mm. The voltage range for the last electrode of the probe forming lens and the double aperture is 50-1000 V. The current

in the beam that is focused into the double aperture should be ~100 nA. The probe size on the double aperture should be ~100 nm.

The temperature of the source should be 1800 K (recommended by the manufacturer) or below. The extraction voltage has a maximum of 5 kV (limitation of setup). The bottom limit is ~4 kV: theory predicts tip dulling for extraction voltages that give lower fields. For high fields faceting can be expected. Both effects change the source performance. Of course the rate of change depends on the tip temperature. The tip radius of the available Schottky source and the operating conditions determine the virtual source size contributing to the probe size. The virtual source size for a tip radius of 0.5 μm is ~ 30 nm at temperatures between 1700-1800 K and for angular intensities between 0.2 and 0.4 mA/sr.

The size of the probe on the double aperture containing 50% of the current (FW50) (image side) can be calculated from the probe size on the object side (where the beam originates) and the magnification of the lens system. The probe size on the object side can be calculated from the (virtual) source size and contributions due to diffraction and spherical & chromatic aberration using the root power sum algorithm. The FW50's of the different aberration contributions [3] are given by

$$d_A = 0.54 \frac{h}{\sqrt{2me}} \frac{1}{\sqrt{U}\alpha} \qquad \text{(Diffraction)} \qquad (1)$$

$$d_s = \frac{1}{2}\left(\frac{1}{2}\right)^{3/2} C_s \alpha^3 \qquad \text{(Spherical aberration)} \qquad (2)$$

$$d_c = 0.6 C_c \frac{\Delta U_{FW50}}{U} \alpha \qquad \text{(Chromatic aberration)} \qquad (3)$$

Where, α is the half opening angle of the beam, U is the extraction potential and ΔU_{FW50} is the FW50 of the energy spread of the beam. C_s and C_c are the spherical and chromatic aberration coefficients respectively.

The total probe size on the double aperture can be found from

$$d_p = M \sqrt{\left(\left(d_A^4 + d_s^4\right)^{1.3/4} + d_v^{1.3}\right)^{2/1.3} + d_c^2} \qquad (4)$$

Where, d_v is the virtual source size and M the total magnification of the lens system of the object side probe size.

5.2.1 Original design of the Schottky gun

First the spherical and chromatic aberration coefficients are calculated for the original design, without beam limiting aperture. The design is given in figure 1.

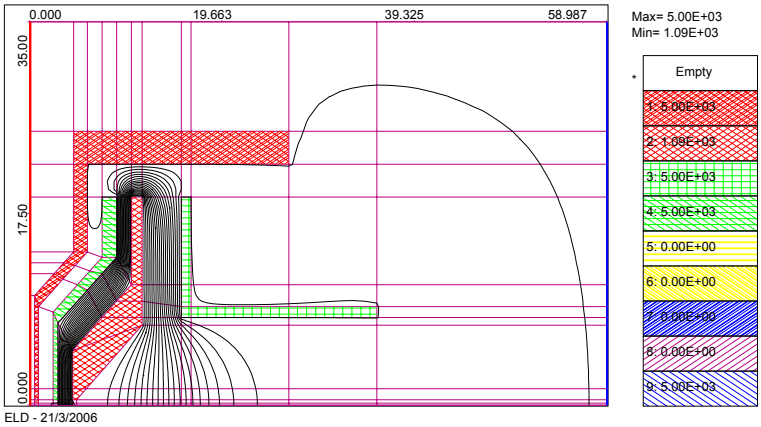

Fig. 1. Original design of the Schottky gun by Daniël Moonen (CPO-TN-Tudelft-2004).

In Fig. 1 the extractor 'bell' & the second extractor plate, and the tube like electrode and the end, are at 5 kV. At the borders on the left and right vertical sheet electrodes are implemented at 5 kV. The lens openings of both extractor plates are 0.38 mm in diameter. The hole in the focusing electrode is 1 mm. The distance between the electrodes is 1.5 mm, which is realized by an insulating ring. Between the focusing electrode and the final electrode there are two rings yielding a total spacing of 4 mm. Figure 1 shows the equipotential lines for a focusing voltage of 1089 V, which gives a lens action such that the beam at 5 kV will leave the gun parallel to the axis. The aberration coefficients for this situation are 82 mm (C_s) and 19 mm (C_c).

5.2.2 The modified Schottky gun design for the ion source

The original design should be more robust with respect to alignment and contain a beam-limiting aperture. The alignment will become more robust when the lens openings are larger. This will also reduce the spherical aberration coefficient. The beam-limiting aperture close to the tip is desirable, to cut the current as soon as possible and thus reduce trajectory displacement. In the new design one of the two spacers between focusing electrode and last electrode is removed. The lens opening of the focusing electrode has increased to a diameter of 3 mm. The second extractor plate has been changed to hold an aperture (create on extractor side centring hole of 3.05 mm in diameter for aperture (0.2 mm deep), glue aperture in centring hole). The new design is given in figure 2.

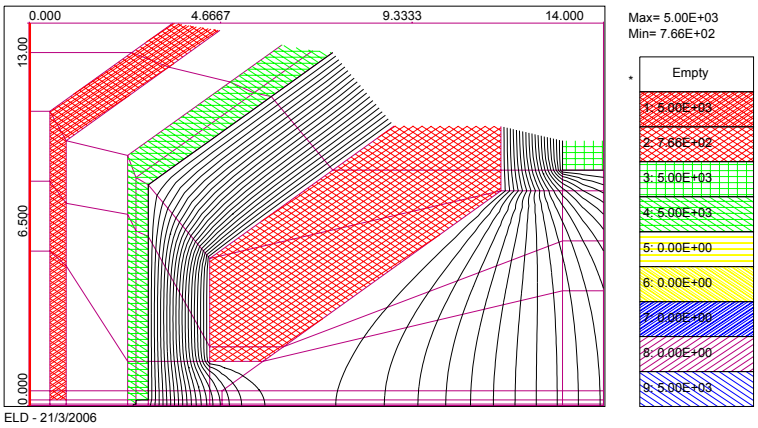

Fig. 2. New design Schottky gun for gas ion source.

The aberration coefficients for lens action that gives a beam leaving the gun parallel to the axis are 29 mm and 24 mm for C_s and C_c respectively. The focusing electrode is at 769 V for this setting. Figure 3 shows for a series of gun lens settings the image position and the aberration coefficients.

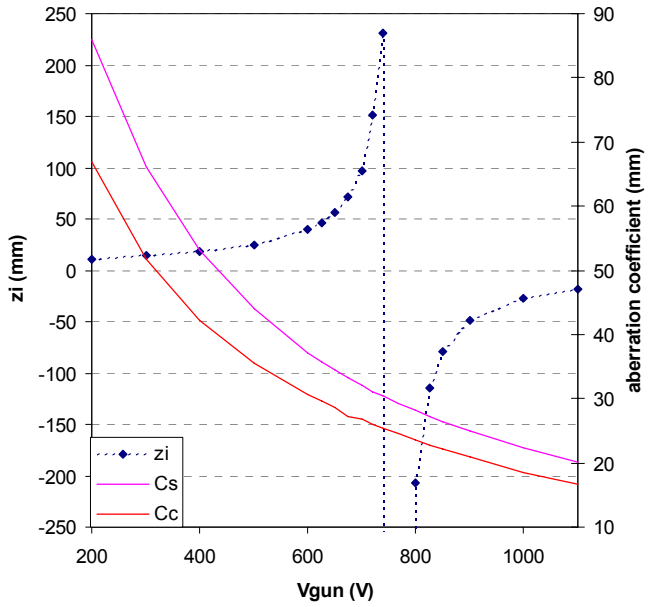

Fig. 3. Image position and aberration coefficients for different gun lens settings. Extraction voltage is 5 kV.

Figure 3 shows a real image for a gun lens voltage below ~769 V. The aberration coefficients increase with decreasing voltage.

5.2.3 Diameter of beam-limiting aperture

The aperture diameter can be calculated from the aperture position with respect to the source, the angular intensity the source will be operated at, and the desired beam current. At the operating temperature recommended by the manufacturer the bottom limit for the extraction voltage (determined by the theoretical force balance) provides a bottom limit of the angular intensity of 0.2 mA/sr. The upper limit is determined by the setup and is at this temperature 0.4 mA/sr.

Assuming an angular intensity of 0.3 mA/sr the half opening angle of a beam containing 100 nA is 10 mrad. For an aperture at 2.4 mm away from the source this requires an aperture diameter of 50 μm. When more or less current is required, the angular intensity should be varied by either changing the source temperature or the extraction voltage. Increasing temperature above 1800 K is discouraged. It will speed up shape change processes and reduce the emitter lifetime.

5.2.4 Aberration contributions

A proper design should yield gun lens aberrations that are at least smaller than the virtual source size. From the half opening angle of 10.4 mrad and the virtual source size it can be calculated that the spherical aberration coefficient C_s should be smaller than 150 mm. To estimate the chromatic aberration contribution the energy spread and the extraction voltage are required. For an extraction voltage of 5 kV and a tip radius of 0.5 micron the FW50 of the energy distribution is estimated to be 0.2-0.3 eV at 0.2-0.4 mA/sr (FEI Company data Dec 21, 2005). To have a contribution from chromatic aberration smaller than the virtual source size, the chromatic aberration coefficient C_c should be smaller than 80 mm. For an extraction potential of 4 kV this would decrease to 64 mm.

Figure 3 shows that for the new design, with beam-limiting aperture and improved robustness, both the spherical and the chromatic aberration coefficient are smaller than 150 mm and 80 mm respectively for gun lens settings between 200 and 1100 V.

The contribution from diffraction for extraction potentials between 4 and 5 kV is ≤ 1 nm.

5.2.5 Tuning beam current

For an aperture diameter of 50 μm the half opening angle of the beam penetrating the aperture is 10.4 mrad. The relation between beam current behind the aperture and the extraction voltage and angular intensity for two different temperatures of the source is given in figure 4. Changing the beam current by changing the tip temperature or the extraction voltage will have an effect on the chromatic aberration contribution, because the energy spread of the electrons in the beam will change. The total energy spread is a combination of the intrinsic energy spread and the Boersch effect. The changes in the intrinsic energy spread are considered to be negligible for temperatures between 1600 and 1800 K. Changes of the contribution from the Boersch effect however are expected to be larger. For a lower angular intensity the Boersch contribution is smaller, yielding a

smaller total energy spread at lower temperatures. This will reduce the chromatic aberration contribution to the probe size. This effect has been ignored in the calculations.

For a different extraction voltage also the potential in the denominator of the chromatic aberration contribution changes. This means that at higher angular intensity the Boersch effect will increase, increasing the energy spread in the numerator, but at the same time the denominator will also increase.

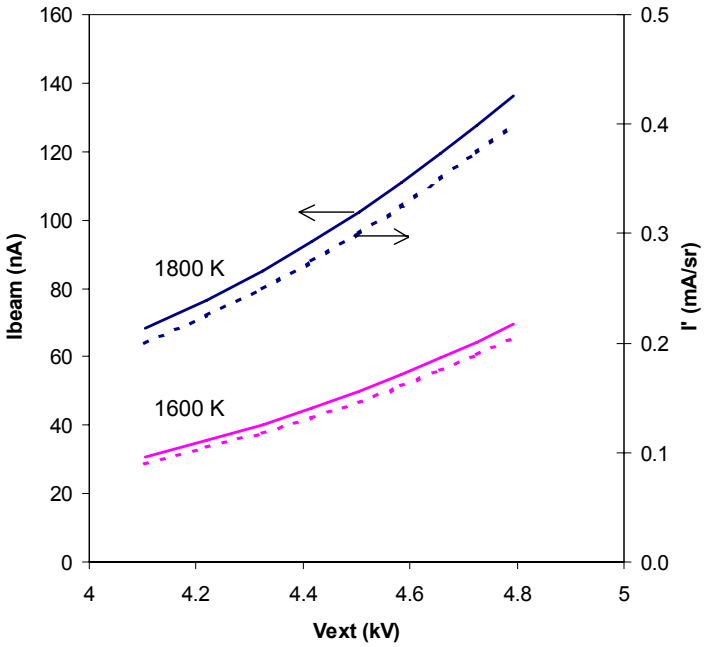

Fig. 4. Expected beam current behind current-limiting aperture versus extraction voltage for two temperatures of the source. Trajectory displacement has been neglected. This could give lower beam current at higher extraction voltage / angular intensity. (Curves constructed using equations from [4] and [5], N.B.: datasheet from FEI Company for source that will be used predicts slightly higher extraction voltages required for the same I')

5.2.6 Probe-forming lens

The beam leaving the gun lens will be focused onto the double aperture with a probe-forming lens close to the double aperture. The design is given in figure 5. In figure 5 the purple vertical line on the right hand side indicates the position of the double aperture, where the last lens should focus the beam.

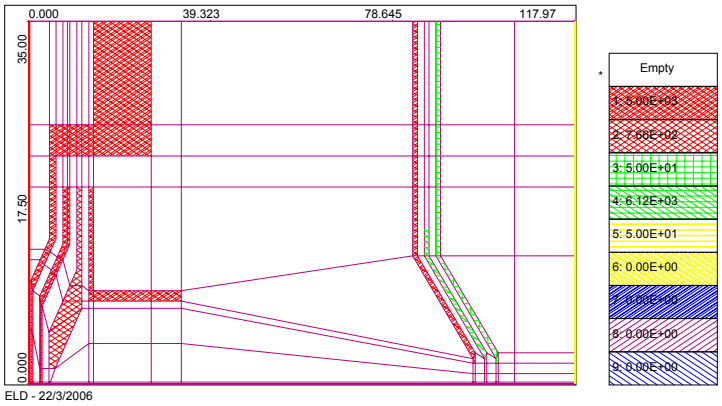

Fig. 5. Lens design for electron gun and probe forming lens that focuses the electron beam onto the gas containing double aperture.

5.2.7 Aberration contributions

The probe-forming lens consists of three identical electrodes with a lens opening of 4 mm in diameter. As an example the aberration coefficients for this lens are shown in figure 6 for different settings of the gun lens and a voltage of the double aperture of 1000 V.

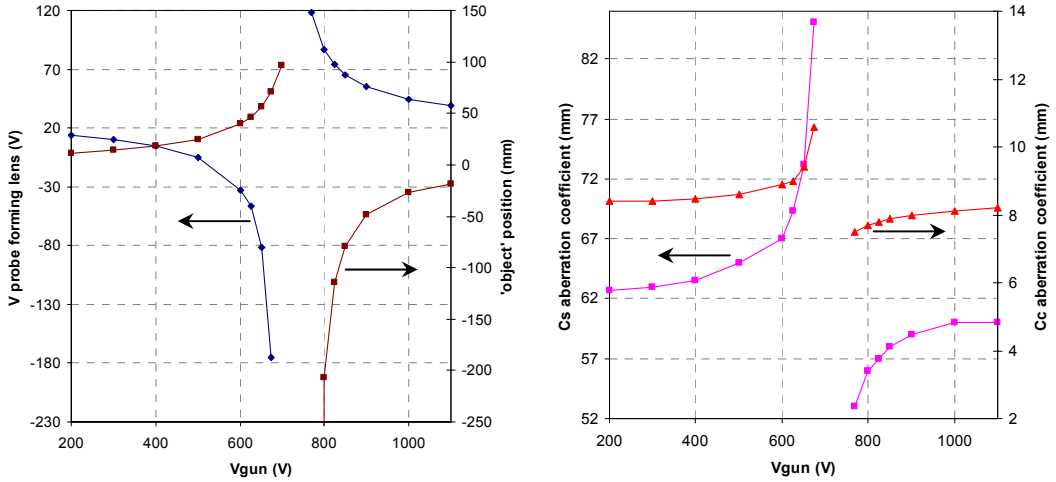

Fig. 6. Probe lens potential and aberration coefficients of probe forming lens for different settings of gun lens. Focus at double aperture. Extraction potential 5 kV, double aperture at 1 kV.

5.2.8 Aberrations and magnification for total lens system

To compare the aberration coefficients of the probe-forming lens to that of the gun lens, the aberration coefficients found for the probe-forming lens can be translated into aberration coefficients on the source side using

$$C_{s,o} = \frac{1}{M^4}\left(\frac{V_{ext}}{V_{da}}\right)^{3/2} C_{s,i} \qquad \text{and} \qquad C_{c,o} = \frac{1}{M^2}\left(\frac{V_{ext}}{V_{da}}\right)^{3/2} C_{c,i} \qquad (5)$$

in which M is the magnification of the total lens system of the source (gun lens plus probe-forming lens) onto the double aperture. Figure 7 shows the aberration contributions of the probe-forming lens on the object side together with the aberration contributions of the gun lens, this time for a voltage of the double aperture of 300 V.

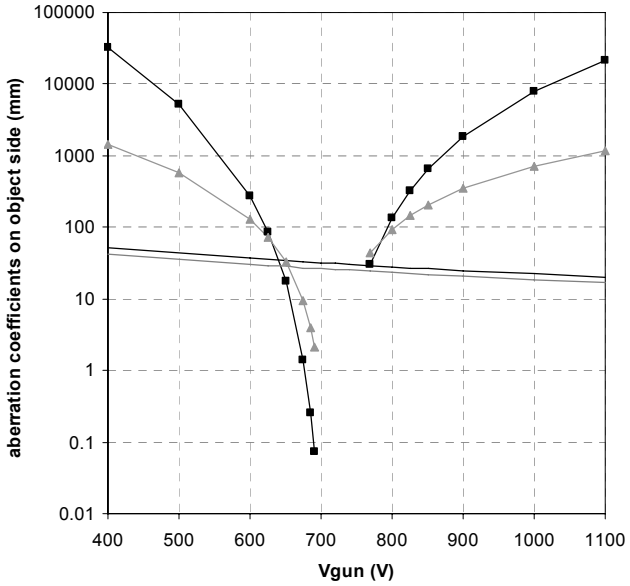

Fig. 7. Spherical (black) and chromatic (grey) aberration coefficients on object side for probe forming lens (with markers) and gun lens. Extraction potential 5 kV, double aperture at 300 V.

Figure 7 shows that for the probe-forming lens a minimum can be found for a gun lens voltage that gives a crossover about halfway between the gun lens and the probe-forming lens. For this minimum the magnification is maximum. For more diverging or converging beams the magnification decreases, which causes the coefficient on the object side to increase according to equations (5).

The aberration contributions and the magnification of the lens system in front of the double aperture change with the gun lens voltage. This is shown in figure 8, where a voltage of 300 V on the double aperture has been chosen as an example.

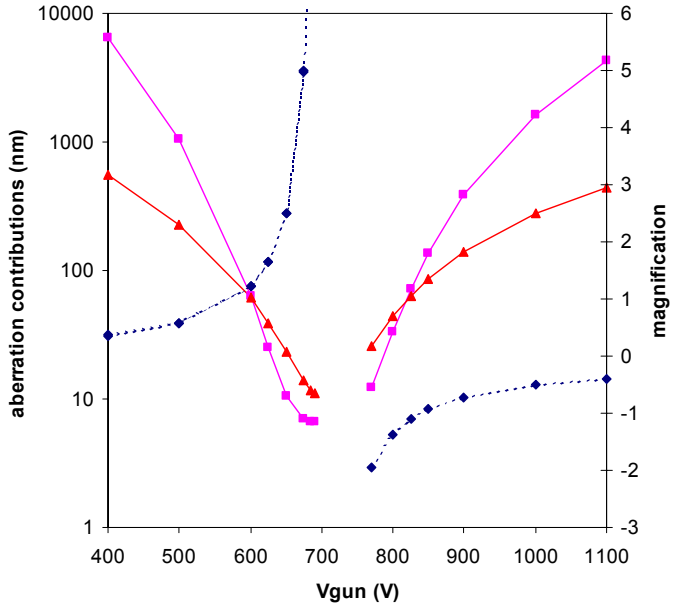

Fig. 8. Total spherical (squares) and chromatic (triangles) aberration contributions versus gun lens voltage. Extraction voltage is 5 kV. Probe lens voltage adapted to give focus at double aperture that is at 300 V. Magnification is indicated in diamonds.

5.2.9 Final probe size on double aperture

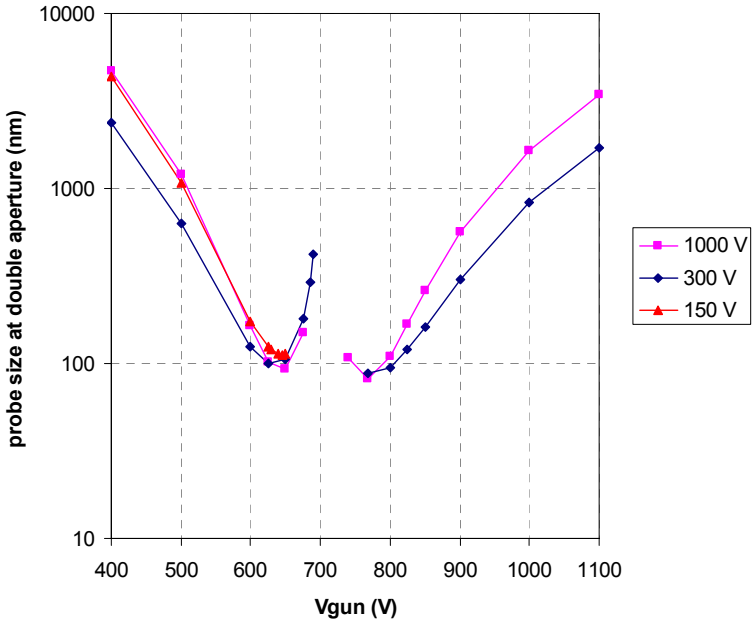

Fig. 9. Probe size at double aperture versus gun lens voltage. Voltage of probe forming lens adapted to give focus at double aperture. Extraction voltage 5 kV, voltage at double aperture 1 kV (diamonds), 300 V (squares) and 150 V (triangles).

From the spherical and chromatic aberration contributions, the contribution from diffraction, the virtual source and the magnification, now the total probe size on the double aperture can be calculated (equation (4)). The probe size for different voltages of the double aperture is given in figure 9. The settings for the probe-forming lens are given in Table I.

Figure 9 shows that the minimum probe size is below 100 nm. Two minima can be seen in figure 9. Around a gun lens voltage of 769 V, which is associated with a parallel beam between gun lens and probe forming lens, and at ~650 V, which is associated with a crossover approximately halfway between the gun lens and probe forming lens. For both situations the magnification is close to (-) 2. For voltages in between the aberration contributions are smallest (figure 8), but the higher magnification yields a higher total probe size on the double aperture.

For the minima the aberrations of both the gun lens and the probe-forming lens contribute, for lower and higher gun lens voltages, the aberrations of the probe-forming lens dominate.

Figure 10 shows for different settings of the double aperture voltage what the minimum probe size is. Table I gives the values and the required settings of the electrode potentials and what magnification this gives.

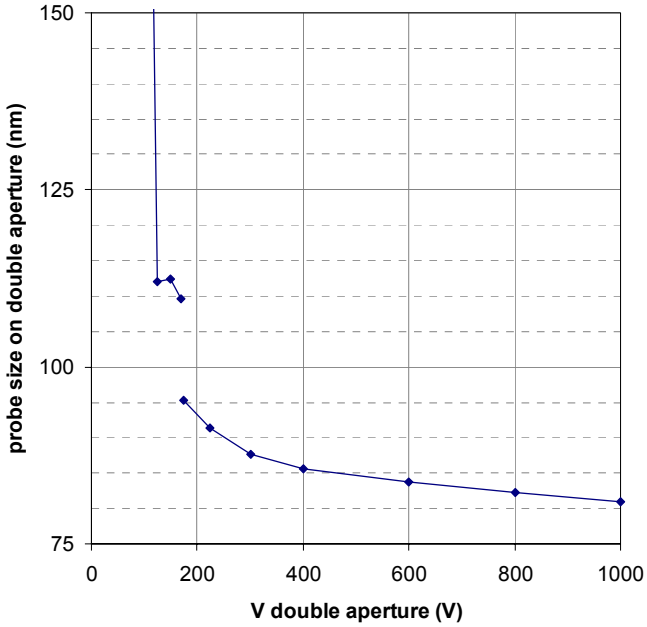

Fig.10. Minimum probe size on double aperture for different settings of the double aperture voltage.

From table I it can be seen that for double aperture voltages above 170 V there is no crossover between gun lens and probe forming lens to obtain the minimum probe size. For these cases the gun lens voltage provides a parallel beam up to the probe-forming lens. For very small double aperture voltages a crossover is required to get the minimum probe size at acceptable electrode potentials.

Table I. Minimum probe size at double aperture, electrode potential settings, magnification and aberration contributions for different settings of the double aperture voltage.

Vda (V)	**50**	**75**	**100**	**125**	**150**	**170**	**175**	**225**	**300**	**400**	**600**	**800**	**1000**
Vgl (V)	695	690	685	655	645	640	769	769	769	769	769	769	769
Vpfl (V)	1646	2380	1944	3139	1861	1529	2857	1602	1092	771	445	256	122
crossover ?	1	1	1	1	1	1	0	0	0	0	0	0	0
M	17.2	9.4	7.0	2.2	2.0	1.9	1.7	1.9	1.9	1.9	1.9	1.8	1.7
dS (nm)	113	63	47	29	31	32	32	25	24	25	29	32	34
dC (nm)	195	119	97	76	79	77	64	58	50	45	39	36	34
dp (nm)	**604**	**335**	**252**	**112**	**112**	**110**	**95**	**91**	**88**	**86**	**84**	**82**	**81**

The probe lens potential and magnification are plotted versus the double aperture voltage in figure 11. The aberration contributions are shown in figure 12.

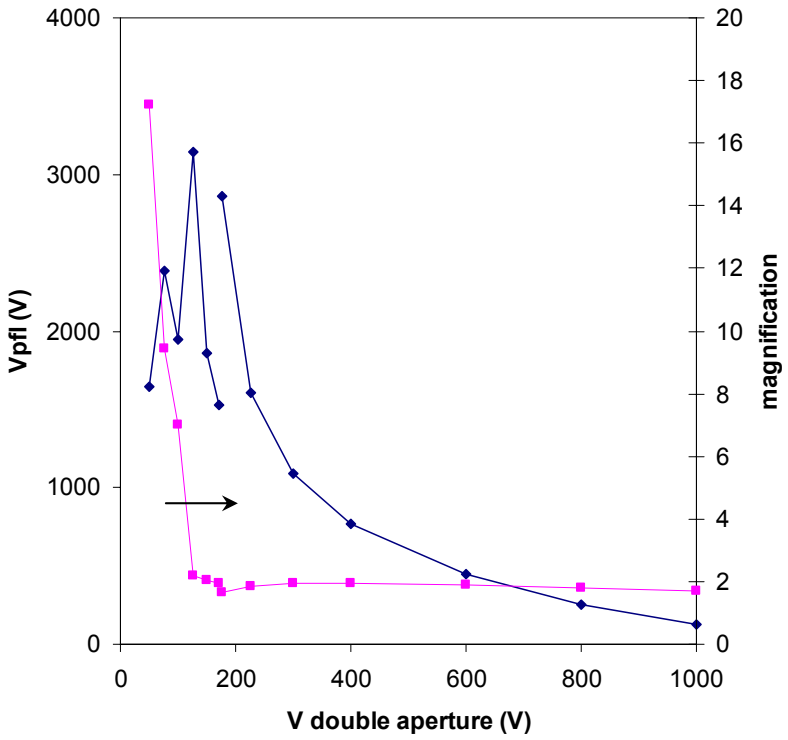

Fig.11. Electrode potential for probe forming lens and magnification to obtain minimum probe size for different settings of the double aperture voltage.

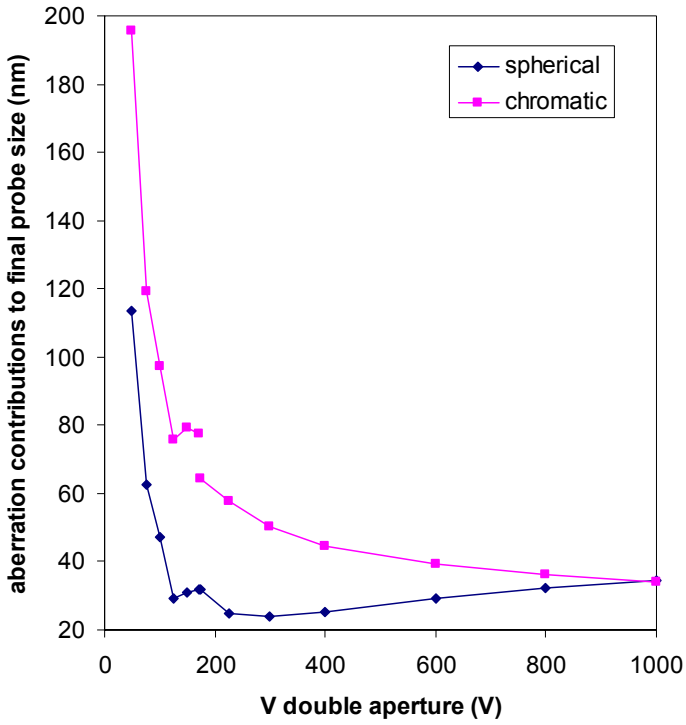

Fig.12. Spherical and chromatic aberration contribution to the minimum probe size that can be obtained for different settings of the double aperture voltage.

5.3 The design of the ion extractor and the ion beam-focusing lens

The figure 13 shows the SIMION ion optical simulation of the ion extractor region. A set of two apertures (10μm and 200μm) is held in front of the ion exit aperture plane of the gas ionization chamber. The 10μm aperture is at distance of 10μm from the ion exit aperture plane of the gas ionization chamber and the 200μm aperture is at 1mm distance from the 10μm aperture. The 10μm aperture is at –10V and the 200μm aperture is at –1010V.

It can be seen that the gas ion beam as well as the electron beam (~1000eV) emerges from the ion exit aperture. However, the gas ion beam (positive ions) travels towards the target (towards right) whereas the electron beam starts retarding and eventually returns back towards the double aperture.

The initial angular spread $[(\Delta E/E)^{1/2}]$ of the ion beam is considered to be ~0.5 radians, where ΔE is ~25meV. This is because ionization occurs at room temperature. The initial energy of ions, E is ~0.1eV. This is because the ion exit aperture is considered at 0.1V.

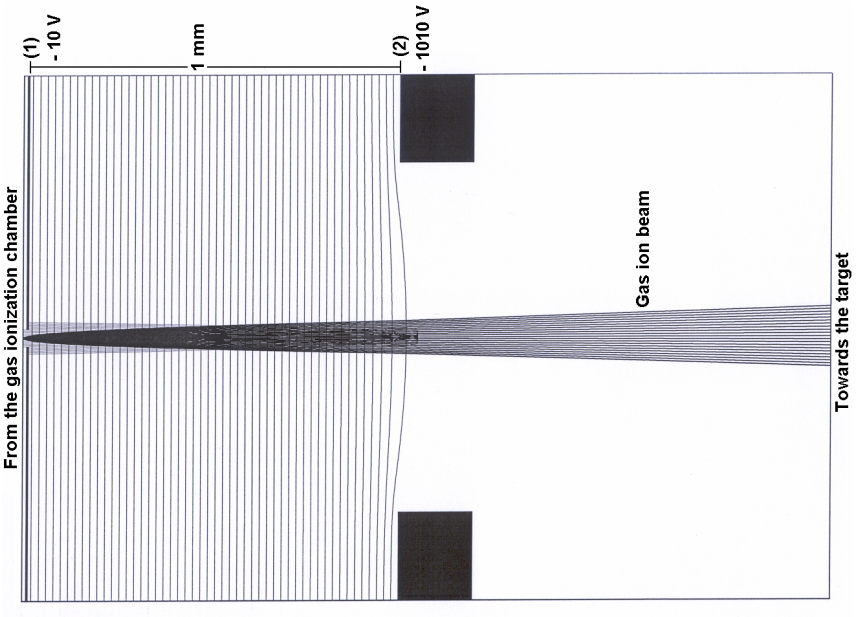

FIG.13. The ion optical simulation near the ion extractor region. However, the gas ion beam (positive ions) travels towards the target (towards right) whereas the electron beam starts retarding and eventually returns back towards the double aperture.

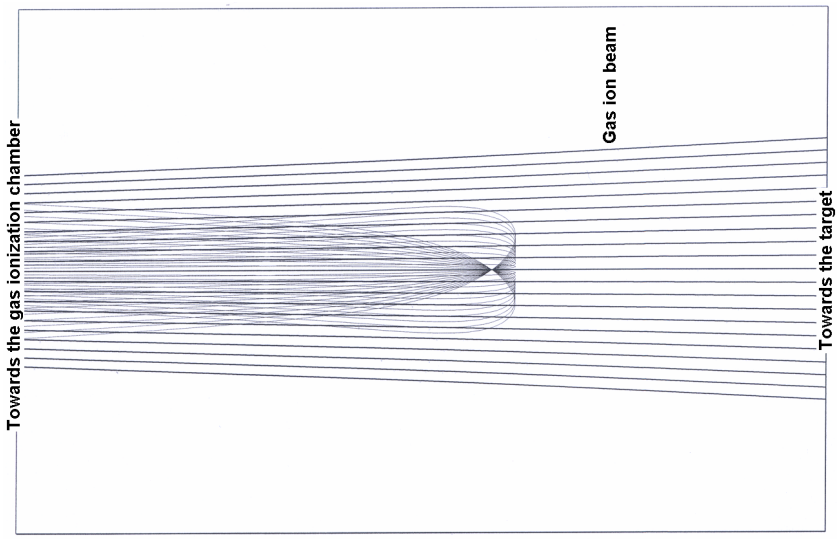

FIG.14. Part of figure 13, where one can see the electron beam is turning back (towards the left) and the gas ions are traveling towards the target (towards the right).

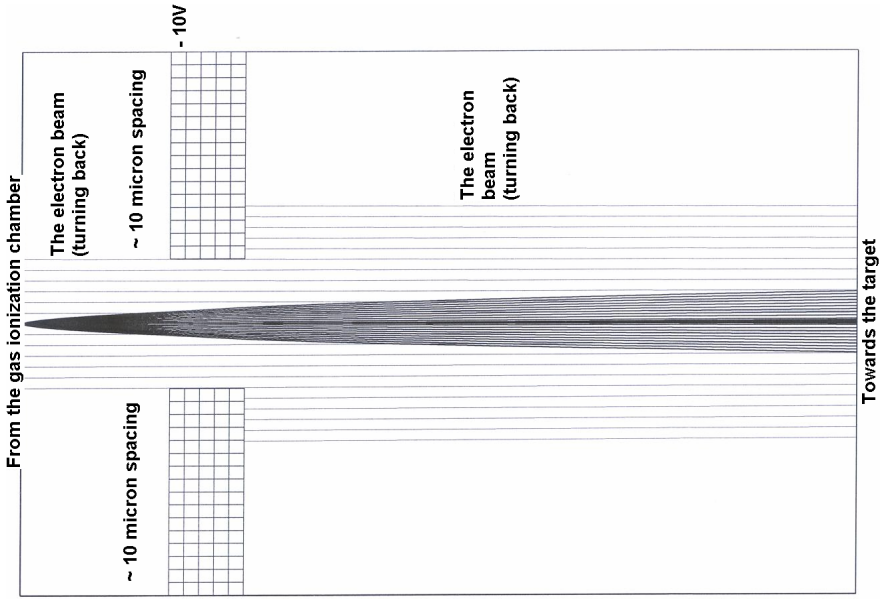

FIG.15. Part of figure 13 (near the ion exit aperture of the gas ionization chamber), where one can see the electron beam and the gas ion beam emerge through the ion exit aperture of the gas ionization chamber. A part of the returning electron beam hits the 10μm aperture. However, another part goes to the ion exit aperture plane of the gas ionization chamber, this is because the electron beam from the Schottky source is tightly focused into the double aperture.

The electrons cannot travel after the 200μm aperture because it is at –1010V. In a field free region, at ~2.2 mm from the ion exit aperture plane of the gas ionization chamber, the beam width and angle of the gas ion beam were measured. The width is found to be ~0.035mm and the angle ~0.39 degrees. This information is considered, while designing a focusing lens (Einzel lens).

The figure 14 and the figure 15 are taken from the figure 13 to illustrate the situation.

The information (ion beam width and angle) collected from figure 13 is used to design an ion beam-focusing lens (Einzel lens). That means at the target, the ion beam spot contains the aberration contribution due to the whole system. The ion beam energy used was ~1010 eV. The beam was focused at 37mm distance from the einzel lens. The total system magnification was ~2, that means, a 200nm diameter-spot at the target, which is an image of the object, the object that is the virtual source size of the ion source 100nm (assumed to be equal to the physical source size).

The contributions (see, equations 2 and 3) due to spherical and chromatic aberrations were found to be less than 200nm at the target.

If we measure the ion current at the target and scan the ion beam to estimate the spot size, we can estimate the ion source reduced brightness.

The deflectors can be mounted within the 37mm region. The energy analyzer can be mounted at the target. The beam angle can be adjusted in such a way that the ion beam should enter perpendicularly into the retarding field energy analyzer. The advantages to

mount the energy analyzer at the target is that most of the current can be collected, as it is a focusing beam and the energy spread measured in this way can not be smaller than the actual energy spread of the ion source.

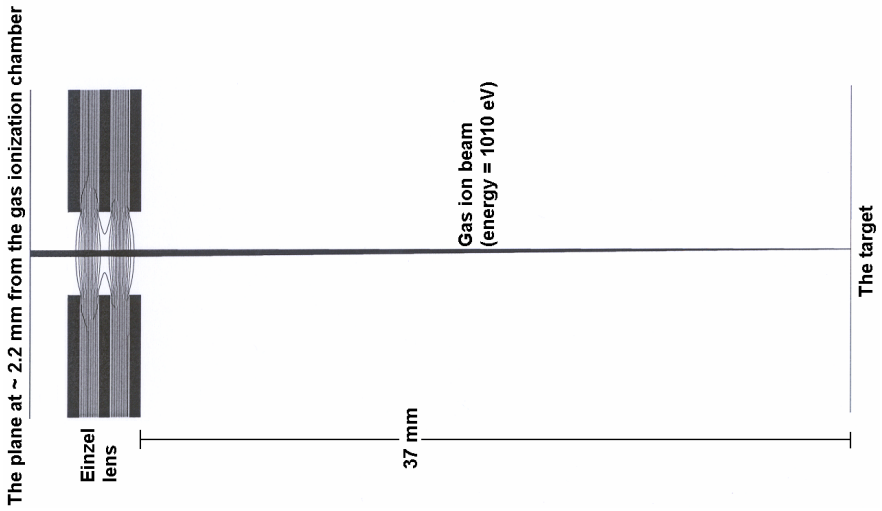

FIG.16. The ion beam focusing lens (Einzel lens).

5.4 The effect of silicon pyramidal hole on the extraction field

As fabricated gas ionization chambers (see, figure 15 in the chapter 4) are not as flat as the situation depicted in the figure 13 and a 10μm ion extraction aperture at ~10μm distance from the ion exit aperture plane can not yet be mounted. The gas ionization chamber is the 100nm apertures drilled into the Si_3N_4 membranes (~20μm×~20μm), which are supported by a 450μm thick silicon wafer (see, figure 15 in the chapter 4). The pyramidal hole (see, figure 15 in the chapter 4) can have destructive effect on the ion beam properties.

The figure 17 shows that if we apply an electric field between the ion exit aperture of the gas ionization chamber and an extractor, it is possible to achieve an ion beam. The electron beam (same as figure 13) can start retarding and eventually turns back towards the ion exit aperture. However it is clear that even >1kV/mm applied electric field is not enough (1kV/mm electric field in optical columns is the safe limit) to avoid an ion beam crossover. This ion beam crossover disc is mostly due to the chromatic aberration contribution. The low extraction field spoils the ion beam quality. This crossover acts, as
an object and therefore, the measured reduced brightness will be too low, as the virtual source size will be greater than the physical source size. In this simulation, for the sake of simplicity, cone geometry was used instead of pyramidal hole. The pyramidal hole will not only introduce a crossover but also astigmatism.

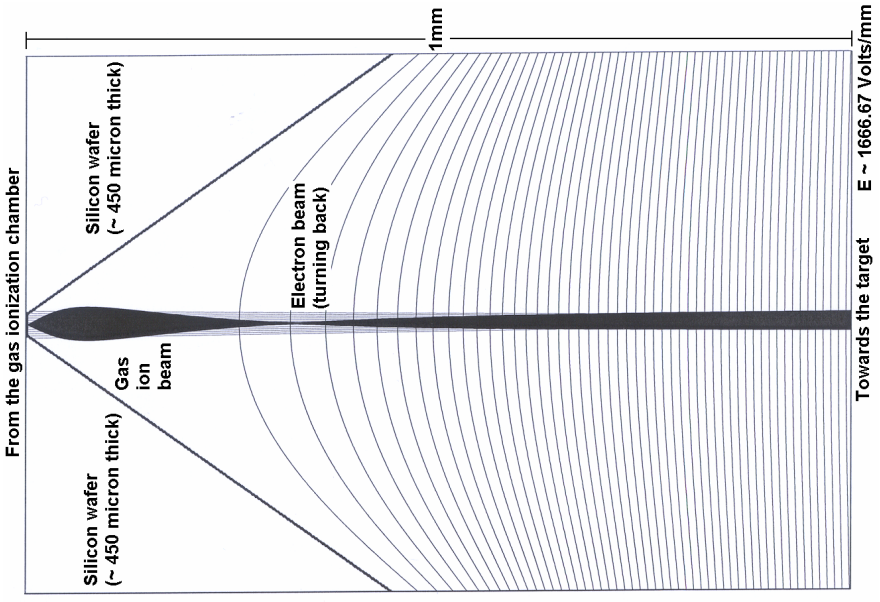

FIG.17. The ion beam crossover takes place due to the lack of extraction field.

Eventually, that means that after the first experiments, we will have to modify the gas ionization chamber to get rid off (or to reduce the effect of) the silicon pyramidal hole.

5.5 Experimental setup

The experimental setup (see, figure 18) of the thermal field electron impact gas ion source consists of various parts namely, (1) thermal field electron source (2) electron gun lens with a beam-limiting aperture (3) the two sets of quadrupole deflectors for electron beam (4) the probe forming lens (5) gas ionization chamber with gas delivery system (6) ion gun lens (7) the two sets of quadrupole deflectors for ion beam (8) the target (double aperture) to position electron beam (9) the target (surface with submicron structure) to find spot size of the ion beam (10) secondary electron detector for electron beam target (11) secondary electron detector for ion beam target and (12) Electronics for power supplies and measurement devices (not shown in figure).

There are two sets of quadrupole deflectors to deflect electron beam. The deflectors are necessary to deflect electron beam and find the submicron aperture of the gas chamber. By mounting these two deflectors at a 45-degree angle around the optical axis with respect to each other, they can also be used as a stigmators. The electron beam can be scanned over the gas ionization chamber and positioned using the secondary electron detectors. The extracted ion beam can be accelerated using the ion gun lens and again using the sets of quadrupole deflectors and secondary electron detectors, it can be focused onto a target.

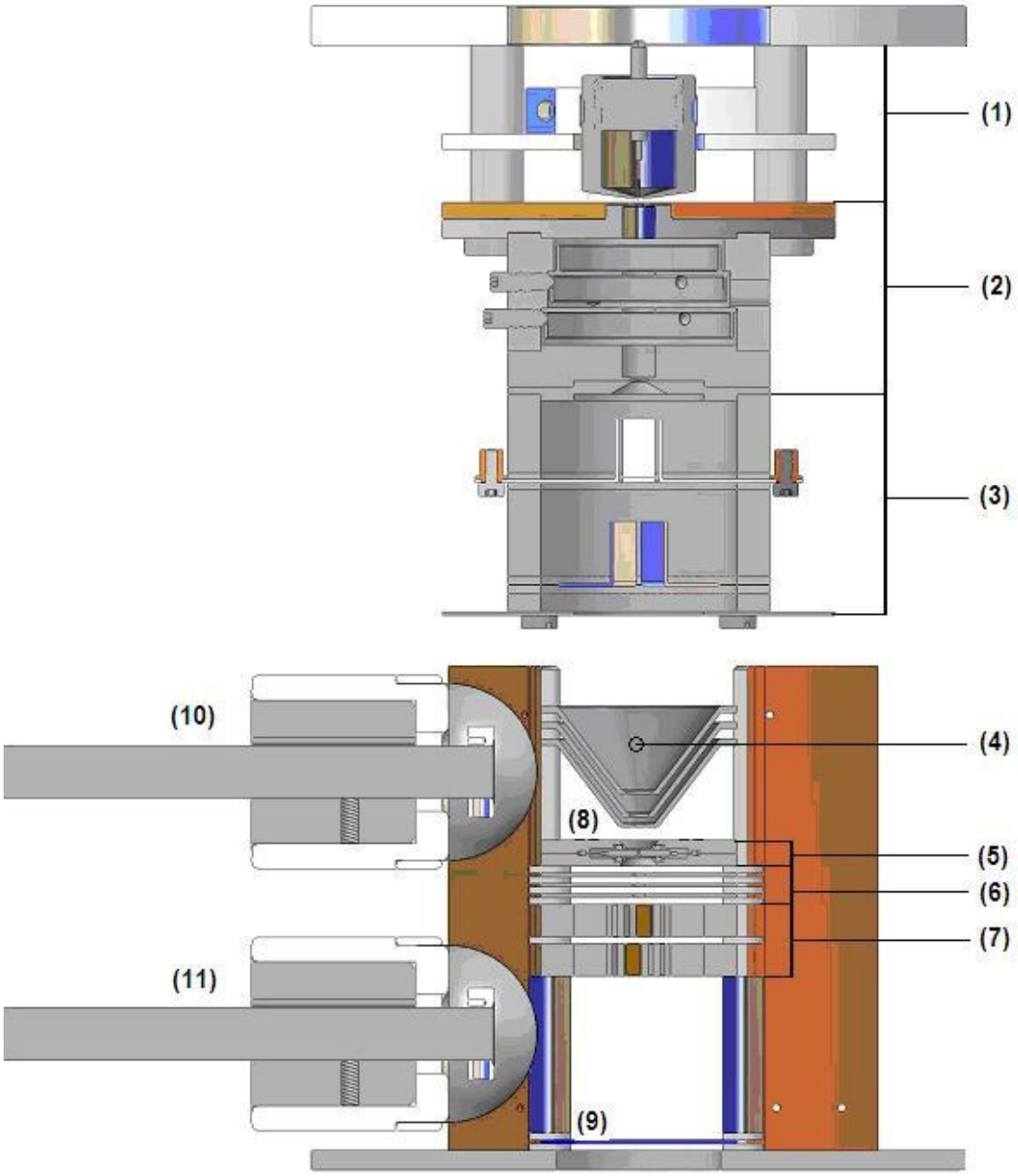

FIG .18. Thermal field electron impact noble gas ion source. The total length of this system is around 20-25 cm. The numbers (1to 11) in the figure indicate (1) thermal field electron source (2) electron gun lens with a beam-limiting aperture (3) the two sets of quadrupole deflectors for electron beam (4) retarding lens (5) gas ionization chamber with gas delivery system (6) ion gun lens (7) the two sets of quadrupole deflectors for ion beam (8) The target (double aperture) to position electron beam (9) the target (surface with submicron structure) to find spot size of the ion beam (10) secondary electron detector for electron beam target (11) secondary electron detector for ion beam target and (12) Electronics for power supplies and measurement devices (not shown in figure).

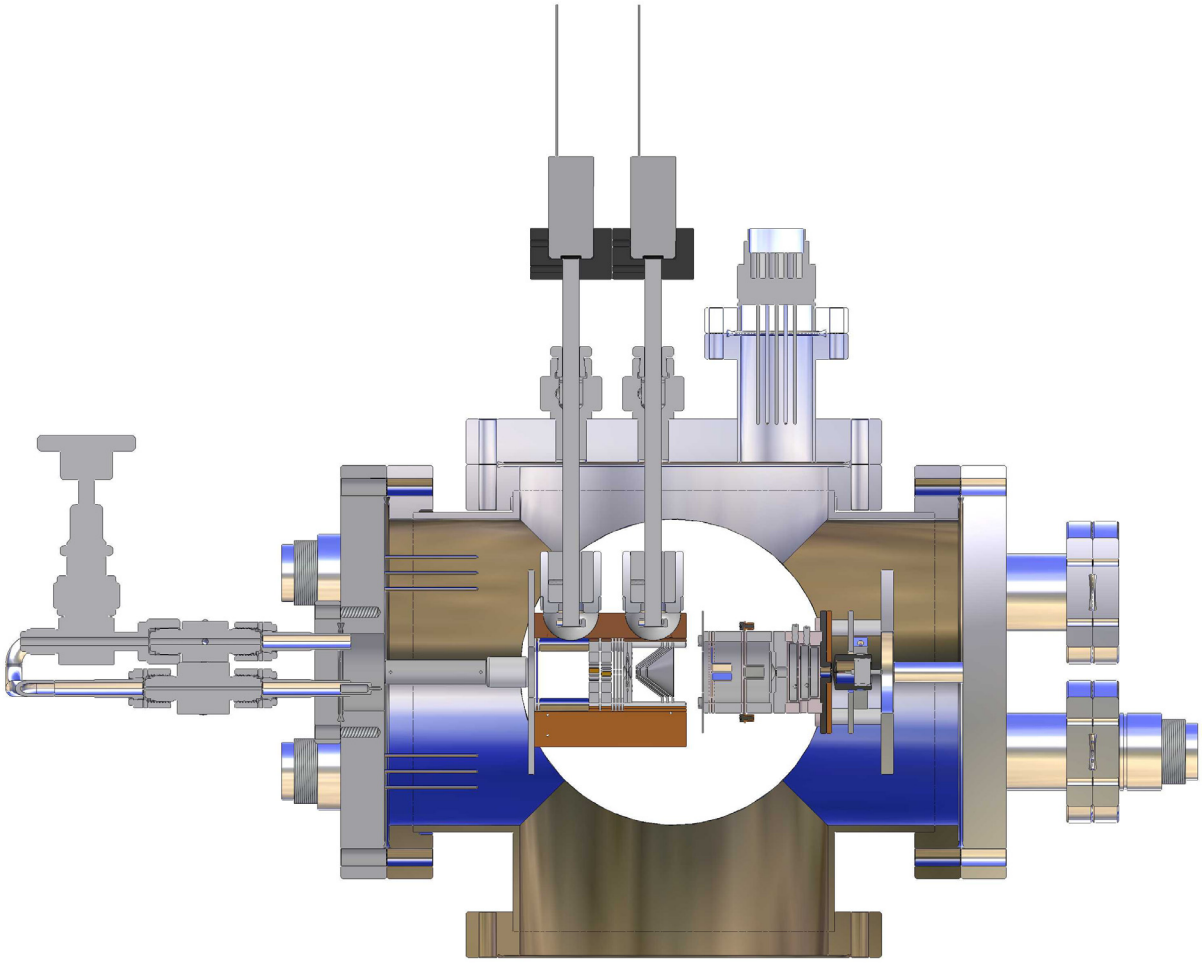

FIG. 19. The same setup described in the figure 18, has been put inside a vacuum system.

If the target has previously known submicron structure then, with the help of secondary electron beam detector the spot size of the focused ion beam can be understood. Hence, if we use the beam half-angle estimated from the ion optical simulation we can find out the reduced brightness of the ion source because we know the current, half angle, spot size and the beam acceleration voltage.

To determine the energy spread of the ion source, a retarding field energy analyser can be inserted just near the ion source. Care has to be taken that the beam comes perpendicularly into the energy analyser.

Figure 20a shows the electron delivery system for the gas ion source. It consists of a Schottky electron source, a gun lens and the two sets of quadrupole deflectors. In Fig. 20b (the top view of figure 20a), the two sets of quadrupole deflectors are visible. Fig. 21 shows the ion optical column stacked together with an electron probe-forming lens.

The ion optical column consists of a double aperture holder, an ion gun lens and the two sets of quadrupole deflectors.

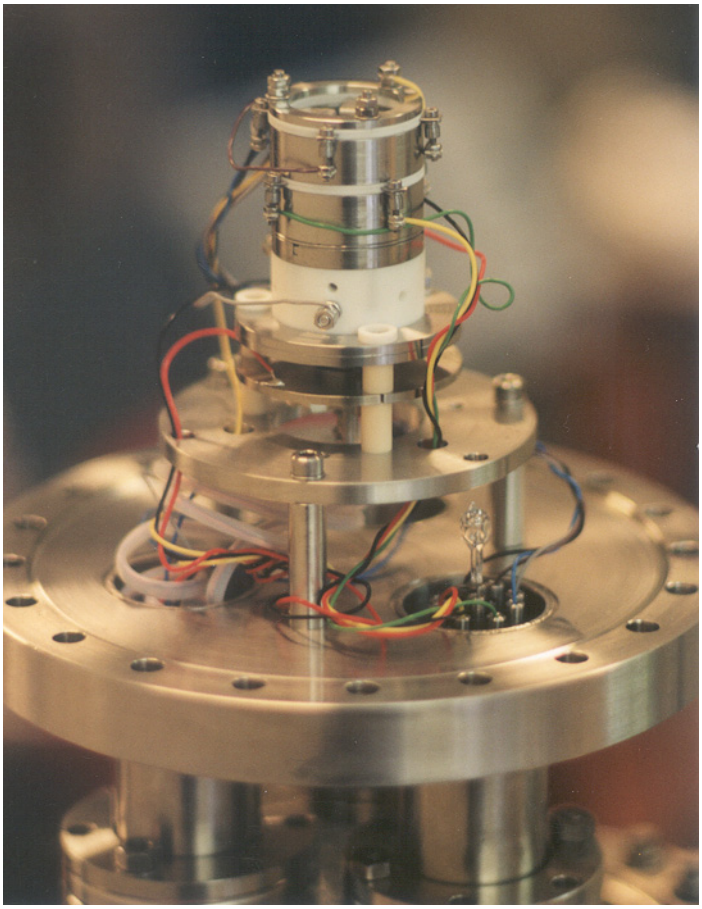

FIG. 20(a). The electron beam delivery system up to the two sets of quadrupole deflectors (the length is around 10-12cm)

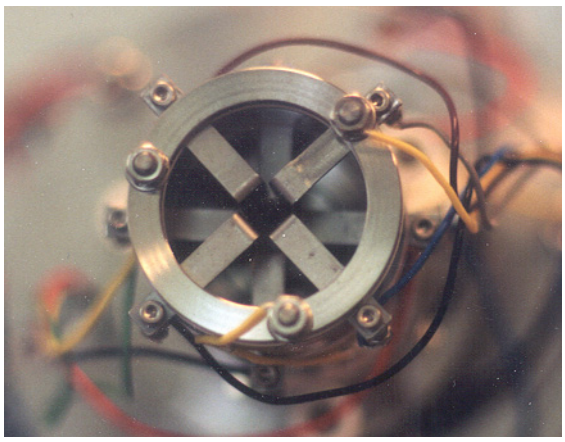

FIG. 20(b). The top view of the electron delivery system shown in the figure 20(a). The two sets of quadrupole deflectors are visible.

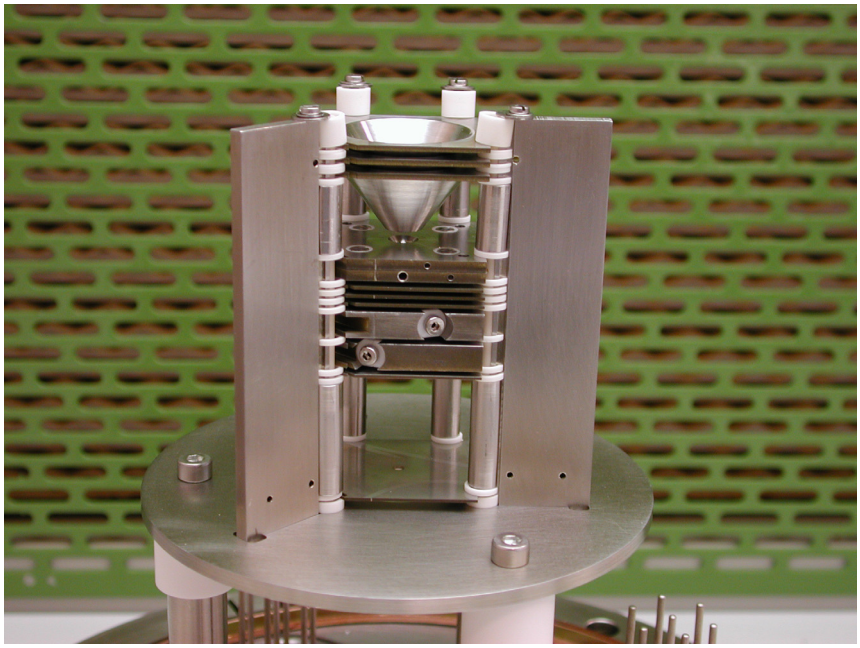

FIG. 21. The ion optical column with the electron probe-forming lens (the length is around 10-12cm).

5.6 Discussion and conclusion

Schottky gun lens components have been redesigned to be more robust with respect to the alignment and to incorporate an aperture to limit the beam current. The aberration contributions of this gun lens and that of the probe forming lens in front of the gas containing double aperture have been calculated using ELD and meet the requirements for an extraction voltage of 5 kV and a voltage on the double aperture of 50 - 1000 V. The minimum probe size on the double aperture meets the requirement of 100 nm for voltages of the double aperture above 170 V and is obtained by setting the gun lens voltage such that a parallel beam is created in between the gun lens and the probe-forming lens (total magnification ~2).The beam current can be changed between ~30-140 nA by changing the extraction voltage and/or the source temperature between 4-5 kV and 1600-1800 K.

The ion beam extractor and focusing lens has been designed. In an ideal situation, the ion beam extractor can be mounted very close to the gas ionization chamber. The proper extraction field avoids a beam crossover and maintains the quality of beam. The effect of the silicon pyramidal hole of the gas ionization chamber is taken into account. The pyramidal hole will not only introduce crossover but also astigmatism. This crossover will act as an object and therefore, the measured reduced brightness will be too low, as the virtual source size will be greater than the physical source size. Eventually, we have to modify the gas ionization chamber to get rid off (or to reduce the effect of) the silicon pyramidal hole.

Anyway, The system is ready to conduct the first ion source experiment. The first thing is to check if electron beam can pass through both the apertures of an empty (no

gas) gas ionization chamber. That means we can position the electron beam using the sets of deflectors and secondary electron detectors. The related electronics work. After inserting a gas into the gas ionization chamber, we have to see if it still functions properly that means, it holds the gas and maintains two apertures electrically isolated. Fortunately, we have several gas ionization chambers as stated in chapter 4. If we see an ion beam then the next thing is to check if ion optics and related electronics works properly. The Focused spot of ion beam on the target will give understanding of the quality of the ion source.

Acknowledgements

We thank P.W. van Harrewijn, J. Nonhebel, F. Berwald, M. Pelle and J. de Looff for their technical assistance in building the experimental setup. This work was part of the research program of the "Stichting voor Fundamenteel Onderzoek der Materie" (FOM), which is supported by the "Nederlandse Organisatie voor Wetenschappelijk Onderzoek"(NWO).

References

[1] ELD, Electron and ion optical simulation software, CPO-IST-TN, TUDelft, The Netherlands.

[2] SIMION 3D (version 7.0), Electron and ion optical simulation software, USA

[3] J.E. Barth and P. Kruit, Optik, **101(3)**, 101 (1996).

[4] Swanson L.W., Schwind G.A., Ch. 2: A review of the ZrO/W Schottky cathode, in 'Handbook of Charged Particle Optics', ed. J.Orloff, CRC Press LLC (1997), p. 77-102

[5] Bronsgeest M.S. and Kruit P., J. Vac. Sci. Technol. B**, 24(2)**, 887 (2006).

Summary and Conclusion

FIB machines are an integral part of material science and the semiconductor industry due to their tremendous day-to-day applications. For example, FIB machines can be used for 1) specimen preparation for transmission electron microscopy, 2) in-situ cross-sectioning and analysis of a fabricated device, 3) gas-assisted milling and deposition, 4) mask repair and micro-machining 5) scanning ion microscopy, 6) lithography, etc. Liquid-metal ion sources (LMIS) are widely used in FIB machines because they meet the minimum ion source requirements such as source brightness and reliability. One of the main drawbacks of FIB machines is that contamination is inevitable due to the use of liquid-metal ions, so a noble-gas ion source is very much desired. Ga ions not only change the electrical properties but can also affect the magnetic properties of the devices. Gallium staining due to deposition of gallium ions in the quartz substrate during FIB repair of a photo-mask is another important issue that limits the use of FIB machines.

Any noble gas ion source with at least similar properties (brightness, energy spread, current stability, and life time) as LMIS is extremely desirable, and there have been several efforts by various researchers to develop such noble gas ion sources. Gas field ionization sources (GFIS) and plasma ion sources have been widely studied. There are several types of GFIS. However, can we obtain a working GFIS as reliable as LMIS? That still remains an open question. Plasma ion sources are more robust, easy to maintain, and more reliable than any GFIS (particularly, GFIS-supertips). They can also produce several gas species. Despite several efforts, plasma ion sources are not as bright as LMIS for FIB applications. To date, we know no plasma ion source that can have a reduced brightness as good as LMIS ~ $1 \cdot 10^6 A/m^2 SrV$. The main reason that plasma ion sources cannot produce high-brightness ion beams is the high temperature, which is an inherent problem in plasma sources.

In Chapter 2, we have proposed a novel device; a sub-micron scale electron impact noble gas ion source. The ion source can be operated at room temperature. The electron impact ionization chamber in this concept consists of two closely spaced (sub-micron) parallel conducting plates each with a small hole on the axis. The plates are electrically isolated from each other. The space between the two plates is filled with noble gas (for example, argon gas) in the molecular flow regime. At such a small device scale (of the double-aperture gas chamber) relatively high pressure of gas in a molecular flow regime can be maintained at the ionization region, while the gas particle density along the optical axis, outside the chamber can be sufficiently small. Electrons from an electron gun enter through one of the apertures and ionize the gas in non-plasma mode, which means at room temperature (T~293K). The ions can be extracted through the second aperture under influence of the electric field. The particle interactions (ion-neutral or ion-ion) outside the ionization region and near the ion exit aperture can be sufficiently small.

We conclude that if this ion source is fabricated using a Schottky electron gun, it will have at least similar or even better optical properties than LMIS. A high reduced brightness ($\geq 10^6 A/m^2 srV$) with a minimum ion current of 1 nA at the source and a low energy spread (< 1 eV) is expected. The reliability and lifetime of this ion source can be comparable to the LMIS as this source does not depend on the material's surface properties.

In Chapter 3, the concept of cold field electron impact noble gas ion sources is discussed. It is essentially the same concept as thermal field electron impact noble gas ion sources, The main difference is the position of the electron source, which is now placed in close proximity to the double aperture. This is to avoid the large construction (almost a low voltage scanning electron microscope) that is required for the thermal field electron impact ion sources. The electron delivery construction can be the main obstacle if one wants to have a miniaturized version of a thermal field electron impact noble gas ion source. The double

aperture gas ionization chamber with cold field emission tip can be fabricated as one assembly using lithographic techniques. Besides miniaturization, another advantage of cold field electron impact noble gas ion sources is that it can be cost effective. However, it is a fact that cold field emitters are notorious for their poor electron emission stability and lifetime. There are several ongoing efforts to make field emitters work in poor vacuum conditions.

The experiments presented in Chapter 3 are to develop stable cold field emitters for poor vacuum conditions and to investigate a number of things that are of interest for electron impact noble gas ion sources. The use of a current regulator circuit and operating the tip below the sputtering threshold could be one of the best options to stabilize the field emission current at stable voltages for a long time. We apply feedback on the tip voltage and therefore to maintain a constant electric current, voltage fluctuations will occur. We know that as far as a useful cold electron gun is concerned, we do not want to vary the voltage and thus introduce an energy spread.

As discussed in section 2.3, voltage fluctuations are due to two effects. Small fluctuations at a very small time scale are needed to control current fluctuations, which are caused by local and temporary geometrical changes due to gas adsorption and desorption. The permanent change in voltage at large time scale is due to sputtering and that is what we want to avoid. Therefore, the tip should be operated below the sputtering threshold to maintain the voltage reasonably stable for the entire period.

The voltage fluctuations on a small timescale are expected to be really small in amplitude. If voltage fluctuations are well below 1-2 V, this may be acceptable. As far as the cold field electron impact noble gas ion source is concerned, it may not be useful to operate the cold field emitter at voltages below the ionization potential of the surrounding gas. Fortunately, different materials have different sputtering thresholds. We hope that at < 50 V for carbon- based materials sputtering should not be a problem. The tip should not be damaged by positive ion bombardment.

Cold field electron impact ion source experiments should be performed with the following three conditions:

a) fabricate the tip and gas ionization chamber as one assembly using lithographic techniques. The system would look like a double-gated field emitter array with a gas delivery system in between the two gates,

b) operate the tip below the sputtering threshold of the tip material (use carbon based materials as far as possible) and expect a good lifetime for the tip, and

c) use a comprehensive feedback on the tip voltage to have a stable emission of electron current at extremely small voltage fluctuations (as we want the incident electron energy to be constant).

Chapter 4 describes the fabrication process of a sub-micron scale gas ionization chamber for a thermal field electron impact gas ion source. The two apertures of the ionization chamber are made of a ~ 100-nm thick Si_3N_4 membrane covered with a 10-nm thick molybdenum layer and supported by Si wafer. Both apertures are electrically isolated by electron beam resist (PMMA950K). We have made a gas ionization chamber of ~ 400-nm aperture diameter with a spacing of ~ 400 nm. The results also show that it is possible to fabricate a gas ionization chamber of ~100-nm aperture size with ~100-nm spacing. A scanning electron micrograph confirms that indeed two separate membranes are present.

Chapter 5 describes the experimental setup of a thermal field electron impact gas ion source. The ion source mainly consists of an electron delivery system into the double aperture at the desired energies < 1000eV. The first task was to build a low-voltage electron optical system equipped with a Schottky source. As the Schottky source is far away from the gas ionization chamber, it should function in a normal way in ultra high vacuum (1×10^{-9} mbar). As there is a facility to scan the electron beam over the gas ionization chamber and detect the

secondary electron beam, the whole construction of the electron delivery system is equivalent to a low-voltage scanning electron microscope. The sub-micron gas ionization chamber is connected to the gas delivery system. The extracted ion beam can be focused on a sub-micron target. The focusing of the electron beam into the gas ionization chamber as well as the focusing of the extracted ion beam onto a sub-micron target can be done with the help of four sets of quadrupole deflectors and two separate secondary electron detectors. An energy analyzer can be incorporated in the same system.

The whole system has been designed using ELD and SIMION-3D electron optical simulation softwares.

Samenvatting en Conclusie

FIB (focused ion beam, gefocusseerde ionenbundel) machines zijn een integraal onderdeel van materiaalwetenschappen en de halfgeleiderindustrie als gevolg van hun enorme hoeveelheid alledaagse toepassingen. Voorbeelden van het gebruik van FIB machines zijn 1) de bereiding van preparaten voor transmissie-elektronenmicroscopie, 2) in-situ doorsnijden en analyseren van geïntegreerde circuits, 3) gas-geassisteerd etsen en deponeren van materiaal 4) reparatie van optische maskers en microbewerking 5) scanning-ionenmicroscopie, 6) lithografie, enz. Vloeibaar-metaal-ionenbronnen (liquid-metal ion sources, LMIS) worden vaak gebruikt in FIB machines omdat ze voldoen aan de minimum vereisten voor ionenbronnen, zoals helderheid en betrouwbaarheid van de bron. Een van de belangrijkste nadelen van FIB machines is dat verontreinigingen onvermijdelijk zijn als gevolg van het gebruik van vloeibaar-metaalionen, dus een edelgas-ionenbron zou zeer gewenst zijn. Galliumionen veranderen niet alleen de elektrische eigenschappen, maar kunnen ook invloed hebben op de magnetische eigenschappen van de bewerkte onderdelen. Het ontstaan van galliumvlekken als gevolg van de afzetting van galliumionen in het kwarts substraat tijdens FIB-reparatie van een optisch masker is een andere belangrijke beperking voor het gebruik van FIB machines.

Iedere edelgas-ionenbron met minimaal soortgelijke eigenschappen (helderheid, energiespreiding, stroomstabiliteit en levensduur) als LMIS zou zeer welkom zijn. Verschillende onderzoekers hebben pogingen gedaan om zulke edelgas-ionenbronnen te ontwikkelen en er is veel onderzoek verricht naar gas-veld-ionenbronnen (GFIS) en plasma-ionenbronnen. Er zijn verscheidene typen GFIS. Echter, is het mogelijk een werkende GFIS te verkrijgen die net zo betrouwbaar is als LMIS? Dat is nog steeds een open vraag. Plasma-ionenbronnen zijn robuuster, makkelijk in onderhoud en betrouwbaarder dan GFIS (in het bijzonder GFIS-supertips). Daarbij kunnen deze ionenbronnen ook verscheidene elementen produceren. Echter, ondanks verschillende pogingen zijn de beste huidige plasma-ionenbronnen niet zo helder als LMIS (gereduceerde helderheid ~ $1 \cdot 10^6 A/m^2SrV$) voor FIB toepassingen. De voornaamste reden dat plasma-ionenbronnen geen ionenbundels met hoge helderheid kunnen produceren, is de hoge temperatuur die een inherent probleem is in plasmabronnen.

In hoofdstuk 2 hebben we een nieuw brontype voorgesteld; een submicron elektronimpact edelgas-ionenbron die kan werken bij kamertemperatuur. De elektronimpact ionisatiekamer in dit concept bestaat uit twee parallelle geleidende platen op kleine afstand (submicron) van elkaar, ieder met een kleine opening op de as. De platen zijn elektrisch van elkaar geïsoleerd. De ruimte tussen de platen is gevuld met een edelgas (bijvoorbeeld argon) in het moleculaire stromingsregime. Op deze kleine schaal (van de dubbel-apertuur ionisatiekamer) kan een relatief hoge gasdruk in het moleculaire stromingsregime in stand worden gehouden in de ionisatiezone, terwijl de dichtheid van de gasdeeltjes langs de optische as, buiten de kamer, zeer klein kan zijn. Elektronen uit een elektronenkanon komen binnen door een van de aperturen en ioniseren het gas in non-plasma modus, dus bij kamertemperatuur (~ 293 K). De ionen kunnen onder invloed van het elektrische veld naar buiten getrokken worden door het tweede apertuur. De interacties tussen de deeltjes (ion-neutraal of ion-ion) buiten de ionisatiezone en in de buurt van het uitgangsapertuur kunnen voldoende klein zijn.

We concluderen dat als deze ionenbron wordt vervaardigd met behulp van een Schottky elektronenkanon de optische eigenschappen vergelijkbaar zijn met of zelfs beter dan die van LMIS. We verwachten een hoge gereduceerde helderheid ($\geq 10^6 A/m^2srV$) met minimaal 1-nA ionenstroom bij de bron en lage energiespreiding (< 1 eV). De

betrouwbaarheid en levensduur van deze ionenbron kan vergelijkbaar zijn met LMIS aangezien deze bron niet afhankelijk is van de oppervlakte-eigenschappen van het materiaal.

In hoofdstuk 3 wordt het concept van koude veldemissie elektronimpact edelgas-ionenbronnen besproken. In essentie is dit concept hetzelfde als dat van thermische veldemissie elektronimpact edelgasionenbronnen. Het voornaamste verschil is de positionering van de elektronenbron, die nu zeer dichtbij de dubbele apertuur wordt geplaatst. Dit is om de grote constructie (bijna een laag-voltage scanning electronenmicroscoop) te vermijden die benodigd is voor thermische veldemissie elektronimpact ionenbronnen. De constructie voor de elektronentoevoer kan het voornaamste obstakel zijn als men een geminiaturiseerde versie van de thermische veldemissie elektronimpact edelgas-ionenbron nastreeft. De dubbel-apertuur gas-ionisatiekamer met koude veld emissietip kan gefabriceerd worden als één onderdeel met gebruikmaking van lithografische technieken. Naast de miniaturisatie is een ander voordeel van koude veld elektronimpact edelgas-ionenbronnen dat deze kosteneffectief kan zijn.

Echter, feit is dat koude veldemitters berucht zijn vanwege hun lage elektronenemissiestabiliteit en korte levensduur. Momenteel worden verschillende pogingen gedaan om veldemitters in slechte vacuüm condities te laten werken.

Het doel van de experimenten die in hoofdstuk 3 worden gepresenteerd is de ontwikkeling van stabiele koude veldemitters voor slechte vacuüm condities en het onderzoeken van een aantal zaken die van belang zijn voor elektronimpact edelgas-ionenbronnen. Het gebruik van een stroomregelcircuit en het laten werken van de tip beneden de sputter drempel zou een van de beste opties kunnen zijn voor het gedurende langere periode stabiliseren van de veldemissiestroom op een stabiele spanning.

We passen terugkoppelingsbesturing op de tipspanning toe en daarom zullen om de elektrische stroom constant te houden spanningsfluctuaties optreden. We weten dat we voor een bruikbaar “koud” elektronenkanon de spanning niet willen variëren omdat dit een energiespreiding introduceert.

Zoals besproken in paragraaf 2.3, treden spanningsfluctuaties op als gevolg van twee effecten. Kleine fluctuaties op erg kleine tijdschaal zijn het gevolg van de regeling van de stroomfluctuaties, die worden veroorzaakt door lokale en tijdelijke geometrische veranderingen door gasadsorptie en -desorptie. Een blijvende verandering in spanning op grote tijdschaal is het gevolg van sputteren en dát is wat we willen vermijden. Daarom moet de tip werken beneden de sputter drempel om de spanning gedurende langere periode redelijk stabiel te houden.

Verwacht wordt dat de amplitude van de voltagefluctuaties op kleine tijdschaal zeer klein zal zijn. Als de spanningsfluctuaties ruim onder de 1-2 V zijn, zou dit acceptabel kunnen zijn. Met betrekking tot de koude veldemissie elektronimpact gas-ionenbron is het wellicht niet nuttig om de koude veldemitter te laten werken bij een spanning die lager is dan de ionisatiepotentiaal van het omringende gas. Gelukkigerwijs hebben verschillende materialen verschillende sputter drempels. We hopen dat bij < 50 Volt voor materialen op basis van koolstof het sputteren geen probleem zal zijn. De tip mag niet beschadigd raken door een bombardement met positieve ionen.

Experimenten met een koude veldemissie elektronimpact ionenbron zouden uitgevoerd moeten worden onder de volgende drie condities:

a) fabriceer de tip en de gas-ionisatiekamer als één onderdeel gebruikmakend van lithografische technieken. Het systeem zou eruit zien als een dubbelpoorts veldemittermatrix met een gastoevoersysteem tussen de twee poorten,

b) zorg dat de tip beneden de sputter drempel van het tipmateriaal werkt (gebruik indien mogelijk materialen gebaseerd op koolstof) en verwacht een goede levensduur voor de tip en

c) gebruik een uitgebreide terugkoppelingsbesturing op de tipspanning voor een stabiele elektronenstroom bij extreem kleine spanningsfluctuaties (aangezien we willen dat de energie van de invallende elektronen constant is).

Hoofdstuk 4 beschrijft het fabricageproces van een gas-ionisatiekamer op submicron schaal voor thermische veldemissie elektronimpact gas-ionenbronnen. De twee aperturen van de ionisatiekamer bestaan ieder uit een met een 10-nm dikke molybdeenlaag bedekt ~ 100-nm dik Si_3N_4 membraan, gedragen door een Si-plak. De aperturen zijn elektrisch geïsoleerd door elektronenbundel-resist (PMMA950K). We hebben een gas-ionisatiekamer met apertuurdiameters van ~ 400 nm en een afstand tussen de aperturen van ~ 400 nm geconstrueerd. De resultaten tonen aan dat het ook mogelijk is om gas-ionisatiekamers te fabriceren met apertuurdiameters van ~100 nm met een tussenafstand van ~100 nm.

Hoofdstuk 5 beschrijft de opstelling voor experimenten met een thermische veldemissie elektronimpact gas-ionenbron. Het belangrijkste onderdeel van de ionenbron is een systeem voor de toevoer van elektronen met de gewenste energie < 1000eV naar het dubbel-apertuur. De eerste taak was om een laag-voltage elektronenoptisch systeem te bouwen uitgerust met een Schottky bron. Aangezien de Schottky bron ver weg is van de gas-ionisatiekamer, zou deze normaal moeten functioneren in ultra-hoog vacuüm (1×10^{-9} mbar). De aanwezigheid van een faciliteit om de elektronenbundel te scannen over de gas-ionisationkamer en de bundel van secundaire elektronen te detecteren maakt de hele constructie van het elektronentoevoersysteem equivalent met een laag-voltage scanning elektronenmicroscoop. De submicron gas-ionisatiekamer is verbonden aan het gastoevoersysteem. De ionenbundel kan gefocusseerd worden op een plaat met submicron structuren. Het focusseren van een elektronenbundel in de gas-ionisatiekamer alsmede het focusseren van de onttrokken ionenbundel op een submicron target kan gedaan worden met behulp van vier sets quadrupool deflectoren en twee afzonderlijke detectoren voor de secundaire elektronen. Een energie-analysator kan in hetzelfde systeem worden opgenomen.

Het hele systeem is ontworpen met behulp van ELD en SIMION-3D, elektronenoptisch simulatieprogramma.

Project Publications

Research articles

1] Critical review: Quest for high brightness, monochromatic noble gas ion sources
V.N. Tondare, J. Vac. Sci. Technol. A **23(6)**, 1498 (2005).

2] Stable field emission from W tips in poor vacuum conditions
V.N. Tondare, N.J. van Druten, C.W. Hagen and P.Kruit,
J. Vac. Sci. Technol. B **21(4)**, 1602 (2003).

3] Chapter 2: High-brightness, monochromatic and reliable noble gas ion source
(To be submitted for publication)

4] Chapter 4: Fabrication of submicron scale ionization chamber
(To be submitted for publication)

Patent

1] European Patent (applied on 22-02-2006)

Title: Particle- optical apparatus equipped with a gas ion source
Inventors: P. Kruit and V.N. Tondare
Application No.: **06110257.0-**

About the author

Vipin Nagnath Tondare was born in Aurangabad City, Maharashtra, India on the 13th of July 1973. In August 1998, he started working in FEM/FIM Laboratory, Department of Physics, University of Pune, Pune City, Maharashtra, India. He received his Master of Philosophy in physics (M. Phil. in physics) degree in February 2001 from the same university. The thesis title was "A Study of Field Electron Emission from HFCVD-Diamond Coated Tungsten Tips". While working for the M. Phil. degree, he also received a Senior Research Fellowship for a year, from Defence Research and Development Organisation, India (DRDO, India).

From August 2001 to date, he is working on a research project (FOM-Project 00PF84-FOM-Philips Laboratorium zonder Muren, in co-operation with FEI Company) in Charged Particle Optics Group, Delft, The Netherlands. The aim of the research project is to investigate new approaches to obtain high-brightness, monochromatic and reliable noble gas ion sources for focused beam applications.